Organisation for Economic Co-operation and Development

ENV/WKP(2022)7

Unclassified

English - Or. English

8 June 2022

ENVIRONMENT DIRECTORATE

Tackling air pollution in dense urban areas

The case of Santiago, Chile

Environment Working Paper No. 195

By Ioannis Tikoudis (1), Tobias Udsholt (1), Walid Oueslati (1)

(1) OECD Environment Directorate

Authorised for publication by Rodolfo Lacy, Director, Environment Directorate.

Keywords: Air pollution, urban transport, carbon tax, road pricing, bus electrification

JEL Codes: Q52, Q53, Q55, R13, R41, R48, H23

OECD Environment Working Papers are available at www.oecd.org/environment/workingpapers.htm

Ioannis Tikoudis (Ioannis.tikoudis@oecd.org)
Walid Oueslati (Walid.oueslati@oecd.org)

JT03497197

OECD ENVIRONMENT WORKING PAPERS

OECD Working Papers should not be reported as representing the official views of the OECD or of its member countries. The opinions expressed and arguments employed are those of the author(s). Working Papers describe preliminary results or research in progress by the author(s) and are published to stimulate discussion on a broad range of issues on which the OECD works.

This series is designed to make available to a wider readership selected studies on environmental issues prepared for use within the OECD. Authorship is usually collective, but principal author(s) are named. The papers are generally available only in their original language – English or French – with a summary in the other language.

Comments on Working Papers are welcomed, and may be sent to:

OECD Environment Directorate

2 rue André-Pascal, 75775 Paris Cedex 16, France

or by email: *env.contact@oecd.org*

OECD Environment Working Papers are published on
www.oecd.org/environment/workingpapers.htm as well as
on the OECD iLibrary (www.oecdilibrary.org)

The statistical data for Israel are supplied by and under the responsibility of the relevant Israeli authorities. The use of such data by the OECD is without prejudice to the status of the Golan Heights, East Jerusalem and Israeli settlements in the West Bank under the terms of international law.

Note by Turkey: The information in this document with reference to “Cyprus” relates to the southern part of the Island. There is no single authority representing both Turkish and Greek Cypriot people on the Island. Turkey recognises the Turkish Republic of Northern Cyprus (TRNC). Until a lasting and equitable solution is found within the context of the United Nations, Turkey shall preserve its position concerning the “Cyprus issue”.

Note by all the European Union Member States of the OECD and the European Union: The Republic of Cyprus is recognised by all members of the United Nations with the exception of Turkey. The information in this document relates to the area under the effective control of the Government of the Republic of Cyprus.

Abstract

Reducing air pollution is a major policy challenge, especially in densely populated urban areas where human exposure to emissions is considerable. This paper develops and examines a series of scenarios for the evolution of transport-related emissions in the area of Santiago, Chile. The study spans the period up to 2050 and focuses on seven air pollutants and CO2. It compares a reference scenario with policy counterfactual scenarios involving a rapid electrification of public buses, a carbon pricing scheme and a kilometre charge differentiated by vehicle type. The reference scenario predicts a 55-80% reduction in air pollutants emitted by the transport system of the city, by 2050. The corresponding reduction of CO2 lies at 6%, highlighting the asymmetric evolution in tailpipe filtering and carbon capture technologies. The analysis suggests that ramping up the efforts to electrify the bus fleet may eliminate 25% of the CO2 and at least 10% of the remaining air pollutant emissions in 2050. These figures increase to 45% and 30%, respectively, if rapid electrification is accompanied by one of the two tax schemes. With a distinct program to recycle the revenue from the tax schemes, the policy reform can be welfare improving for all groups and its environmental objectives can be achieved without adverse distributional consequences. The paper highlights the potential synergies of policies curbing climate change and tacking air pollution from the viewpoint of urban transport.

Keywords: air pollution, urban transport, carbon tax, road pricing, bus electrification

JEL Codes: Q52, Q53, Q55, R13, R41, R48, H23

Résumé

La réduction de la pollution atmosphérique est un défi politique majeur, en particulier dans les zones urbaines densément peuplées où l'exposition humaine aux émissions est considérable. Ce papier développe et examine une série de scénarios pour l'évolution des émissions liées au transport dans la région de Santiago, au Chili. L'étude couvre la période allant jusqu'en 2050 et se concentre sur sept polluants atmosphériques ainsi que les émissions de CO2. Le papier compare un scénario de référence avec des scénarios politiques contrefactuels impliquant une électrification rapide des bus publics, un système de tarification du carbone et une redevance kilométrique différenciée par type de véhicule. Le scénario de référence prévoit une réduction de 55 à 80 % des polluants atmosphériques émis par le système de transport de la ville, d'ici 2050. La réduction correspondante de CO2 se situe à 6 %, soulignant l'évolution asymétrique des technologies de filtrage et de capture du carbone. L'analyse suggère que l'intensification des efforts d'électrification de la flotte d'autobus pourrait éliminer 25 % du CO2 et au moins 10 % des émissions restantes de polluants atmosphériques en 2050. Ces chiffres passent respectivement à 45 % et 30 % si l'électrification rapide est accompagnée par un des deux régimes fiscaux, à savoir la tarification du carbone ou une redevance kilométrique par type de véhicule. Avec un programme distinct pour recycler les recettes des régimes fiscaux, la réforme politique peut améliorer le bien-être de tous les groupes et ses objectifs environnementaux peuvent être atteints sans conséquences distributives négatives. Le document met en évidence les synergies des politiques de lutte contre le changement climatique et de lutte contre la pollution atmosphérique du point de vue des transports urbains.

Mots clés : Pollution atmosphérique, transports urbains, taxe carbone, tarification routière, électrification des bus

Classification JEL: Q52, Q53, Q55, R13, R41, R48, H23

Acknowledgements

This working paper is an output of the OECD Environment Policy Committee (EPOC) and its Working Party on Integrating Environmental and Economic Policies (WPIEEP).

It is authored by Ioannis Tikoudis, Tobias Udsholt and Walid Oueslati. The work was conducted under the overall supervision of Shardul Agrawala, Head of the Environment and Economy Integration Division of the OECD's Environment Directorate. The authors are grateful to former Chilean government Ministers Marcelo Mena and Gloria Hutt, and to the WPIEEP delegates, in particular Javier Garcia and Felipe Saavedra for helpful comments on earlier drafts of this paper. The assistance from numerous colleagues in the Chilean Ministries of the Environment, Housing and Urban Planning, and Transport and Communications in the preliminary stages of the study is greatly acknowledged. The authors thank Illias Mousse Iye for the editorial assistance. The responsibility for the content of this publication lies with the authors.

Table of Contents

Tables

Figures

Executive summary

Reducing air pollution and greenhouse gas emissions from urban transport is a timely policy challenge. Coming up with a socially desirable remedy can be complicated, as the ideal policy mix has to improve environmental quality, ensure economic efficiency and satisfy fiscal constraints. At the same time, it should not interfere with economic growth or exacerbate existing inequalities. To jointly satisfy these requirements, policy making should be supported by evidence-based analysis that utilises the maximum amount of information and state-of-the-art modelling methods. This study uses multiple data inputs, projection techniques and the OECD's model of land use and transport, MOLES, to examine the impact of various policies on local air pollution and greenhouse gas emissions in Santiago, Chile.

The study offers a comparative analysis of a series of scenarios. It presents a reference scenario for the evolution of transport-related emissions of CO_2, CO, NO_X, VOC, $PM_{2.5}$, SO_2, N_2O and NH_3 from 2020 to 2050. During this time, the current policy framework that applies to the transport sector in Santiago is kept constant. The study juxtaposes that scenario against a series of counterfactuals constructed out of three new core policies. These include: (i) the rapid electrification of the city's public bus fleet, (ii) a stringent carbon pricing scheme and (iii) a kilometre charge differentiated by vehicle type. The policy analysis investigates the effectiveness of the various policy combinations in reducing emissions. Simultaneously, it takes into consideration the potential impact they may have on the balance of public budgets, household welfare and equity.

The analysis of the reference scenario uncovers a striking difference between the trajectories of greenhouse gases emissions and air pollutants. Aggregate CO_2 emissions from urban transport can be remarkably unresponsive to technical progress. The carbon footprint of Santiago's transport system in 2050 is projected to be just 6% lower than its current level. In contrast, the aggregate emissions of CO, VOC, NO_X and $PM_{2.5}$ in the reference scenario are projected to fall by 55-80%. The key difference is the asymmetric evolution of technologies (i) filtering tailpipe emissions and (ii) capturing carbon from internal combustion engine vehicles. The former technologies advanced substantially during the last 40 years, and are expected to continue improving throughout the time window of the study. In contrast, the latter technologies are in their infancy and any assumption about their long-run evolution would be purely speculative.

The analyses of counterfactual scenarios yield a set of policy recommendations. These include: (i) the acceleration of the bus electrification process, which is one of the main levers to ensure that policies promoting public transport will generate the largest possible environmental benefits, (ii) the implementation of a tax scheme aligning the external effects of car use with its private costs, and (iii) the introduction of a recycling mechanism ensuring that the road and carbon tax revenue returns to the local economy. The latter can be designed in a way that ensures that the tax reform is fiscally balanced and welfare improving for all.

The paper highlights the importance of ramping up the efforts to electrify the passenger bus fleet. The benefit from increasing the share of electric buses in the fleet is twofold. Primarily, it decreases the current emissions from buses, which may be high in cities where the use of public transport is prevalent. Secondarily, investing in an electric bus fleet can be an important complement to tax-based policies that increase the pecuniary cost of car use. While such policies may cause a considerable switch to public transport, the environmental benefits of this switch are maximised only when buses operate in the cleanest possible way. The study yields three major recommendations.

The carbon tax and the vehicle-differentiated kilometre charge are found to induce a decrease in the carbon footprint of urban transport and to reduce air pollution. Each of the two schemes can contribute to pursuing both environmental goals, as their tax bases greatly overlap. This finding suggests that any local or national authority in charge of a kilometric or motor fuel tax can help mitigating both environmental issues by adjusting the tax to this end.

The two tax schemes are not likely to be welfare improving as stand-alone mechanisms. Combining them with a distinct revenue recycling mechanism could ensure that the immediate benefits exceed the imposed tax burdens. The analysis shows that recycling the tax revenues with a horizontal lump-sum transfer can secure that the reform is welfare improving, even before the benefits from carbon savings and air pollution reduction are factored in. Importantly, the inclusion of this revenue recycling mechanism will have a positive impact in both lower- and higher-income segments. Therefore, the political acceptability of any such scheme will be largely determined by the presence of a dedicated mechanism to recycle the revenue from these tax instruments.

The results also question the degree to which the two tax instruments can fully achieve their environmental goals as stand-alone policies. In particular, aggregate emissions of CO_2 and various air pollutants are found to be rather unresponsive to increases in either of the two tax schemes. In contrast, the inclusion of these taxes in a wider policy programme, for instance one that invests in a greener public bus fleet, scales up the emissions savings that these taxes can generate. This occurs because the switch from car to bus, which both taxes induce, has a larger environmental benefit when the difference in the environmental footprint of the two transport modes is larger.

The results of the study may be highly valid for urban contexts similar to Santiago. They are particularly relevant for dense urban areas with a rather monocentric structure, where the use of public transport is already prevalent. In many of these cities, curbing air pollution and reducing greenhouse gas emissions are joint priorities. The study's findings will also be informative for countries sharing some of the most distinct characteristics of the Chilean economy, such as the rapidly increasing car ownership. This characteristic is a critical driver behind multiple findings in the study and constitutes a common phenomenon in many emerging economies with an expanding middle class. As it has been the case with Chile, it is likely that the issue of air pollution will rise on the political agenda of these countries in parallel with their rapid economic growth and urbanisation. Therefore, it is expected that the overarching policy recommendations of this study are partially transferrable to these contexts.

1 Introduction

Curbing the emissions of air pollutants and greenhouse gases is both a policy goal and a major socioeconomic challenge. Reducing CO_2 emissions is an urgent policy priority due to the impact that climate change may have on natural systems (IPCC, 2019[1]) and the global economy (OECD, 2015[2]). Managing air pollution is a key public health priority, as poor air quality is responsible for one in every nine deaths globally (WHO, 2016[3]). Air pollution imposes a significant social cost, since exposure to it results in higher rates of morbidity, absenteeism, partial disability and productivity losses (OECD, 2016[4]). Cities are key in the effort to reduce both types of emissions. Urban areas are major energy consumers, generating the largest part of global greenhouse gas emissions (UN Habitat, 2014[5]). They are also the loci where the issue of air pollution is mostly pronounced, as large concentrations of air pollutants are typically observed in densely populated areas (Lanzi and Dellink, 2019[6]).

The role of urban transport in curbing air pollution is crucial. In Latin America, the transport sector generates a large part of the most detrimental emissions: 55% of nitrogen oxide (NO_X), over 30% of carbon monoxide (CO) and roughly 20% of $PM_{2.5}$ emissions (IEA, 2016[7]). Moreover, transport generates a substantial proportion of sulphur dioxide (SO_2) and volatile organic compounds (VOC) emissions, pollutants that are associated with a range of negative health impacts. These contributions, which are likely to be higher in urban environments due to the density of motorised vehicle use, place transport policies at the forefront of initiatives to mitigate air pollution.

Furthermore, the decarbonisation of economic activity has to focus on curbing CO_2 emissions from transport sector.[1] In Chile, these emissions rose by 44% in the period 2000-2013, currently accounting for 25% of the country's total CO_2e emissions (Gallardo et al., 2018[8]). The goal of decarbonising transport is highly related to that of reducing air pollution, as both types of emissions largely originate from the combustion of motor fuels. Although the social cost of CO_2 does not depend on where it is emitted, spatially refined policies are nevertheless of high importance. Passenger transport in cities holds a considerable share of transport-related CO_2. Curbing that requires a mix of transport and land use policies, whose intensity can be adjusted across urban space (OECD, 2020[6]; Tikoudis and Oueslati, 2021[7]).

This study examines different pathways to reducing emissions of greenhouse gases and air pollutants in Santiago. In 2016, the capital of Chile was among the 10% most polluted large metropolitan areas in the OECD (OECD, 2016[9]). The study presents a reference scenario for the evolution of transport-related emissions of CO_2, CO, NO_X, VOC, $PM_{2.5}$, SO_2, N_2O and NH_3 in a period spanning the years from 2020 to 2050. During this time, the current policy framework in the transport sector is kept constant. Thus, the reference scenario is a business-as-usual continuation of the existing taxes applying to motor fuels, vehicles, and their circulation. This scenario keeps the local regulatory mechanisms and road infrastructure constant, but it accounts for the planned expansion of the city's subway network. Moreover, the study juxtaposes the reference scenario against a series of counterfactuals, which are constructed out of three core policies: (i) the rapid electrification of the city's public bus fleet, (ii) a carbon pricing scheme targeting the transport sector, and (iii) a local kilometre charge that is differentiated by vehicle type. The analysis is

[1]Chile committed to reduce the amount of CO_2e per unit of GDP in 2030 by 30% compared to its level in 2007. The commitment increases to 45% if sufficient international support is provided (Climate Action Tracker, 2019[33]).

based primarily on the environmental effectiveness of policies combining the above elements, i.e. on their capacity to reduce emissions. However, it takes into consideration the potential impact these policies may have on the economy, both in aggregate terms and separately on low and high-income households in Chile.

A series of data inputs, instruments and tools enable the analyses in this report. The study projects the emission factors of future conventional buses in Santiago. To this end, it combines the emission factors of various types of buses with Chilean data on the share of these bus types in the conventional bus fleet of Santiago. Data from the Chilean national travel survey are used to approximate the share of different vehicle classes in the fleet. Furthermore, a combination of the travel survey data with demographic information enables the explicit modelling of household location and travel patterns in Santiago. One of the most important sources of employed data is the emission inventory published by the European Monitoring and Evaluation Programme (EMEP) and the European Environment Agency (EEA). This inventory (European Environment Agency, 2019[10]) is used to conservatively project the emission factors of light duty passenger vehicles entering the market in the next three decades. The degree to which their filtering technologies will be superior to those embodied in currently available cars is predicted using historical observations of the emission factors during the last 50 years. This period spans filtering technologies from the pre-Euro era to the most recent EURO 5 and EURO 6 cars.

The core of the analysis is conducted with the use of OECD's urban Computable General Equilibrium (u-CGE) model, MOLES (Tikoudis and Oueslati, 2017[11]). The model enables the examination of the environmental effectiveness and economic efficiency of urban policies targeting transport and land-use. MOLES simultaneously accounts for the key drivers of the emissions intensity of a city by quantifying technological innovations, policy interventions, price shocks and adjustments in individual behaviour. The version of the model used in this paper is tailored to consider the differences in the economic and travel behaviour between low-income and high-income groups.[2] Despite being a stylised model, it accounts for a number of city-specific characteristics. These include the spatial morphology of Santiago, the configuration of its transport networks, the observed mobility patterns and the overall traffic conditions.

The findings indicate that the baseline trajectories of greenhouse gas emissions and air pollutants may differ widely. CO_2 emissions can be remarkably rigid to technological progress, as the aggregate carbon footprint of Santiago's transport system in 2050 is projected to be just 6% lower than its current level. Despite the expected progress in the fuel efficiency of future vehicles, and a significant penetration of electric vehicles in the next three decades, several factors contribute to offsetting the associated environmental gains from these developments. Population growth, increase in income, car ownership and travel demand, as well as rebound effects from fuel economy improvements constitute the key offsetting variables.[3] Unlike the rigid trajectory of CO_2, transport-related emissions of CO, VOC, NO_X and $PM_{2.5}$ are projected to fall by 55% to 80% in the next three decades. The key factor behind this striking difference is the asymmetric progress in the capacity to filter tailpipe emissions of air pollutants and capture CO_2 from conventional vehicles. Filtering technologies have largely advanced during the last 40 years. They are expected to continue improving throughout the time window of the study. In contrast, carbon capture of vehicle emissions is in its infancy and any optimistic assumption about its long-run potential would be purely speculative.

The analysis reveals the crucial role of passenger bus fleet electrification. A drastic increase in the share of electric buses in purchases can provide substantial mitigation effects, even as a stand-alone policy.

[2]The version of the model used in this paper is an extension of a precursor version used in a case study focusing on the decarbonisation of sprawled urban areas (OECD, 2020[57]). See Tikoudis and Oueslati (2021[63]) for the specification of this precursor model.

[3]This finding corroborates similar evidence from simulations performed for the urban area of Auckland (OECD, 2020[57]).

Quintupling the share of electric buses in purchases could result in at least two thirds of the fleet being electric by 2050. This would eliminate 25% of transport-related CO_2 emissions and lower the emissions of all air pollutants by between 10% and 50%. The benefits of increasing the share of electric buses in the fleet are twofold. First, it reduces current emissions from buses, which may be high in cities like Santiago where the use of public transport is prevalent. Second, investing in an electric bus fleet can be an important complement to tax-based policies that increase the pecuniary cost of car use. While such policies may cause a considerable switch to public transport, the environmental benefits of this switch are maximised only when buses operate in the cleanest possible way.

The two tax-based schemes can be part of a wider strategy to mitigate climate change and air pollution. The carbon tax and the vehicle-differentiated kilometre charge are found to serve both environmental goals pursued in the analysis, as their tax bases greatly overlap. This finding suggests that a local or national authority in charge of any of these tax instruments can partially mitigate both environmental issues by adjusting the tax accordingly. At the same time, the results question the degree to which these instruments can fully achieve such goals as stand-alone policies. In particular, aggregate emissions of CO_2 and the various pollutants are found to respond in a rather rigid way to increases in either of the two tax schemes. In contrast, the inclusion of these taxes in a wider policy program, for instance the one investing in a greener public bus fleet, scales up the emissions savings. In line with this finding, the results indicate that combining either of the two tax schemes with an intensive bus electrification strategy could eliminate 45% of the remaining CO_2 and 30-50% of the emissions of the most detrimental air pollutants (CO, VOC, NO_X and $PM_{2.5}$) in 2050.

While the analyses employed in the paper apply to the case of Santiago, their relevance to similar contexts should be substantial. The study is particularly relevant to settings where rapid growth in income levels (OECD, 2018[12]; OECD, 2016[9]) and car ownership coexists with the widespread use of a public transport system that undergoes an overall modernisation.[4]

The rest of the paper is structured as follows. Section 2 provides general information on the existing policy context of air pollution regulation in Santiago. It charts pathways towards further reductions in emissions from transport and heating. Section 3 provides the methodological details of the study. That includes the reference scenario, the three core policy interventions examined in the simulations, as well as the way in which they are combined to form counterfactual policy scenarios. Section 4 presents the findings from simulating the various scenarios and discusses their policy implications. Section 5 concludes. Section 6 is dedicated to the documentation of MOLES 1.2, the version of the OECD's urban transport and land-use model MOLES tailored for the case of Santiago.

[4]In Chile, the rapid economic progress of the last twenty years contributed to a remarkable growth of car ownership, as the country's vehicle stock doubled between 2000 and 2016 (OECD, 2016[9]).

2 The challenges related to tackling air pollution in dense urban areas

2.1. Policy context of air pollution regulation in Santiago

Air pollution is a key concern for policymakers in the Santiago Metropolitan Region (hereafter, Santiago) and Chile, as a combination of factors contribute to high emission levels. Santiago is home to 7 million people and lies in the Chilean Central Valley, surrounded by mountains. The growing number of private vehicles, the proximity of emission-intensive industries to densely populated areas and the dependence on firewood for residential heating are the main drivers of the high levels of emissions. Due to the topography and meteorological conditions of the region, air pollutants are prevented from dispersing. Air pollution episodes are particularly prevalent during winter, when certain meteorological conditions[5] and the absence of precipitation increase the concentration of pollutants at lower altitudes (Jorquera et al., 2005[13]; Garreaud and Rutllant, 2003[14]). A reliance on firewood for residential heating significantly adds to the high concentration of air pollutants during the winter.

The Chilean government has adopted a range of policies to address air pollution and climate change. The effort to monitor air pollutants dates back several decades, as large scale regulatory efforts began in the 1990s (Gallardo et al., 2018[8]). Since then, Chile enacted a wide range of policies to reduce emissions of air pollutants. These include stricter standards for vehicles and measures to encourage households to switch to cleaner forms of residential heating.

There has been some success in reducing the overall levels of air pollution and the frequency of its episodes in Santiago. The daily average pollution exceeded the alert threshold during 27 days in 2017 versus 109 days in 2000 for PM_{10}.[6] An important contributor has been the full integration of the public transport system, which was initiated in 2005 under the Transantiago banner. This has significantly increased public transport capacity, particularly that of the subway network (Pino et al., 2015[15]). The gradual implementation of Euro emission standards has also contributed to reducing the release of air pollutants per vehicle-kilometre travelled. As a result of these policies, the average contribution of motor vehicles to PM concentration levels fell significantly between the periods 2005-2006 and 2010-2011 (Barraza et al., 2017[16]).

However, the challenge of air pollution is far from being fully addressed and Santiago remains among the 10% most polluted large metropolitan areas in the OECD despite extensive measures to tackle the issue of air pollution (OECD, 2016[9]). In particular, emissions of particulate matter (PM) from transport remain high. Additionally, emissions of some air pollutants are still increasing. The levels of nitrogen dioxide (hereafter NO_2), which is primarily emitted from motor transport in cities, rose by 28.6% between 2004 and 2014 (Duncan et al., 2016[17]). Furthermore, PM emissions from residential wood burning did not decline

[5]Meteorological conditions include thermal inversions and coastal lows. A coastal low is a transient meteorological phenomenon substantially limiting the dispersion of pollutants (Garreaud and Rutllant, 2003[14]).

[6] See (Secretaría Regional Ministerial del Medio Ambiente Región Metropolitana, 2018[34])

in the period 1998-2012 (Barraza et al., 2017[16]). This suggests that the policy to ban open chimneys, in place since 1997, and the prohibition of residential wood burning during high pollution episodes have not been effective (Barraza et al., 2017[16]). The persistent use of wood for residential heating underlines the need for affordable alternatives if efforts to reduce emissions are to be successful.

Emissions of air pollutants in Chile entail a substantial social cost. The Chilean Ministry of Environment estimates that air pollution costs USD 670 million annually in health care expenses and productivity losses (El Ministerio del Medio Ambiente, 2013[18]). A considerable fraction of this burden is generated in Santiago. Further losses are likely associated with the shutdown of polluting factories in urban areas during high air pollution episodes.

Greenhouse gas emissions have also risen in line with Chile's rapid economic growth: CO_2 emissions from the transport sector alone rose by 44% between 2000 and 2013. Therefore, current policy measures and improvements in technology have not been sufficient in addressing high levels of air pollution and rising greenhouse gas emissions.

2.2. Pathways to reduce emissions using transport policies

This study addresses how policy and technological progress will affect emissions of air pollutants and greenhouse gases between 2020 and 2050. The current policy mix is used to construct a *reference scenario*, against which the effectiveness of policies implemented in hypothetical counterfactual scenarios are assessed. These policies target emissions from urban transport. They do so by promoting and electrifying public transport, by discouraging the use of private cars and by affecting the size of fossil fuel vehicles in the long run. The channels through which such measures affect air pollution and greenhouse gas emissions are explained in detail below.

Public transport represents an efficient way of transporting large numbers of people in cities. Santiago already operates an extensive subway and bus network. Ongoing work to expand the subway network will provide further opportunities for a modal shift towards public transport. Greater access to and use of the public transport system would reduce air pollution and greenhouse gas emissions. Furthermore, it would likely lead to less congestion. Electrification is also key, as the extent to which air pollution can be reduced through a shift to public transport depends on the extent to which public transport vehicles are electric. Currently, the bus fleet is primarily comprised of diesel buses, although a degree of electrification is under way. A shift to a bus fleet composed exclusively of electric vehicles would eliminate tailpipe emissions of air pollutants. In turn, the effect of electrification of public transport on greenhouse gas emissions would depend on the carbon intensity of electricity generation. A higher share of electricity generated by low-emission energy sources would result in larger emission reductions. In 2017, 36% of electricity in Chile was generated by solar panels, wind and hydro (IEA, 2018[19]). This represents a decline from 1995 when the share of low-emission energy sources was 66%, indicating that growing energy demand energy has been met with less green alternatives.

Another pathway to reducing emissions from transportation is by improving the energy efficiency of existing internal combustion engine (ICE) vehicles. A more fuel-efficient fleet implies lower emissions per kilometre travelled. This can be achieved by encouraging the sale of conventional vehicles that are less polluting. The effect of such support measures depends on the extent to which these vehicles function as substitutes to older, more polluting cars and the degree to which they will induce users of public transport to adopt them. The net effect is context-specific and requires thorough economic analysis to be estimated.

Policies can also provide incentives for the adoption of private electric vehicles. Similarly to the effect of increased use of public transportation discussed above, the effects of an increase in the share of electric vehicles on air pollution would be immediate and positive. However, the extent to which such initiatives will lower CO_2 emissions depends on the carbon intensity of the electricity generation sector and the extent to which these policies will reduce public transport ridership.

2.3. Other relevant policies

In addition to the aforementioned measures, there are several other policies that could affect emissions and human exposure to these emissions.

The urban form and the development pattern of a city affect its emissions profile. Santiago is a compact city, parts of which are characterised by high population density. The spatial variation of residential and employment density determines commuting distances and, by extension, the emissions generated by commuting. Compared to sprawled urban areas, cities of high population density like Santiago are likely to have a smaller *per capita* carbon footprint from transport activity.

On the other hand, a high population density implies that a larger part of the population may be exposed to substantial levels of air pollution. Santiago's population density is high, particularly in areas close to the city's inner core. The amount of traffic in these areas is considerable, as Santiago fits the profile of a typical monocentric city. That is, the majority of non-industrial jobs, services and shopping facilities are located in its central business district. Therefore, during a typical day, a large part of the population lies in areas where most of the traffic takes place.

The argument developed above suggests that reducing human exposure to air pollution may be possible by implementing policies to achieve a more decentralised urban form. Decentralisation could be achieved in the long run with incentives that induce firms, preferably heavy industries and services, to relocate to more peripheral locations. This could partially reverse commuting from the outer suburbs to these employment hubs, spreading the overall traffic across space. Consequently, such a reform on urban structure could alter the spatial concentration patterns of air pollutants and reduce total human exposure to them.

A substantial share of air pollution is linked to firewood burning for residential heating. During the winter, firewood burning is responsible for approximately 30% of total amount of ambient $PM_{2.5}$. Emissions from firewood heating primarily result from poorly operated heaters and the high humidity of firewood (OECD, 2016[9]). Thus, these emissions can be reduced through measures encouraging the use of more efficient residential heating systems (Ministerio del Medio Ambiente, 2017[20]) and through an upgrade of the energy efficiency of dwellings.

3 Design of the study

3.1. Exogenous factors, endogenous variables and policy instruments

The modelling exercise involved in the study uses two types of inputs. *Exogenous factors* are inputs that may affect the results of the policy simulations, but not *vice versa*. A list of the study's exogenous variables is provided in Table 3.1. Some of them are prices and wages determined outside the urban economy. For instance, fuel pre-tax prices are determined in the international markets and wage rates are determined at the national level. The exogenous input encompasses taxes and fees that are fixed over time and across policy experiments, as well as relevant technological constraints determining travel speeds, travel times and energy consumption. Importantly, the exogenous input includes the evolution of Santiago's total population and its distribution across low and high-income cohorts. For the latter, it is assumed that the low-income cohort is comprised of individuals in the 1st and 2nd quartile of the income distribution, while the high-income cohort is comprised of individuals in the 3rd and 4th quartiles. Therefore, the percentage of the total population in each cohort remains fixed at 50% over time, but the total size of each group grows at the same rate as the total population.

Table 3.1. Exogenous variables imported to the model

Variable	Explanation
Population	The total number of individuals residing in the city. [a]
Cohort composition	The percentage of population in the low and high-income groups.
Wages	The annual average earnings of a commuter, net of income taxes. [a, b]
Pre-tax vehicle price	The real purchase price of a representative vehicle from a class of vehicles, net of excise and value-added taxes.
Kilometric lifetime of a private vehicle	The number of kilometres a vehicle is expected to be operational.
Pre-tax fuel & electricity price	The real average prices of fuel (CLP/lt) and of electricity (CLP/kWh), net of excise, *ad-valorem* and environmental tax components. [a]
Time-invariant tax components	Excise and *ad-valorem* tax rates on gasoline, diesel and electricity. Annual vehicle registration and circulation tax.
Public transport fares	Real pecuniary cost of a trip using bus or metro.
Fuel economy of conventional vehicles	The fuel consumption (litres/km) of an internal combustion engine (ICE) vehicle representing its class. [c]
Energy efficiency of electric vehicles	The electricity consumption (kWh/km) of a representative electric vehicle (EV) in a given year. [a]
Maximum speed	Free-flow speeds of cars and buses, average speed of subway
Carbon intensity of grid	The amount of carbon embodied in electricity (kg CO_2/kWh). [a]
Evolution of public transport network	The stations and capacity additions to the subway network active in a given year.

Notes: [a] Evolves across years; [b] Differs across population cohorts; [c] Differentiated across types of internal combustion engine vehicles according to their fuel type and their vintage.

Table 3.2. Policy instruments

Instrument	Explanation
Carbon tax on transport	Charges gasoline, diesel fuel and electricity with a tax per unit of final fuel (CLP/litre, CLP/kWh). The tax reflects the social cost of damages caused by the carbon content embodied in that unit.
Vehicle-specific kilometre tax	Charges a driven kilometre at a rate that depends on the filtering technology of the car.
Rapid bus electrification	Accelerates the replacement of old diesel buses exiting the fleet with electric buses. The purchase share is assumed to be: 50% for 2020-2030, 75% for 2030-2040 and 100% thereafter. [a]

Notes: [a] Corresponding purchase rates in the reference: 10% (2020-2030), 15% (2030-2040) and 20% (2040-2050).

Table 3.3. Variables projected by the model

Variable	Explanation
Locational probability	The percentage of a population cohort residing in a residential zone of the city. [a, b, c]
Employment distribution	The percentage of a population cohort supplying labour to a given employment hub. [a, b, c]
Incomes	The expected income of an individual given the average wages at different parts of the city. [a, b, c]
Vehicle ownership, fleet size	Percentage of population owning a car. [a, b, c]
Expenditure share distribution	The percentage of an individual's income spent on consumption goods, housing rents and transport services. [a, b, c]
Value of time	The willingness-to-pay in order to save one hour of travel time. [a, b, c]
Labour supply & commuting trips (L-trips)	The number of days an individual goes to work each year. [a, b, c]
Other trips (O-trips)	The number of shopping and leisure trips of an individual per year. [a, b, c]
Mode & route choice probability	The probability of choosing a transport mode and route in a trip. [a, b, c, f]
O-trip destination probability	The probability that a non-commuting trip ends up in a location. [a, b, c]
Vehicle class share in fleet size	The percentage of cars that belong to a vehicle class. [a, c]
Modal split	The share of cars, public transport and soft mobility modes in total traffic. [a, e, h]
Traffic level and speed	The volume of road traffic and the resulting speed [a, c, g, h, i]
Travel times	The time needed for a two way trip [a, c, g, h, i]
Housing & land rents	The annual rental rate per m^2 [a, c]
Emission levels	Aggregate annual emissions of a pollutant during a time period [a, c]

Notes: [a] Evolves across years; [b] Differs across population cohorts; [c] Varies across urban space; [d] Differs across vehicle classes; [e] Differs when calculated based on kilometres or trips; [f] Differs by trip type; [g] Differs between cars and buses; [h] Differs across time periods; [i] Differs by transport mode.

Policy instruments are taxes and regulations that may be active or inactive in the simulation. Whenever tax instruments are active, their levels are predetermined, so the simulation exercise does not attempt to optimise them. The study focuses on three instruments. The first is an implementation of a carbon tax scheme through urban transport instruments. When the carbon tax is active, an additional tax per litre of gasoline and diesel fuel (CLP/litre) and a tax per kWh of consumed electricity (CLP/kWh) is imposed. The level of these taxes reflects the social cost of damages caused by the carbon content embodied in one unit of final fuel. The value used in this study scales (by a factor of 3.0) the social cost of carbon dioxide (US$/metric tonne of CO_2) proposed by U.S. EPA (2016[21]). That cost is expressed in 2007 prices.[7] It

[7]Correcting for inflation reduces the scale factor to 2.4. Deriving this requires to denote the social costs of carbon (in year t), expressed in 2007 prices by c^t_{2007}. The same cost expressed in 2020 prices is then c^t_{2020}. Using an inflator of 1.25, it holds that $c^t_{2020} = 1.25 \cdot c^t_{2007}$. Thus: $2.4 \cdot c^t_{2020} = 3.0 \cdot c^t_{2007}$.

embodies a 5% probability, with which climate change may cause high-impact events. It also incorporates an annual rate of 3%, with which the monetised consequences are discounted. That value is then converted to CLP per litre of gasoline and diesel and to CLP per kWh using the carbon content embodied a unit of final fuel.[1] The tax on gasoline and diesel is characterised by an increasing time trend, as the social cost of carbon increases over time.[8] On the other hand, the tax on electricity declines, as the carbon content of a kWh is projected to decrease faster than the pace at which the social cost of carbon increases. The evolution of the three tax components included in the *carbon pricing scheme on urban transport* are displayed in Figure 3.1.

Figure 3.1. Carbon tax on urban transport

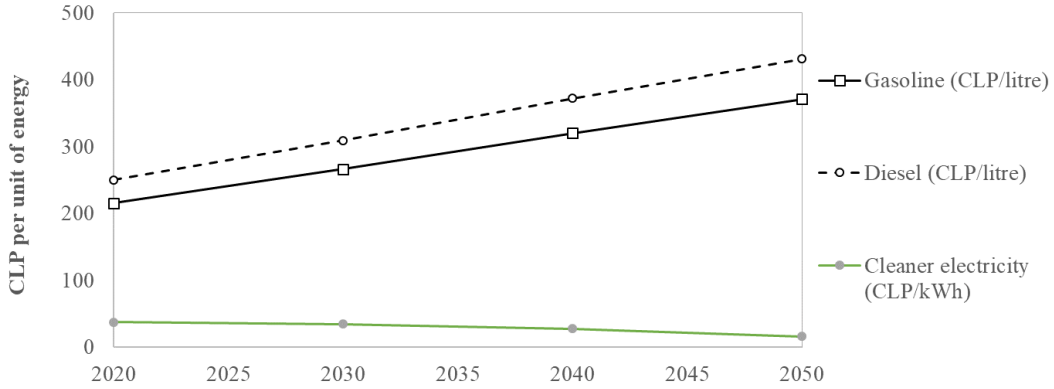

Notes: See endnotes for the conversion of carbon social cost to tax on final fuel. Graph generated by the authors.

The second tax scheme is primarily designed to manage air pollution, but functions as an alternative way to tax carbon emissions as well. That is, it involves a kilometre tax system that increases the generalised cost of car use to levels that are comparable to those induced by the carbon tax. The system is designed around a maximum kilometre price, which is the ceiling charge that can be imposed on any vehicle in the active fleet at a given year. The maximum kilometre price increases every year. The rationale behind this is similar to that driving up the environmental taxes on gasoline and diesel. Within any given year, the kilometre charge is differentiated across vehicles. The older vehicles, whose circulation is more detrimental from an environmental viewpoint, contribute relatively more. As time goes by, the charge imposed on a kilometre driven by a vehicle x increases. This occurs because (i) the external effects of road use increase, thus all kilometre charges increase, and (ii) the vehicle's relative age increases, thus its relative contribution to pollution increases. The evolution of the charges imposed on different vehicle classes used in the simulation is displayed in Figure 3.2.

[8]At the same time, the study assumes away any progress in the carbon capture technologies applied in urban transport. Thus, the carbon emitted in the air through the combustion of one litre of gasoline and diesel equal, always, the respective carbon content in a litre of these fuels.

Figure 3.2. Vehicle-specific kilometre tax system

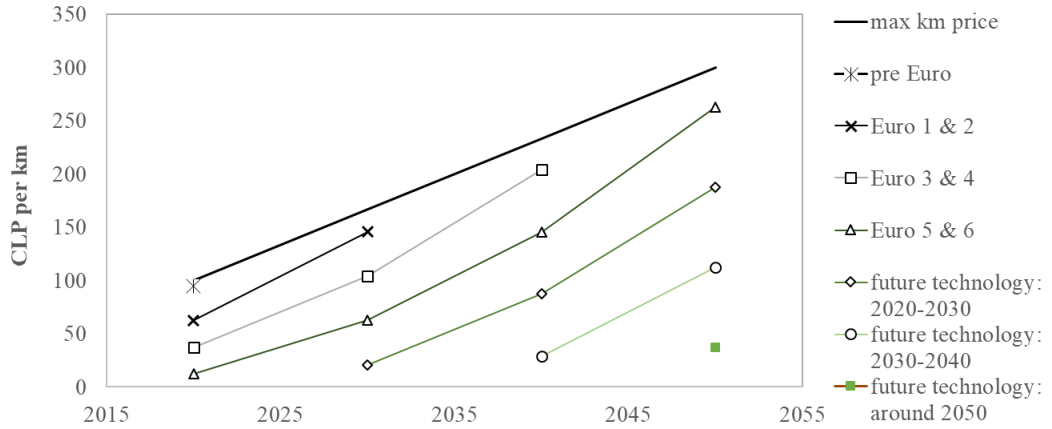

Notes: Graph generated by the authors.

Figure 3.3. Rapid bus electrification

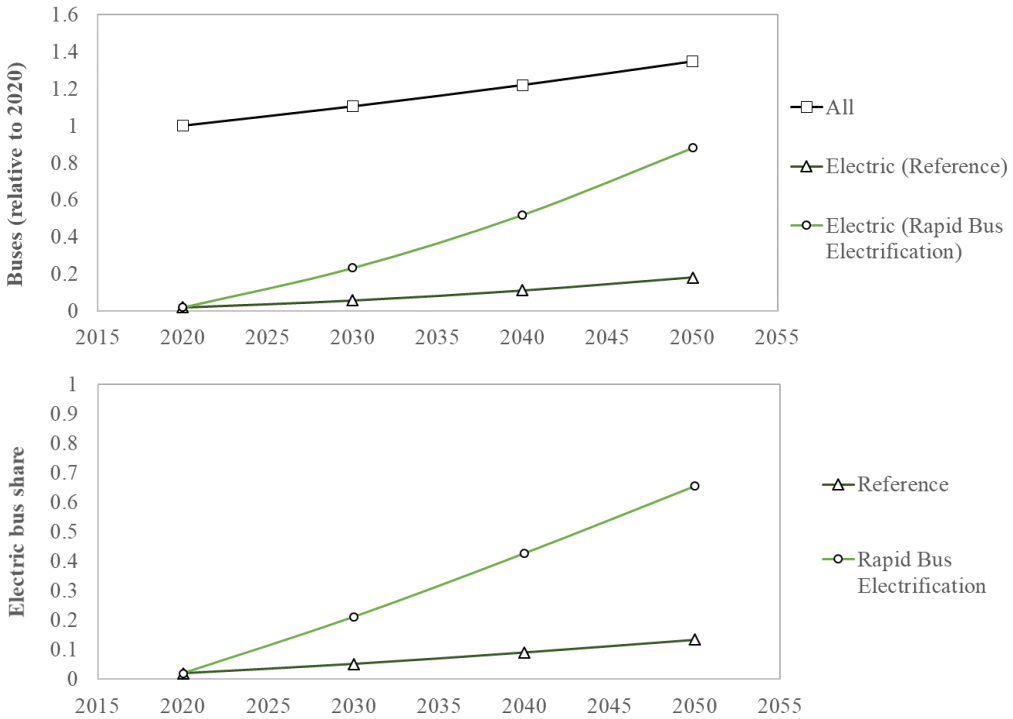

Notes: The computations assume that the total fleet size (solid black curve) increases at the same rate as the population of Santiago; Assumed annual depreciation rate of the bus stock: 4%; initial stock size estimate: 6600 buses. Combining these with the purchase rates in Table 3.2 and benchmarking on the initial size of the stock yields the curves in the graphs. Graph generated by the authors.

The third policy instrument involves the rapid electrification of the bus fleet. In policy simulations where the instrument is active, the share of electric buses in the purchases of a given year is substantially higher than that assumed in the reference scenario. The policy ensures that 50% of the buses purchased in the years preceding 2030 will be electric, versus 10% in the reference scenario. The rate increases to 75% for the period 2030-2040 and 100% for the period 2040-2050, while the corresponding rates in the reference scenario are 15% and 20% respectively. The differential impact of the policy is reflected in the expected share of electric buses in the fleet, shown in the lower panel of Figure 3.3.

The study focuses on five counterfactual scenarios, which are juxtaposed against the reference scenario. Three of them involve a single policy from Table 3.2, while two counterfactual scenarios involve a combination of a tax-based scheme with the rapid bus electrification programme. In the reference scenario, none of the policies outlined in this section is active. The reference scenario represents a continuation of current land-use and transport policies in the future. Therefore, it constitutes a business-as-usual benchmark, against which other counterfactual policy options can be assessed. The evolution of all time-varying elements included in Table 3.1 is common in all six scenarios of the study.

Table 3.4. Scenarios

Name	Specification
Reference scenario	All instruments in Table 3.2 are inactive
Carbon pricing scheme (CPS)	Applies exclusively the *carbon tax on transport* in Table 3.2.
Kilometre tax	Applies exclusively the *vehicle-specific kilometre tax* in Table 3.2
Rapid bus electrification	Applies exclusively the *rapid bus electrification program* in Table 3.2.
CPS-based duplex	Applies simultaneously the *carbon tax on transport* and the *rapid bus electrification program* in Table 3.2 [a]
Kilometre tax based duplex	Applies simultaneously the *vehicle-specific kilometre tax* and the *rapid bus electrification program* in Table 3.2 [a]

Notes: Tax revenue returns to the urban economy in all scenarios.

Figure 3.4. Spatial configuration of the study

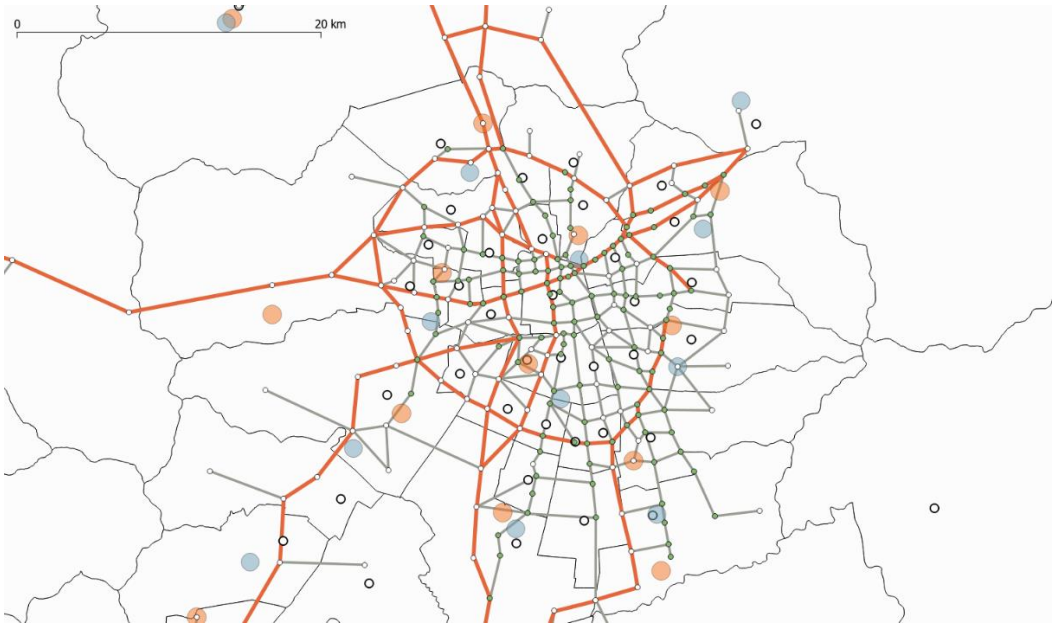

Notes: Medium-sized white dots: residential nodes; Orange dots: employment hubs; Blue dots: attractors of non-commuting trips; small white dots: transport network nodes without metro access; small green dots: transport network nodes with metro access.
Source: Image generated by authors.

3.2. Spatial and transport network configuration

The modelling exercise materialises upon a stylised representation of Santiago. This representation accounts for the key points of economic activity and the configuration of the city's transport networks. The

resolution of the configuration, shown in Figure 3.4, is bounded by the computational limitations of the model.

Table 3.5. Spatial resolution of the model

Layer	Resolution and visualization
Residential zones	52 zones represented by their centroids, displayed in Figure 3.5.
Employment hubs	16 destination points of commuting and education trips, identified with a combination of land-use and travel survey data. Displayed in Figure 3.6.
O-trip attractors	17 aggregate attractors of O-trips, i.e. non-commuting trips for leisure and shopping purposes. Displayed in Figure 3.6.
Road network nodes	262 nodes displayed in Figure 3.7.
Urban road network links	508 unidirectional links of low and medium capacity displayed in Figure 3.7.
Highway network links	292 unidirectional links of high capacity displayed in Figure 3.7.
Metro stops	130 aggregate metro stops, each representing one or more actual metro stops, shown in Figure 3.7.

3.2.1. Residential zones and key activity points

The model comprises 52 residential zones, which constitute concatenations of administrative units in Santiago. The centroids of these areas do not exactly represent the starting points of home-based trips, especially in peripheral zones. This occurs because the urban fabric is not evenly distributed within the surface of a zone. Due to this, the study uses fine-tuned household locations, which spatially deviate from zonal centroids. The home locations are displayed by dots in Figure 3.5. The spatial adjustment of centroids is performed with Open Street Map land use data. The adjusted centroids indicate the areas where developed land used for residential purposes is relatively concentrated.

Figure 3.5. Centroids of residential areas

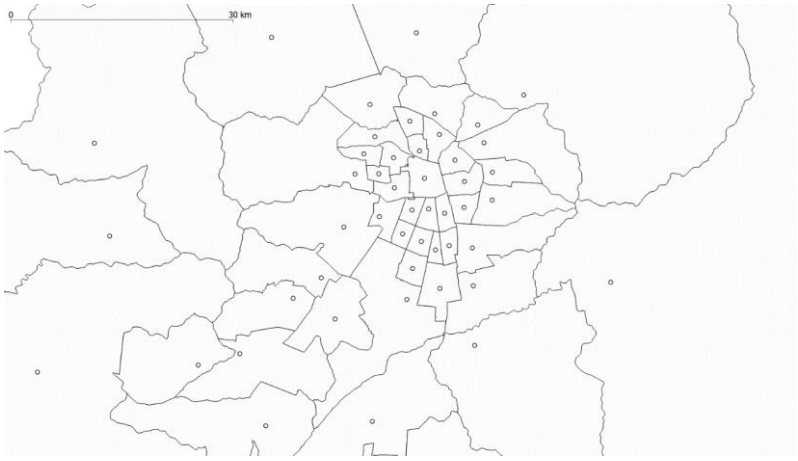

Notes: Dots represent aggregate household locations and may deviate from zonal centroids.
Source: Image generated by authors.

All *synthetic* trips simulated in the model terminate at destination points that constitute the centroids of trip-attracting hubs. Each such hub spans a circular area, within which a high number of *actual* trips, i.e. trips observed in travel survey data, terminate. The model uses 16 destination points of work and education trips (L-trips) and 17 destination points of other trips (O-trips), each surrounded by a buffer zone. These zones are displayed in the upper and lower panels of Figure 3.6, respectively. They capture the vast majority of actual trip termination points in the national travel survey. These comprise 55512 L-trips and

29327 *O*-trips, whose destination points are displayed by the dots in Figure 3.6. Trips terminating within the buffer zone of a particular hub increase the share of trips that hub attracts. A trip destination may also fall into the buffer zone of multiple hubs. In that case, all involved hubs are given a credit that is inversely related to the distance between their centroid and the trip destination point.

Figure 3.6. Identification of trip destinations

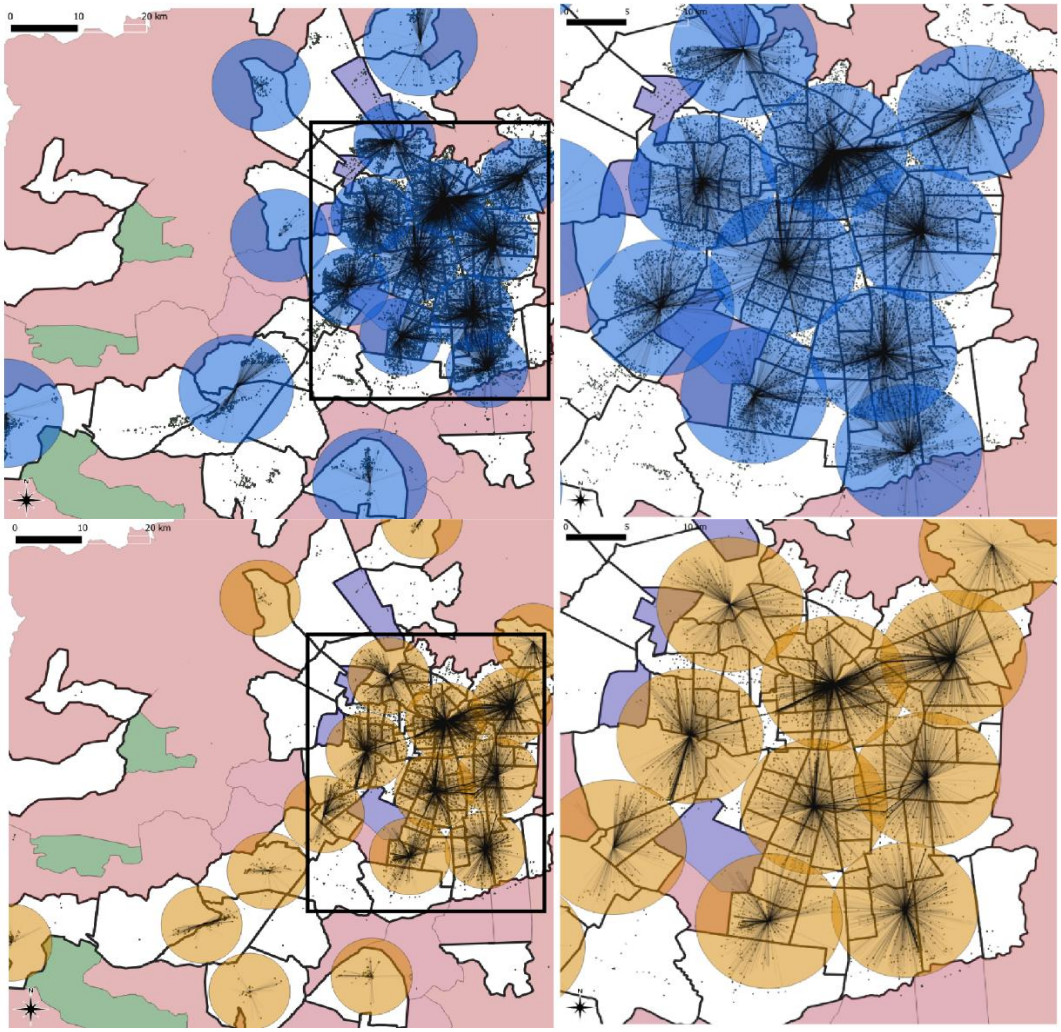

Note: Miscellaneous trips connected with miscellaneous key activity points.
Source: Underlying data by Observatorio Social (UAH) (2014[22]). Image generated by authors.

3.2.2. Transport network

Trips between residential locations in Figure 3.5 and the points of economic activity in Figure 3.6 are taken using the stylised transport system, displayed in Figure 3.7. This system consists of a road network, which is utilised by private vehicles and buses, and a subway network. The former network contains urban road links and highway segments constructed using Google Maps data. Traffic on the network takes place under congested conditions, i.e. a change in traffic volume causes an adjustment in the speed of cars and buses. The latter network is a simplified version of the city's actual subway system. For simplicity, subway traffic is assumed to be free of congestion.

Figure 3.7. Transport network

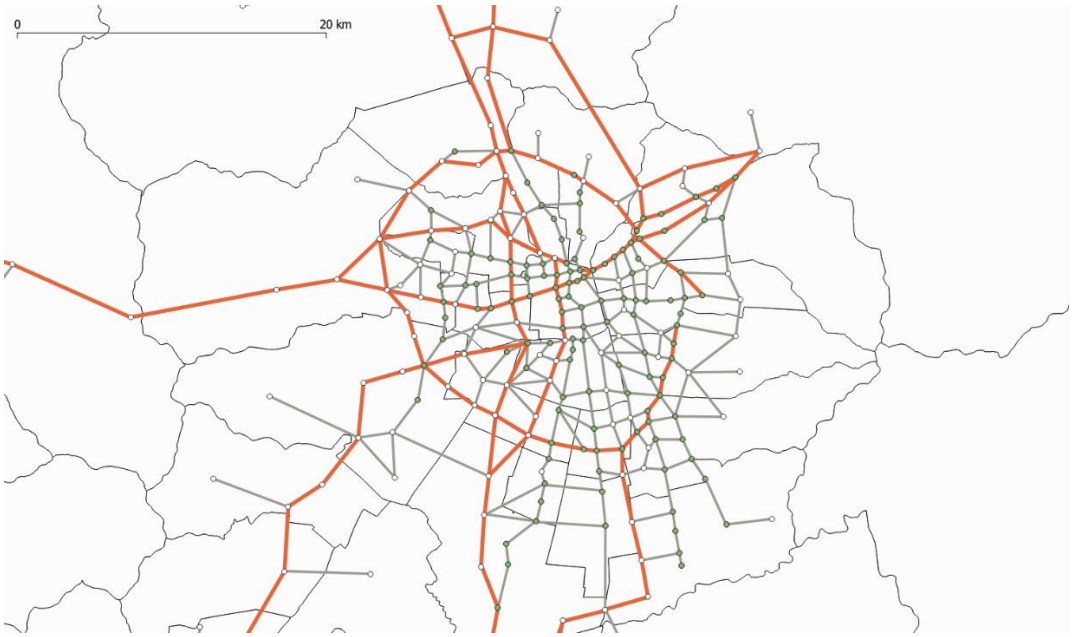

Source: Image generated by authors.

The study uses data from actual bus routes of 387 lines operating in Santiago, displayed in the left panel of Figure 3.8. The sequence of recorded stops by each bus line in that graph is projected onto the stylised network and converted into a sequence of nodes displayed in Figure 3.7.[2] Similarly, the metro network is simplified using actual data by Transantiago on current and future metro stations.[9] Each metro line in the right panel of Figure 3.8 is projected to the stylised network and converted into a sequence of nodes in Figure 3.7 with the same technique illustrated in endnote 2. That technique allows approximating the minimum number of line transits required when travelling between any pair of nodes in Figure 3.7.[3] The light rail network (Metrotren) is modelled as part of the metro network.

[9]When the travel survey was conducted in 2013, there were five metro lines in operation (lines 1, 2, 4, 4A and 5) as well as a light rail train (Metrotren). Since then, two additional metro lines have been added to the network (lines 3 and 6). By 2030, the government plans to extend lines 2, 3, 4 and 6 as well as to construct three additional metro lines (7, 8 and 9).

Figure 3.8. Actual bus and metro networks

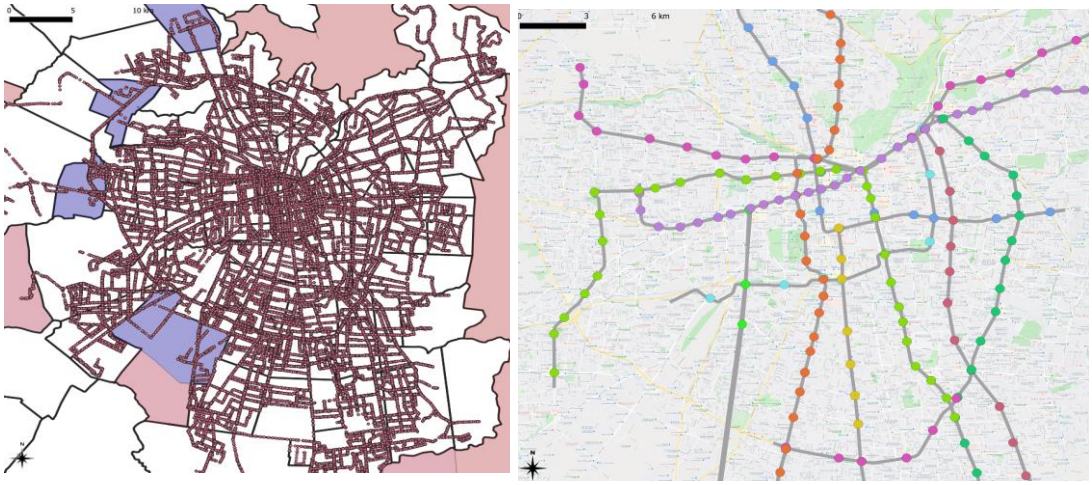

Note: Left panel: routes of bus network in operation in Santiago; right panel: the expanded network, as it is planned to be operational by 2030. *Source:* Images generated by authors.

Figure 3.9. Travel survey origins and destinations plotted and visualised with heat map

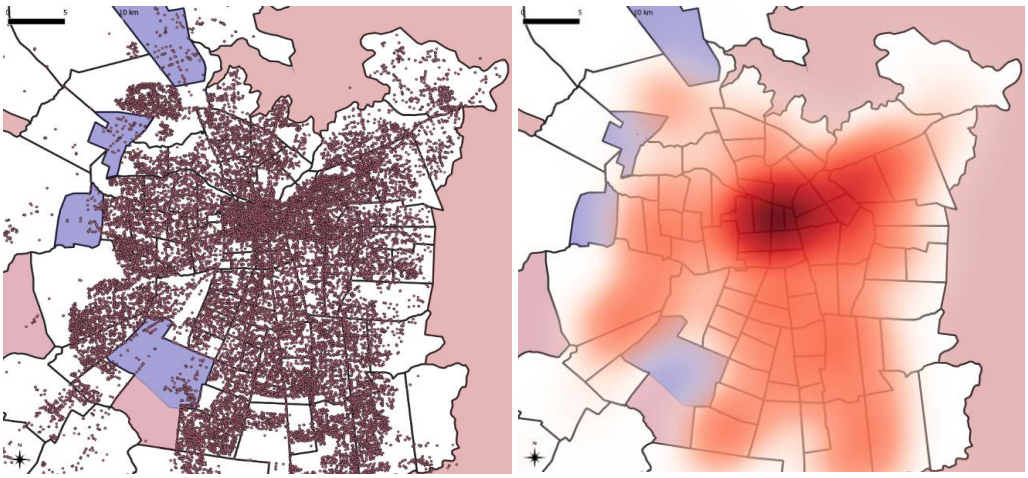

Notes: Polygons: uncoloured = residential; purple = industrial; pink = public lands; left panel: dots represent trip origins and destinations; right panel; trip origin and destinations density heat map.
Source: Observatorio Social (UAH) (2014[22]). Image generated by authors.

3.3. Modal split, car ownership and travel patterns

The study uses information from the travel survey conducted in Santiago in 2012-2013 to infer the general trends in mobility patterns (Observatorio Social (UAH), 2014[22]). The data contain 96 000 trips taken by 40 000 individuals. The origins and destinations of the trips included in the survey are visualised in Figure 3.9. The corresponding heat map of starting and ending trip points in the same figure indicates that Santiago is highly monocentric. The density and aggregation of population at the centre of the city is closely linked to the issue of air pollution. The density of trip origins and destinations declines with distance from the city centre, with a particularly large number of trips taking place in western and southern suburbs of the city.

The travel survey also contains information on the mode of travel, the time and purpose of the trip, as well as the age and manufacturer of the vehicle used. The age, employment status and income of the person travelling are also available. Trips in the following tables are grouped into three time categories: (i) on-peak period of a weekday, (ii) off-peak period of a weekday, (iii) weekends. The time intervals of each period are detailed in Table 3.6. The modelling work that is exhibited in subsequent sections further disaggregates weekend trips according to whether they took place on Saturday or Sunday.

Table 3.6. Time intervals of each period

On-peak weekday	All weekdays from 07:00 to 09:59 and from 16: 00 to 19:59.
Off-peak weekday	All weekdays from 10:00 to 15:59 and from 20:00 to 06:59.
Weekends	Saturday and Sunday from 00:00 to 23:59.

Trips are grouped into two categories based on their purpose. The first category consists of work-related and education-related trips, which involve regular or semi-regular commuting. Throughout the paper, these are referred to as L-trips and represent 52% of trips. The remaining 48% consists of non-commuting trips undertaken for miscellaneous purposes, such as shopping, recreation, errands and health-related purposes. These trips are grouped under the label O-trips.

To a large extent, the modal split of Santiago is transit oriented. Almost half of all trips (48%) are made by public transport. When trips are weighted by distance, the share of public transport grows even further, to 63%. The large majority of public transport trips are undertaken by Transantiago bus. Buses make up 83% of all single-mode trips undertaken by public transport. The role of private vehicles is also important, as they hold the second largest share of trips, approximately 32%, and account for 35% of the travelled distances (passenger kilometres). The vast majority of these trips are taken with personal vehicles. Non-motorised travel makes less than 20% of trips, with the larger part being walking (16%) and the smaller being biking (3.5%). When weighting by distance, the share of non-motorised modes in total passenger-kilometres travelled falls to 4%, as non-motorised trips are significantly shorter. The breakdown of trips by purpose, mode and time period is presented in Table 3.7.

Table 3.7. Modal split of passenger kilometres for all trips

Purpose	Mode	Period	Share of total trips	Share of total distance travelled
Work and education trips (L-trips)	Private vehicle	On peak weekday	8.83%	10.54%
		Off peak weekday	4.09%	5.14%
		Weekend	1.39%	1.90%
		Total	14.31%	17.58%
	Public transport	On peak weekday	18.84%	26.96%
		Off peak weekday	8.50%	13.25%
		Weekend	2.73%	4.22%
		Total	30.07%	44.43%
	Walking	On peak weekday	3.44%	0.56%
		Off peak weekday	1.76%	0.26%
		Weekend	0.30%	0.05%
		Total	5.50%	0.87%
	Biking	On peak weekday	1.36%	0.63%
		Off peak weekday	0.60%	0.26%
		Weekend	0.27%	0.14%
		Total	2.23%	1.03%
Other trip purposes (O-trips)	Private vehicle	On peak weekday	5.37%	3.83%
		Off peak weekday	6.95%	5.63%
		Weekend	5.57%	6.24%
		Total	17.89%	15.70%
	Public transport	On peak weekday	4.89%	5.10%
		Off peak weekday	9.02%	8.94%
		Weekend	4.37%	4.71%
		Total	18.28%	18.75%
	Walking	On peak weekday	3.12%	0.37%
		Off peak weekday	4.82%	0.55%
		Weekend	2.62%	0.31%
		Total	10.56%	1.23%
	Biking	On peak weekday	0.35%	0.11%
		Off peak weekday	0.48%	0.16%
		Weekend	0.31%	0.14%
		Total	1.14%	0.41%
Total			100%	100%

Note: Miscellaneous trip purposes include shopping, recreation, social and health related trips. Public transport includes journeys by metro, bus and shared taxi.
Source: Observatorio Social (UAH) (2014[22]).

The vast majority (92.7%) of the cars and motorbikes listed in the 2013 travel survey run on petrol, while 7.12% are diesel-powered. Less than 0.05% of the fleet is hybrid or electric. The mean age of vehicles in 2013 was 11 years. Stylised travel speeds are constructed by dividing the road and highway network into four types: rural roads, urban roads, rural highways and urban highways. Urban roads and highways lie within Santiago's city ring. Rural roads and highways lie beyond the city ring. Proxies for the average speed at each part of the network and time period are obtained using repeated draws from Google Maps.

Table 3.8. Vehicle speeds on different road and highway segments at different times

Period	Rural road	Urban road	Rural highway	Urban highway
Free flow	54.9	28.2	102.0	81.1
Weekday on-peak	44.1	14.2	74.4	53.7
Weekday off-peak	48.6	22.1	89.3	65.8
Weekend	51.0	21.3	93.9	68.0

Source: Generated by authors using Google Maps data.

Figure 3.10. Evolution of the Chilean electricity generation composition.

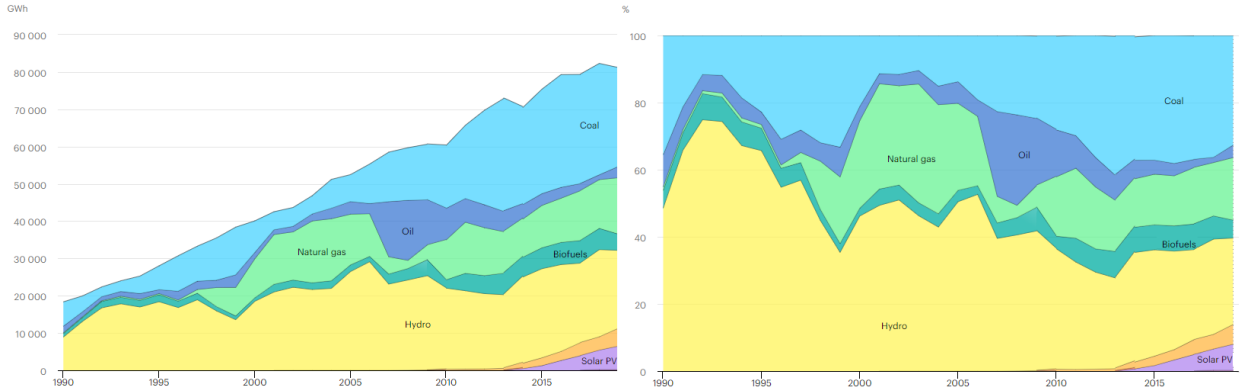

Source: Charts generated on the IEA website (www.iea.org).

3.4. Carbon intensity of electricity generation

In the past 30 years, the growth of the Chilean economy boosted energy demand. As a result, electricity generation has more than tripled (IEA, 2018[23]). Responding to the rapidly increasing demand has been achieved through expanding the use of coal. Figure 3.10 displays the evolution of total electricity generation and the contribution of various sources, both in aggregate (left panel) and relative (right panel) terms. The return to coal observed between 1993-1998 and 2003-2013 contributed to a steep increase in the carbon intensity of electricity generation. This is shown in Figure 3.11 which uses annual OECD (2015[24]) estimates on the carbon dioxide embodied in a kilowatt-hour (kWh) of electricity. The same figure displays an adjusted time series of the 5-year index provided by IEA (2020[25]). Despite surging between 2003 and 2013, the relative contribution of coal in the electricity mix has now stabilised. The contribution of wind and solar energy sources increases at a constant pace since 2012, signalling an upcoming decrease in the emission intensity of the grid. The projected emission factors used in this study are a conservative version of the carbon intensity predicted under IEA's Stated Policy Scenario for Chile. That is, the study assumes a substantial decrease in the carbon intensity of electricity generation between 2020 and 2050. This is displayed by the dashed curve in Figure 3.11, where the amount of CO_2 embodied in a kWh decreases in a linear fashion, from 0.4 kg/kWh in 2020 to 0.28 kg/kWh in 2050. These projected values fall within the range of values that the emissions factor attained from 1990 to 2020. Its plausibility depends on the degree to which the various pledges, intentions and commitments of the country will be accompanied by improvements in energy efficiency.[10]

[10]The country has committed to reducing total greenhouse gas emissions by 30% below the 2007 level by 2030 under the Paris Agreement (UNFCCC, 2015[49]). To achieve this in a context of growing electricity demand, renewables are targeted to account for 60% of the electricity mix by 2035 and for 70% by 2050.

Figure 3.11. Past and future CO_2 intensity of the Chilean electricity generation.

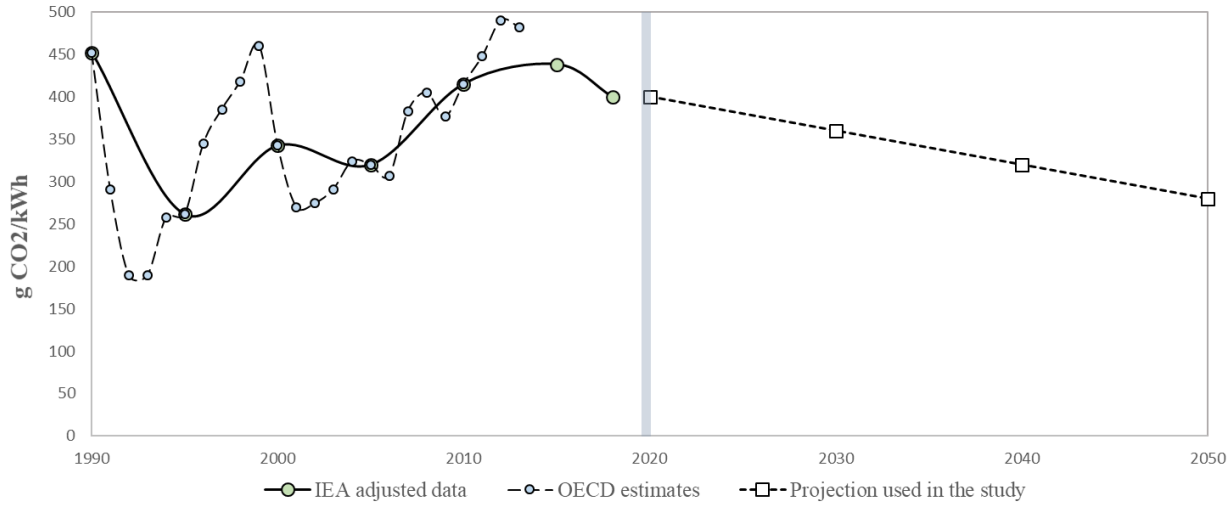

Notes: The data of annual frequency are obtained by the OECD (2015[24]); the 5-year index on the carbon intensity of power generation (IEA, 2020[25]) approximates the CO_2/kWh at year t relative to 2020, and thus equals 100 in 2020. Here, the IEA series is pre-multiplied with $\alpha_{2020}/100$, where α_{2020} is CO_2/kWh in year 2020 in the OECD time series. Thus, the level of the IEA series is adjusted to the OECD observations. Graph generated by the authors.

3.5. Technological evolution in cars

The model allows various vehicle technologies with different degrees of vintage to overlap. At any year t, car owners choose one vehicle from the set $\mathcal{V}_t$, which contains vehicle classes differentiated by fuel type and by the period at which the vehicle was introduced in the market. With respect to fuel type, the differentiation regards diesel, gasoline and electric vehicles. With respect to age, the model incorporates a gasoline car from the pre-Euro era, and one representative car for every decade from 1990 to 2050. That gives rise to 34 vehicle classes with partially overlapping lifecycles, as displayed in Table 3.9.

The fuel economy of gasoline and diesel vehicles evolves according to a negative exponential model, while the fuel economy of electric vehicles is predicted using a logarithmic model.[4] The evolution of fuel economy is displayed in Figure 3.12.

Table 3.9. Model representation of filtering technologies in internal combustion engine vehicles.

Category	Introduction period	Simulated lifecycle [c]
Internal combustion		
Pre Euro [a]	1970-1990	2020
Euro I & II [b]	1991-2000	2020
Euro III & IV [b]	2001-2010	2020, 2030
Euro V & VI [b]	2011-2020	2020, 2030, 2040
Future technology I [b]	2021-2030	2030, 2040, 2050
Future technology II [b]	2031-2040	2040, 2050
Future technology III [b]	2041-2050	2050
Electric		
Current technology	2011-2020	2020, 2030, 2040
Future technology I	2021-2030	2030, 2040, 2050
Future technology II	2031-2040	2040, 2050
Future technology III	2041-2050	2050

Notes: [a] Only gasoline; [b] Gasoline and Diesel; [c] Years at which the vehicle appears in the simulation; Table generated by the authors.

Figure 3.12. The evolution of average fuel economy

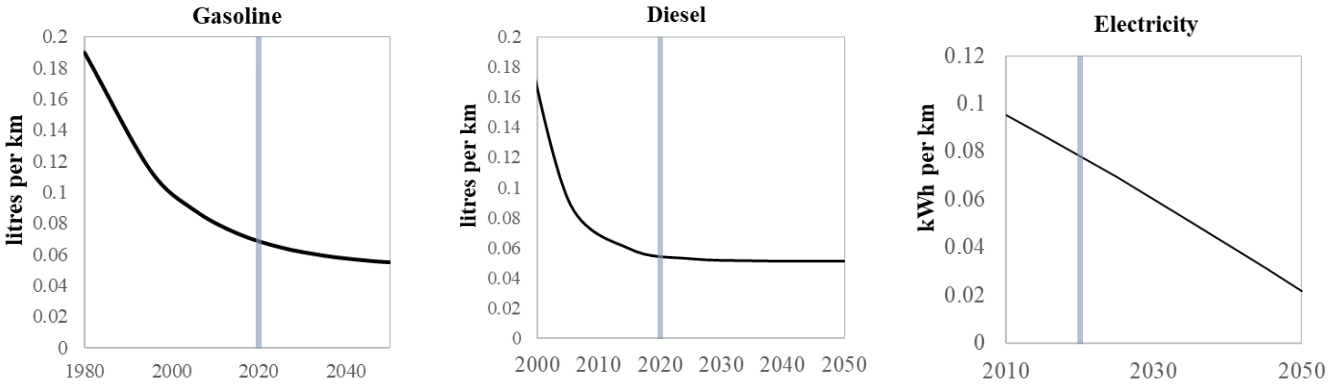

Notes: Graph generated by the authors.

The study uses projections for the emission factors of CO, VOC, NO_X, N_2O, NH_3 and $PM_{2.5}$ of future internal combustion engine cars. The key input is the historical evolution of emission factors reported by the European Environment Agency (2019[10]) for gasoline and diesel cars that entered the market from the pre-Euro era up to 2019. The study tests different models to fit these data, adopting the one that yields the most plausible within-sample prediction. Then, the current rate of progress, as well as its evolution across different decades are used to compute future emission factors. These do not only reflect recent technological progress, but the rate at which innovation in filtering has evolved during the whole period spanned by the sample. This allows a recent slowdown in innovation to further reduce the pace of technological change in the future, yielding a conservative projection.[5]

Figure 3.13. The evolution of emission factors in gasoline and diesel vehicles

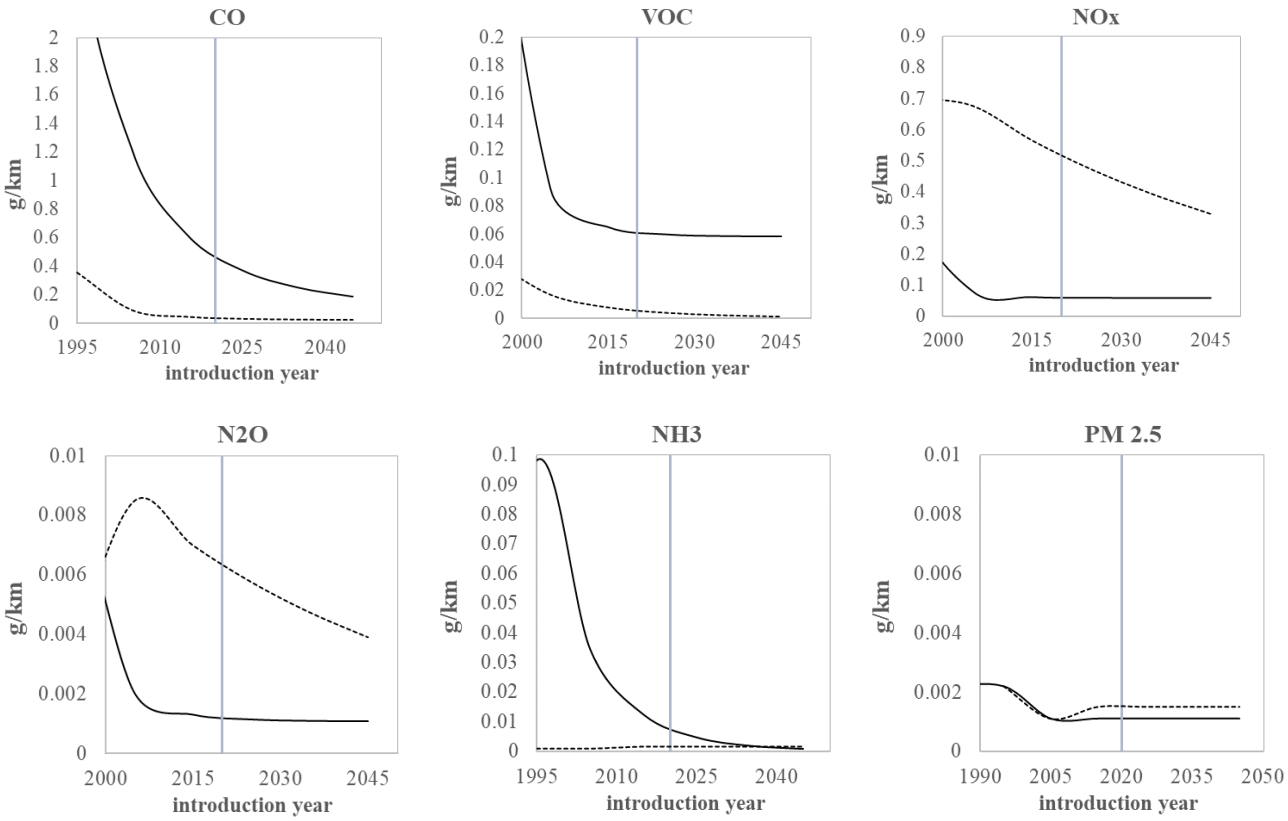

Notes: Solid curves represent gasoline cars; dashed curves represent diesel cars; a year estimate refers to the emission intensity of vehicles produced that year, not to the emission intensity of the active fleet of private cars that year. Graph generated by the authors.

3.6. Technological evolution of public transport vehicles

The study provides mid-term (2020-2030) and long-run (2030-2050) projections for the emission levels expected from a representative bus. The projection is based on bus fleet data from Santiago provided by the Directory of Metropolitan Public Transport. The DTPM dataset reports the size of the bus fleet by emission level between 2012 and 2018. This dataset allows to approximate the share of each filtering technology in the bus fleet. Currently, the fleet is dominated by Euro 3, Euro 5 and Euro 6 buses, as together these categories comprise 97% of the fleet. The DTPM dataset is complemented with crude information from open sources. The merged data enable the extraction of trends on the evolution of the share of Euro 3, Euro 5 and Euro 6 buses in the fleet between 2012 and 2020. As Euro 6 buses were introduced only recently to the bus fleet of the city, the market share for these buses is estimated only from 2016 to 2018.

Figure 3.14. Estimates on past and mid-term future composition of bus fleet

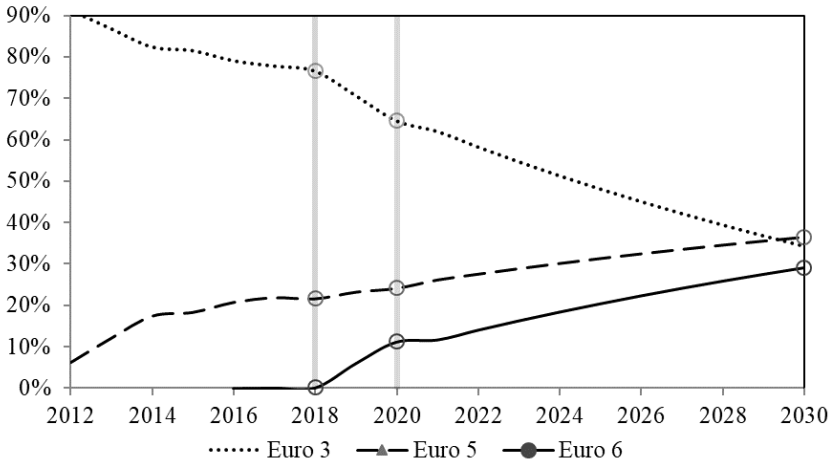

Notes: Graph generated by the authors.

The mid-term projection for the bus emission factors is based on a mid-term projection of the shares of the three bus categories. It assumes that the emissions factors of these three technologies (i.e. Euro 3, Euro 5, and Euro 6) remain fixed between 2020 and 2030. However, the emission intensity of the average bus with an internal combustion engine still evolves. This occurs because the emissions factors of the representative conventional bus are modelled as weighted averages of the emission factors of Euro 3, 5, and 6 buses. Figure 3.14 shows that these weights should be expected to drastically change in the mid-term, altering the expected emission intensity of the public bus fleet. Once again, using the estimates for the average emission factors of Euro 3, 5, and 6 buses provided by the European Environment Agency (2019[10]) yields the averages reported in Table 3.10.[6]

Table 3.10. Expected emissions of an average conventional bus in the mid-term.

Years	CO	VOC	NO_X	N2O	NH3	PM 2.5
2018	2.1277	0.3232	7.9823	0.0079	0.0047	0.1713
2020	1.8037	0.2720	6.8736	0.0129	0.0055	0.1451
2030	1.0622	0.154723	4.5205	0.0237	0.007639	0.088551

Notes: Authors' own calculations. Table generated by the authors.

The long-run projection of the emission factors extrapolates the information in Table 3.10. The projection does not make any restricting assumption about the composition of the fleet or the future filtering technologies that will be available from 2030 on.

Figure 3.15. Estimates on past and mid-term future composition of bus fleet

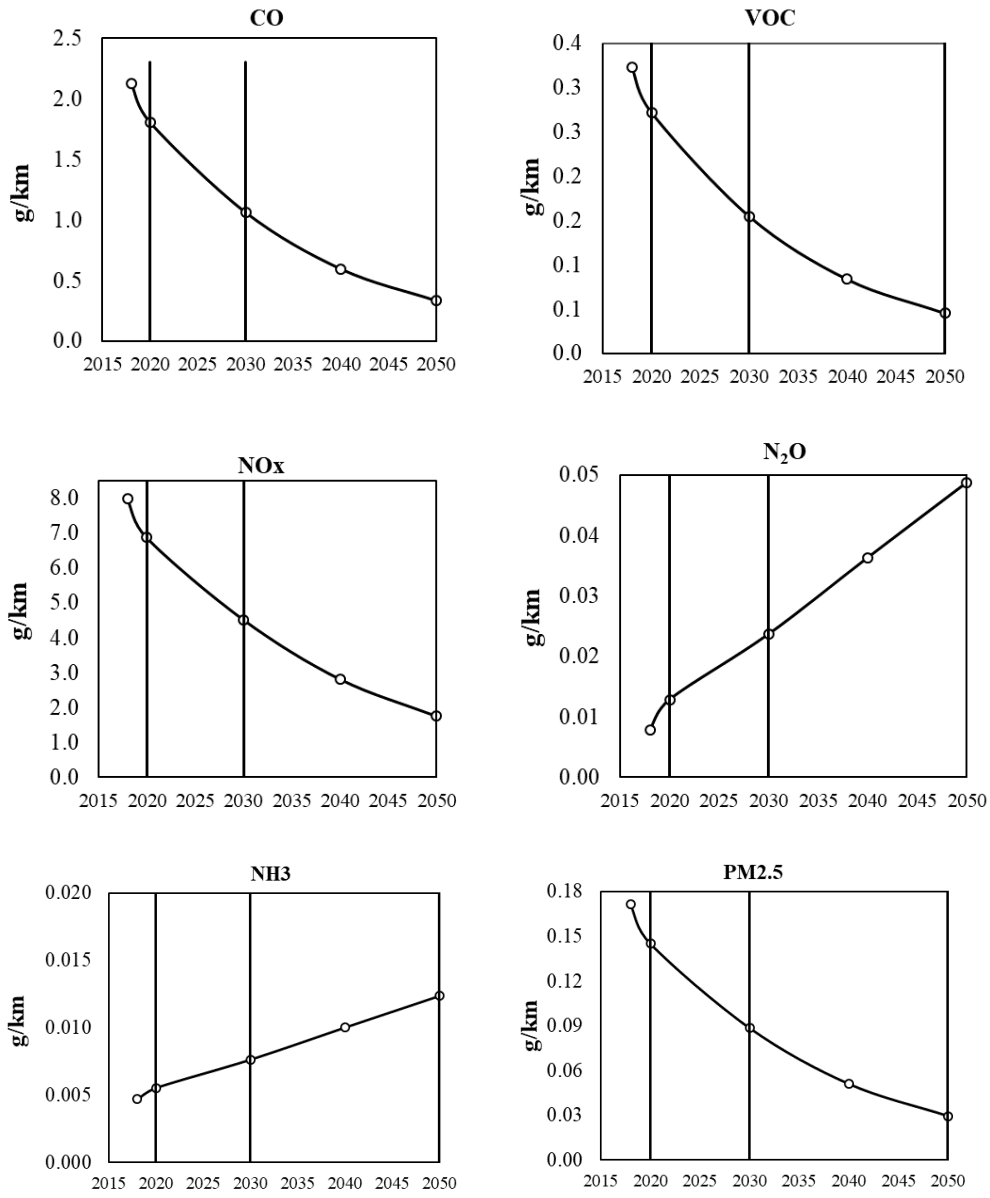

Notes: Graphs generated by the authors.

Finally, the study uses projections about the future diesel consumption of conventional buses, as well as the electricity consumption of future buses and metro wagons. These projections are displayed in Figure 3.16. There is currently limited information on the historical evolution of the fuel efficiency of diesel buses. The study obtains an estimate on the fuel consumption of different bus categories using data from the Ministry of Transport and Telecommunications of Chile.[11] It then uses a similar methodology to that proposed for projecting the future emissions of the bus fleet to also project bus fuel consumption.

[11]The Chilean Ministry of Transport and Telecommunications provides yearly data on the characteristics of the new buses entering the fleet at https://www.mtt.gob.cl/. These data are used to obtain the fuel consumption in litres/100 km for Euro 3, Euro 5 and Euro 6 buses.

Figure 3.16. Assumed energy consumption of public transport vehicles in the simulation

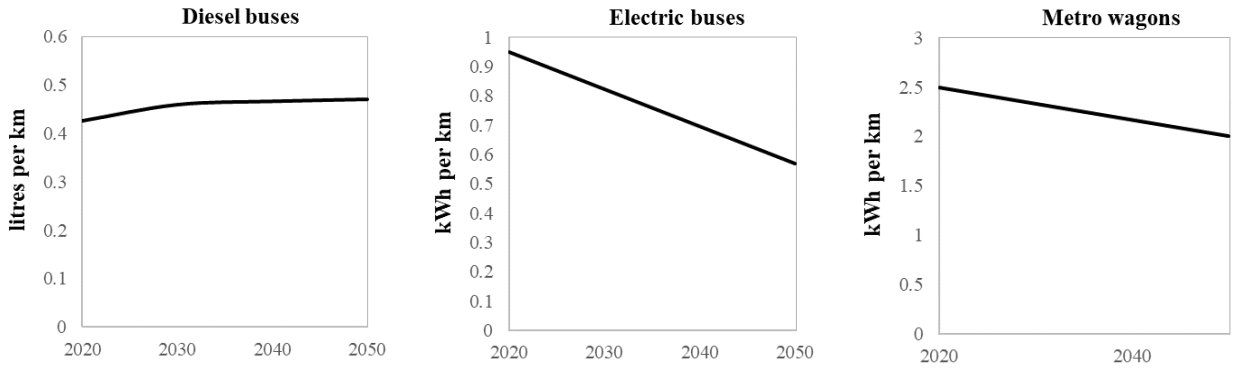

Notes: Graphs generated by the authors.

To project the electricity consumption of a metro wagon per kilometre, the study uses historical observations on (i) the total electricity consumption of metro trains[12] and (ii) the total number of wagon kilometres materialised each year[13] in the period 2013-2019. The electricity consumption of a wagon kilometre is approximated by dividing the former by the latter. The projection in the right panel of Figure 3.16 is conservative because the estimated electricity consumption displays limited variation.

[12]Data are obtained from the 2015 and 2019 Sustainability Reports of the Chilean state company Metro S.A, which operates the metro in Santiago. The sustainability reports are available at: https://www.metro.cl/documentos/reporte_sostenibilidad_metro_2019.pdf.

[13]Annual metro wagon-kilometres are obtained from annual Management Reports of the Directory of Metropolitan Public Transport (DTPM), which publishes these data on a yearly basis. The Management reports can be found here: http://www.dtpm.cl/.

4 Results

This section presents the findings from the application of OECD model MOLES in Santiago. It details the results from simulating the *reference* scenario, as well as the five *counterfactual* policy scenarios outlined in Section 3.

Figure 4.1. Predicted evolution of car ownership and fleet size in reference scenario.

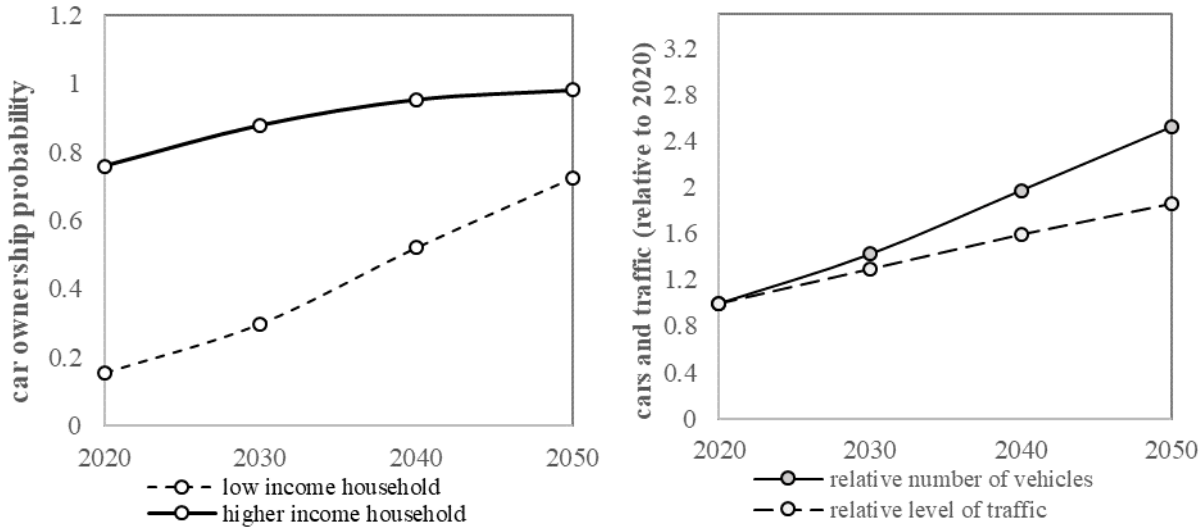

Notes: Dotted circles on all curves mark the years at which the simulation experiments are performed. Right panel: the vertical distance between the solid and dashed curve can be attributed to congestion feedback effects, which discourage a portion of the trips. The model overestimates these effects, as road capacity is held constant throughout the entire time window of the simulation. Graph generated by the authors.

4.1. Results from simulating the reference scenario

The reference scenario predicts a steep increase in the ownership of private vehicles in the first two quartiles of the income distribution. The left panel of Figure 4.1 displays the predicted evolution of car ownership by households of relatively low and high income. The probability that a random individual from the low-income group owns a car quintuples within the time horizon of the simulation. The car ownership rate in high-income groups begins from a relatively saturated level and grows at a slower pace. In the terminal year of the simulation, almost every individual with income above the median will have access to a private vehicle.[14] In the same year, the car ownership status of low-income groups will resemble that of high-income groups today.

[14]The study does not make any explicit assumptions about shared schemes that go beyond the traditional within-household ownership model. In general, a proliferation of shared car ownership schemes would imply a smaller fleet size, flattening the curves in the right panel of Figure 4.1. The degree to which such ownership schemes can be cost saving in contexts where time constraints strongly correlate across households (e.g. similar working hours) is currently unknown.

The projected evolution of car ownership implies a growing fleet size and larger traffic volumes. Combining the predicted demand for private vehicles with the projected population change yields the evolution of the car fleet size in Santiago. This is displayed by the solid curve in the right panel of Figure 4.1, relative to the corresponding fleet size in 2020. The aggregate traffic, measured in vehicle kilometres travelled relative to 2020, has also a clear positive trend. However, the growth rate of traffic is substantially lower than that of the fleet size, as the model accounts for the feedback effect of congestion on the number of generated trips.

The baseline simulation offers several insights about the possible lifecycle of current and future vehicles in Santiago. Euro 5 and 6 gasoline cars possess the largest market share in the benchmark equilibrium, i.e. year 2020. This share will steadily fall, and will have considerably shrank by 2030. The simulation accounts for a new representative vehicle technology entering the car market every decade, with characteristics detailed in Section 3. In 2050, future technologies are projected to dominate the market. Moreover, the model predicts that electric vehicles of various technologies will gradually gain considerable momentum, accounting for 25% of the fleet in 2050.

Figure 4.2. Predicted lifecycle of current and future vehicle technologies.

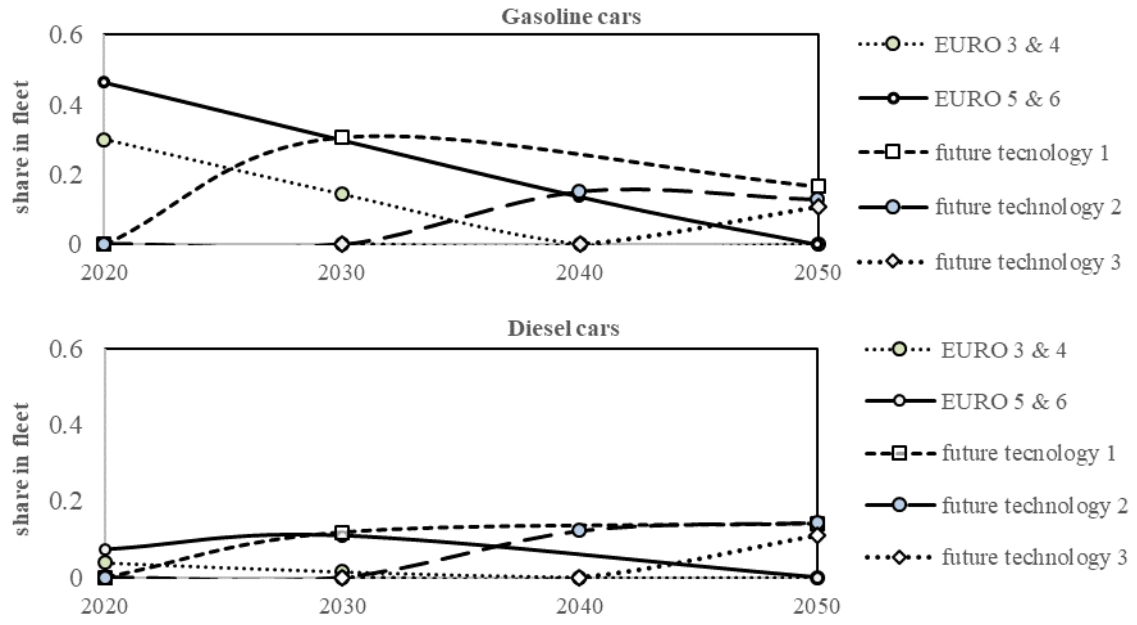

Notes: Graphs generated by the authors. Dotted circles on all curves mark the years at which the simulation experiments are performed. The model does not account for the secondary vehicle market. The lifetime of each category is exogenous, but the market share of each active vehicle class is endogenous.

The series displayed in Figure 4.1 and Figure 4.2 as well as the technological progress in cars and buses laid out in Section 3 have implications on the emissions of the urban transport system. Figure 4.3 presents the amount of CO_2 and several air pollutants emitted by cars and buses within the time window of the simulation.

Carbon dioxide (CO_2) emissions are modelled as linear functions of fuel consumption. Therefore, the analysis does not account for carbon capture technologies that could enter the market in the future. There are various opposing forces contributing to the slight reduction in aggregate CO_2 emissions, *i.e.* 6% lower than the current level in 2050. Vehicle fuel efficiency improves in all cars and metro wagons. Barriers in the adoption of electric vehicles fade out and a substantial portion of the bus fleet electrifies. Furthermore,

electricity generation becomes less carbon intensive. On the other hand, population growth, income growth and the rebound effects of technological change prevent the deep decarbonisation of the city's transport system. Emissions of sulphur dioxide (SO_2) are also proportionally related to fuel combustion, thus they follow a similar path to those of CO_2.

Figure 4.3. Predicted evolution of transport emissions relative to their level in 2020.

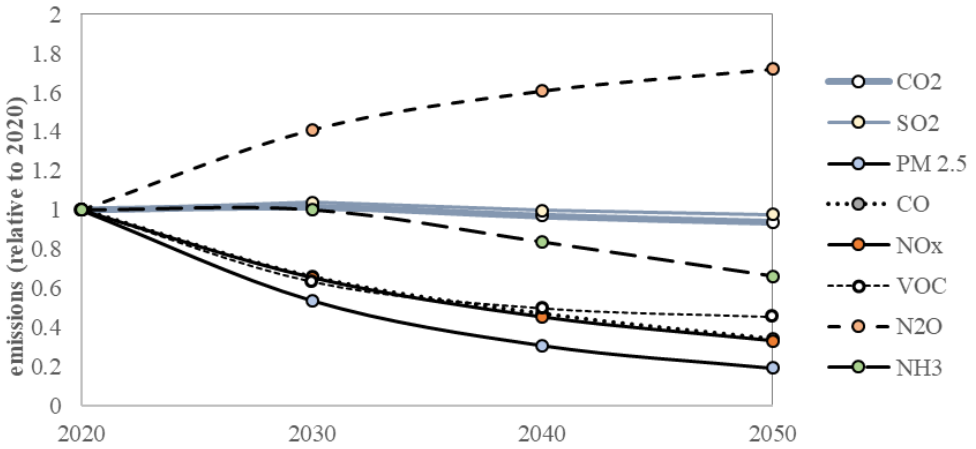

Notes: Graphs generated by the authors.

Unlike CO_2, the emissions of most air pollutants examined in the paper exhibit a clear negative trend. Carbon monoxide (CO), nitrogen oxides (NO_X) and volatile organic compounds (VOC) follow a similar, steeply declining trajectory. The main driver behind this trend is the constantly improving filtering technology incorporated in cars and buses. Available data indicate an immense progress achieved between the last generation of cars and those of the pre-EURO or early EURO era. This progress is not confined to fuel efficiency, but extents to the capacity of pollutant-retaining filters incorporated in cars. The progress in filtering capacity of buses is also large, but less remarkable compared to that observed in cars. The simulation is based on conservative projections of filtering technology detailed in Section 3.

Future cars and buses in Santiago will emit only a fraction of the CO, NO_X and VOC that they emit today. Despite that, the aggregate emissions of the future vehicle fleet will still be far from zero, ranging between 33% and 45% of the levels calculated for 2020. The main offsetting factors are the speed at which the fleet modernizes, as well as its growing size. The former factor introduces a delay effect, since technical progress in filters takes years to be reflected in the fleet composition. The latter factor has also a negative impact, since a growing fleet implies a larger base of emitters.

The model estimates that the dominant share of exhaust $PM_{2.5}$ emissions currently originate from buses, despite the fact that the largest portion of traffic is generated by private vehicles. The reason for this disproportional contribution is that the present bus fleet is relatively old. A relatively old diesel bus is estimated to emit up to 130 times the amount of $PM_{2.5}$ of a modern EURO 5-6 car. However, its ridership is estimated to be approximately 20 times that of a car. This implies that the $PM_{2.5}$ footprint of a passenger-kilometre served by an old diesel bus is much greater than that served by a modern car. The estimate has important policy implications, as it highlights a potential trade-off regarding policies that promote the use of public transport. That is, switching a passenger from car to bus could reduce her personal contribution

to congestion by 85%; but with a bus fleet composed of old vehicles, this switch may substantially increase the $PM_{2.5}$ footprint of this passenger.[15]

The outlook of aggregate exhaust $PM_{2.5}$ emissions from Santiago's transport sector is promising, as the model predicts a decrease of more than 80% by 2050. This mainly stems from the projected technological progress in bus filtering technology, which is expected to eradicate 78% of the exhaust $PM_{2.5}$ a conventional bus emits. At the same time, the reference scenario assumes that roughly 15% of the bus fleet in 2050 will be electric. As a result of this combination, the average bus in the city will be producing only 19% of the $PM_{2.5}$ it currently generates. The data do not enable a similar projection for the progress in car filtering technology, which appears to have plateaued. The $PM_{2.5}$ reduction displayed in Figure 4.3 could shrink to a number below 40% if non-exhaust $PM_{2.5}$ emissions are factored in. These emissions currently account for approximately 50% of primary $PM_{2.5}$ and are persistent to a switch in electromobility. Furthermore, they increase as the aggregate level of traffic increases.

The paths of nitrous oxide (N_2O) and ammonia (NH_3) emissions qualitatively differ from the counterparts of other air pollutants. The former is projected to decrease in future cars but also to increase rapidly in buses. The model predicts that the aggregate level of N_2O emitted by the transport sector will be 72% higher than its current level. Additionally, the share of transport modes in the generation of N_2O is projected to drastically change. While the share is estimated to be currently balanced between buses and cars, buses will be producing 77% of N_2O in the future. Emissions of NH_3 exhibit a negative trend, which is nevertheless different from that of CO, VOC and NO_X. As is possibly the case with N_2O, technical progress in the filtering technology of cars coincides with a less stringent regulatory framework regarding the NH_3 filtering technology of buses. The former contributor prevails, giving the trajectory of relative NH_3 the shape it has in Figure 4.3.

[15]For instance, with an off-peak ridership of 15%, and a bus maximum capacity at 60 people, the $PM_{2.5}$ emission per passenger kilometre in a diesel bus can be more than 11 times higher than that in a EURO 6 car.

Figure 4.4. The e-distribution of CO and VOC and its intertemporal evolution

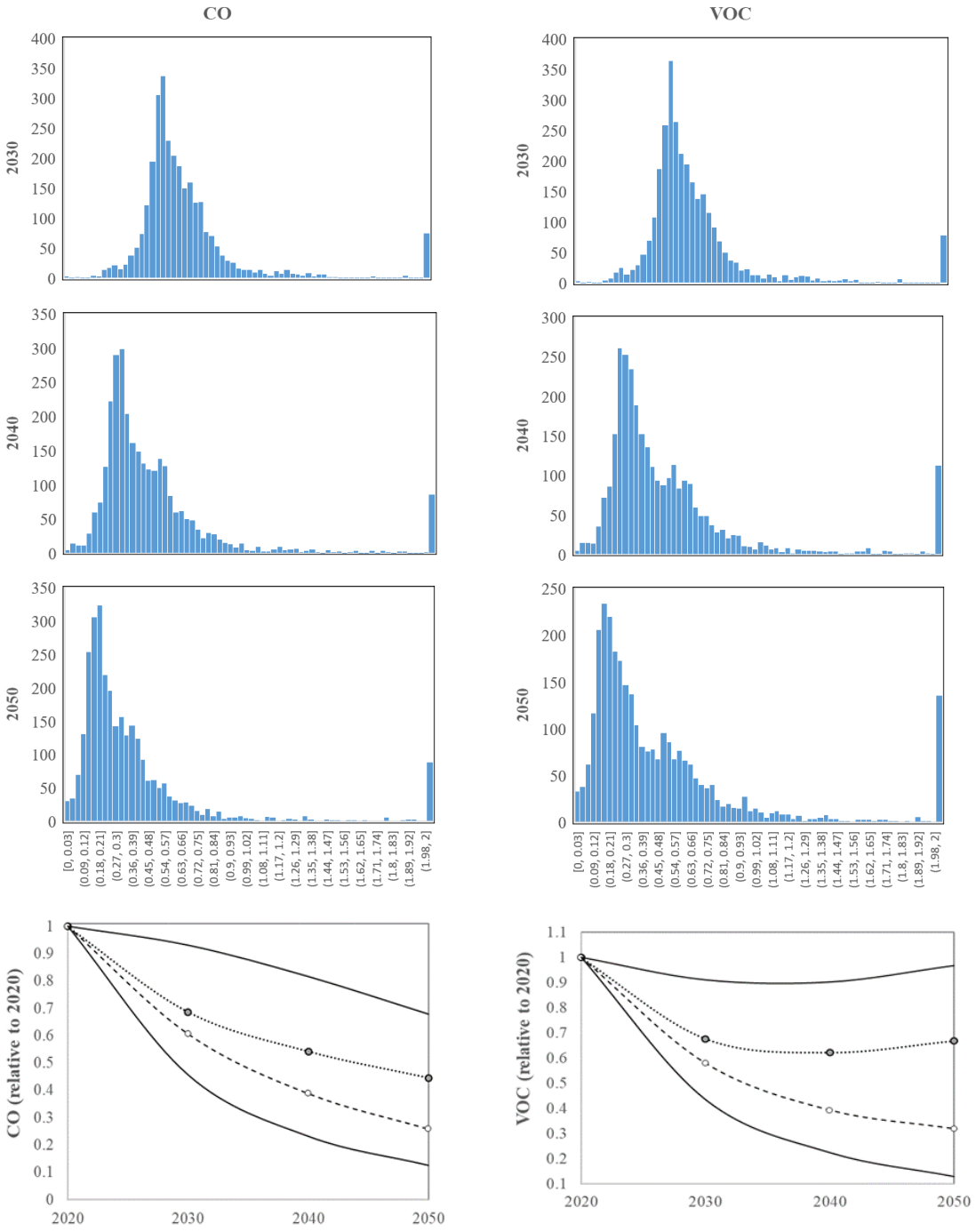

Notes: Graphs generated by the authors. Horizontal axis in histograms is expressed in relative emissions ($e_{B,t}$). The lowest panels encapsulate the evolution of mean, median, 10th and 90th percentile and are replicated from Figure 4.5.

The change in emissions will not occur in a uniform manner across space. The model considers approximately 750 unidirectional links and four time periods within a typical week. Therefore, it accounts for emissions in at least 3000 pairs of locations and time points. Denoting the amount of pollutant e emitted

in location x in year t by $e(x,t)$ allows to benchmark it with respect to the corresponding emission in year 2020. The benchmarked emission is:

$$e_{B,t}(x) = \frac{e(x,t)}{e(x,2020)}, \qquad (4.1)$$

and can be treated as a random variable which has a different *spatial distribution* for every year included in the simulation. This distribution is referred to as the *e-distribution of pollutant x in year t*. Figure 4.4 shows how the e-distribution evolves in the cases of CO and VOC. All histograms are displayed upon the same range of $e_{B,t}$, from 0.0 to 2.0.[16] The bar at the edge of this range indicates the relative frequency of all locations where $e_{B,t}$ values exceed the value of 2.0. This is the probability that in a random location the emission of pollutant e in year t will be at least two times its level in 2020. The graphs suggest that this probability is far from negligible, and constitutes the main reason for which the mean of the e-distribution deviates upwards from the respective median.[17] The threshold value of 1.0 is also critical in the e-distributions displayed in Figure 4.4**.** Locations in which $e_{B,t}$ falls short of this value experience a decrease in emission levels in year t, compared to 2020. The histograms indicate that the vast majority of locations are falling in this category and will thus be better off in all future years.

Due to the intertemporal evolution of the e-distribution, its mean, median and percentiles also evolve across the years. The lower panel of Figure 4.4 summarises in a single graph the evolution of these statistics from the histograms in 2030, 2040 and 2050. Figure 4.5 displays the same statistics for all six pollutants examined in the paper (CO, VOC, NO_X, $PM_{2.5}$, N_2O and NH_3). The e-distibutions of all pollutants in year 2020 are degenerate, as $e_{B,2020}(x)$ is by definition equal to one. The median, 10th and 90th percentile of the e-distribution of pollutant x in year t express the percentage of that pollutant that is "still emitted" in the *median, 10th and 90th percentile locations* in year t. To find these values for a given year t, locations are ranked according to the fraction in (4.1). In this ranking, locations in which the emissions of pollutant x in year t is relatively low (compared to 2020) precede locations in which emissions are relatively high. The 10th percentile location, median location, and 90th percentile location are denoted by $x_t^{0.1}$, x_t^M and $x_t^{0.9}$. For instance, the x_{2030}^M of CO is 0.606, implying that the amount of CO emitted in the median location of Santiago in 2030 is predicted to be 60.6% of the respective amount of CO emitted in the same location in 2020.[18]

Figure 4.5 suggests that the emissions of CO, VOC, NO_X and $PM_{2.5}$ in the median locations will see declines in emissions over time. These trends qualitatively resemble to, but quantitatively differ from, those displayed for aggregate emissions in Figure 4.3.

[16]The e-distribution has a lower bound of zero since emissions cannot be negative.

[17]However, the vast majority of the locations falling in this category are peripheral areas where emission levels were relatively low in 2020. A major limitation of centring the spatial analysis on the distribution of $e_{B,t}(x)$ across locations x is that $e_{B,t}(x)$ is particularly sensitive to low values of $e_{B,2020}(x)$.

[18]Stated mathematically, $CO_{B,2030}(x_{2030}^M) = \frac{CO(x_{2030}^M, 2030)}{CO(x_{2030}^M, 2020)} = 0.606$.

Figure 4.5. Evolution of means, medians and percentiles of e-distribution

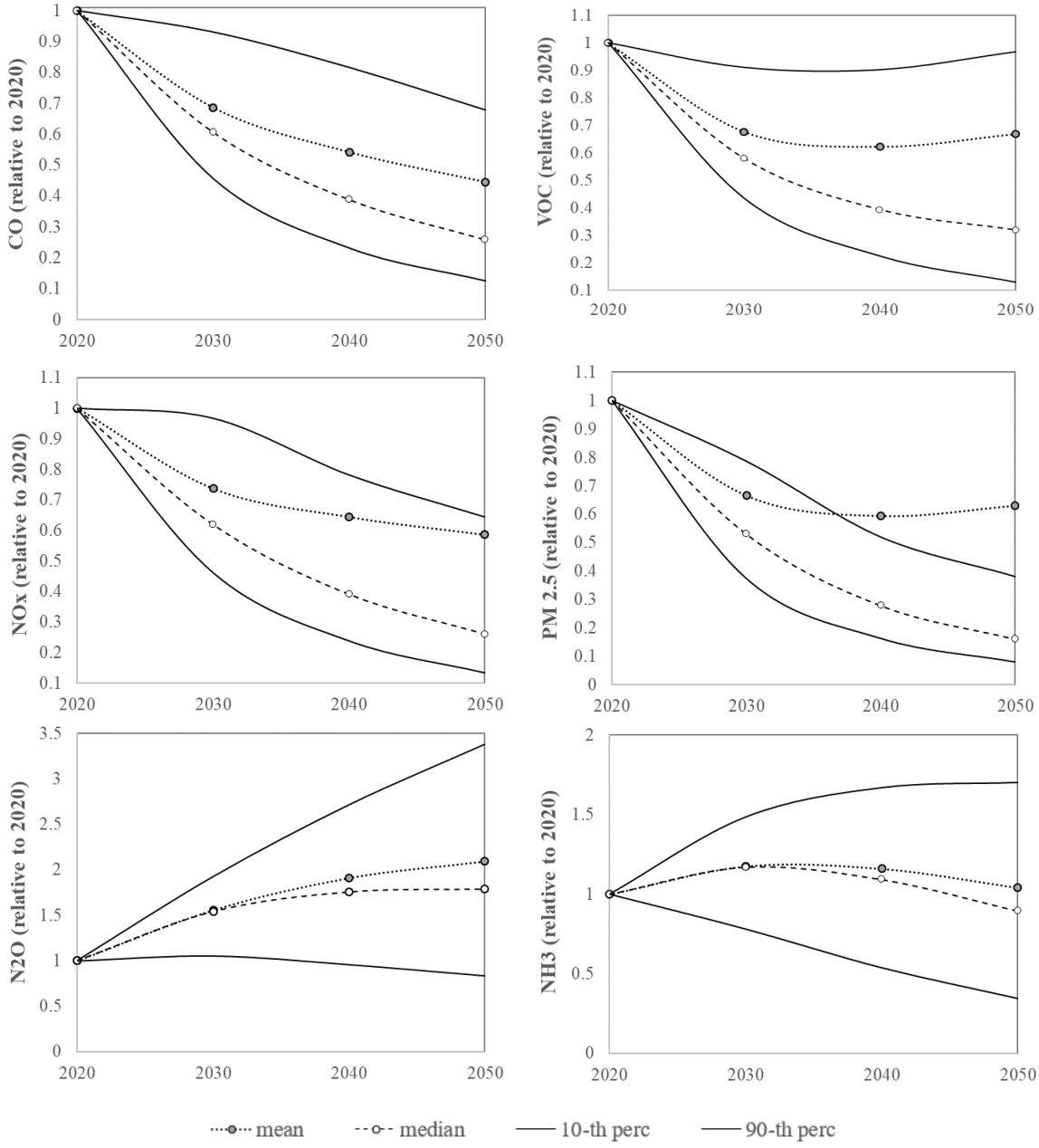

Notes: Graphs generated by the authors.

The 10th and 90th percentile of the *e*-distribution contain information about how heterogeneously the various locations will be affected by the changes in emission levels that take place over time.[19] Figure 4.5 reveals that this variation is significant with respect to all pollutants. For instance, while CO emissions in 2030 are predicted to be 40% lower than 2020 in the median location of the city, this reduction will exceed 54% in

[19]That holds insofar the spatial distribution of emissions correlates with that of concentrations. The model does not incorporate any biophysical module for translating emissions to concentrations.

at least 10% of locations in the city.[20] Additionally, 90% of locations will experience a reduction of at least 7%.[21] The evolution of the 90th percentile reveals that the large majority of locations will see an overall reduction in CO, NO_X, VOC and $PM_{2.5}$ in the years to come. This implies that projected emissions reductions are likely to occur in a spatially inclusive way.

The preceding analysis focused on the relative amount of air pollutants emitted at the various locations in the model. The change in emission levels in a given location x, here predicted by $1 - e_{B,t}(x)$, constitutes only an initial indication of expected change in human exposure to air pollution in location x. Obtaining informed estimates of the latter requires information on the population density in location x and an emissions-transportation model. The latter uses weather conditions, morphological variables, as well as the physical and chemical properties of each pollutant to predict how emitted amounts move, concentrate and disperse across space and time. However, the complexity of such an endeavour is considerable and goes beyond the scope of this paper. In particular, it requires a model that generates one high frequency time-series (rather than a set of time-averaged annual figures) for each location x and each pollutant.

4.2. Results from simulating the counterfactual scenarios

Figure 4.6 shows the outcome of the modelled policy interventions on aggregate CO_2 emissions. One of the most distinct findings is the key role that *rapid bus electrification* program could play in decarbonising urban transport. Its impact on emissions at the time horizon of the simulation is substantial. By 2050, this measure can diametrically alter the composition of diesel and electric buses in the active fleet. Approximately 65% of buses will be electric, a figure that lies far above the corresponding share of electric buses in absence of the policy, i.e. 15%. In combination with the considerable share of public transport in the city's modal split, such a shift could eliminate 28% of the CO_2 emitted in 2050 under the reference scenario. The corresponding figure for year 2040 is also considerable, i.e. 17%. However, the mid-term impact of the program is substantially smaller, as time constitutes a key element in the implementation of the policy.[22] In line with that, CO_2 emissions will be 7% lower in 2030, and approach the levels predicted by the reference scenario for the very short run. The decarbonisation effect of electrifying public transport could possibly be accelerated with additional policy interventions increasing the modal share of public transport without generating a steep increase in travel demand.[7]

[20]That is, $CO_{B,2030}(x_{2030}^{0.1}) = \frac{CO(x_{2030}^{0.1},2030)}{CO(x_{2030}^{0.1},2020)} = 0.457$, implying a change of -54.3%.

[21]That is, $CO_{B,2030}(x_{2030}^{0.9}) = \frac{CO(x_{2030}^{0.9},2030)}{CO(x_{2030}^{0.9},2020)} = 0.93$, implying a change of -7.0%. Thus in 10% of locations, emissions between 2020 and 2030 will either increase or go down by a maximum of 7.0%.

[22]The programme is based upon a higher frequency of replacing an old diesel bus that exits the fleet with an electric bus, rather than a new diesel bus. The rate at which the stock of public buses depreciates is identical in all scenarios. Therefore, time is required in order to substantially increase the share of electric buses in the fleet. See Section Results for a detailed description of the policy and its impact on the bus fleet composition over time.

Figure 4.6. Aggregate CO_2 emissions across different scenarios

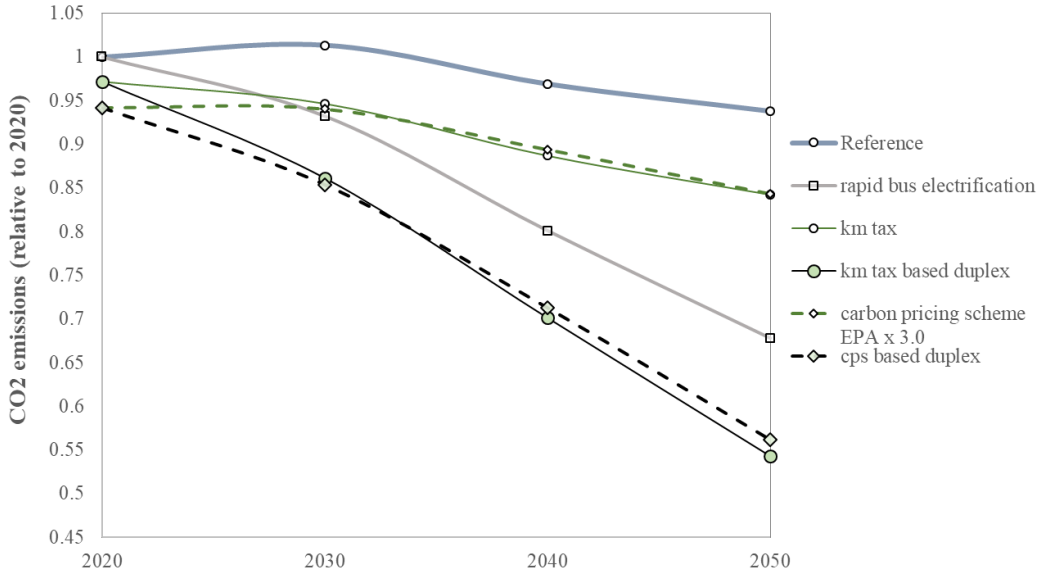

Notes: Graphs generated by the authors. Reference emissions in year t are expressed in relative terms as: $e_t^R = \hat{e}_t^R / \hat{e}_{2020}^R$, where $\hat{e}_t^R$ denotes nominal emissions at year t. Emissions associated with any policy i are also expressed relative to $\hat{e}_{2020}^R$, i.e. $e_t^i = \hat{e}_t^i / \hat{e}_{2020}^R$.Thus $e_t^i / e_t^R = \hat{e}_t^i / \hat{e}_t^R$.

In the short-run, only the tax-based policies outlined in Section 3 can cause a noticeable deviation of CO_2 emissions from their reference level. The *enhanced carbon pricing scheme* imposes a tax on all fuels used in the transport system, i.e. gasoline, diesel and electricity, that is proportional to their carbon content. This has an immediate mitigation impact of 6%. The *vehicle-distance tax scheme* has a smaller short-run mitigation potential, as it sets out with fairly low kilometre charges for the vast majority of the vehicles in the fleet. The addition of a more rapid bus electrification programme has no immediate effect on the decarbonisation potential of the two instruments. The reason is the lag between the launch of the policy and the year at which a substantial portion of the bus fleet becomes electric. The mechanics underlying this time lag, and the pace at which the policy matures are detailed in Section 3.

In the mid-term and long-run, the CO_2 mitigation potential of both policy interventions increases, but remains moderate. Both instruments cause a decrease in CO_2 emissions of approximately 7% in 2030, 8% in 2040 and 10% in 2050, where all of these reductions are expressed as deviations from the corresponding emissions in the reference scenario. The decarbonisation potential of rapid bus electrification is reinforced when the program is combined with the two tax schemes. Up to 3% of CO_2 emissions reductions can be attributed to the combined implementation of the electrification program and a tax scheme, but not to either of the two separately. This *reinforced effect* occurs because the examined tax schemes increase the share of public transport in the modal split, which in turn increases the net decarbonising potential of bus electrification.[8]

Figure 4.7. Aggregate CO and VOC emissions across different scenarios

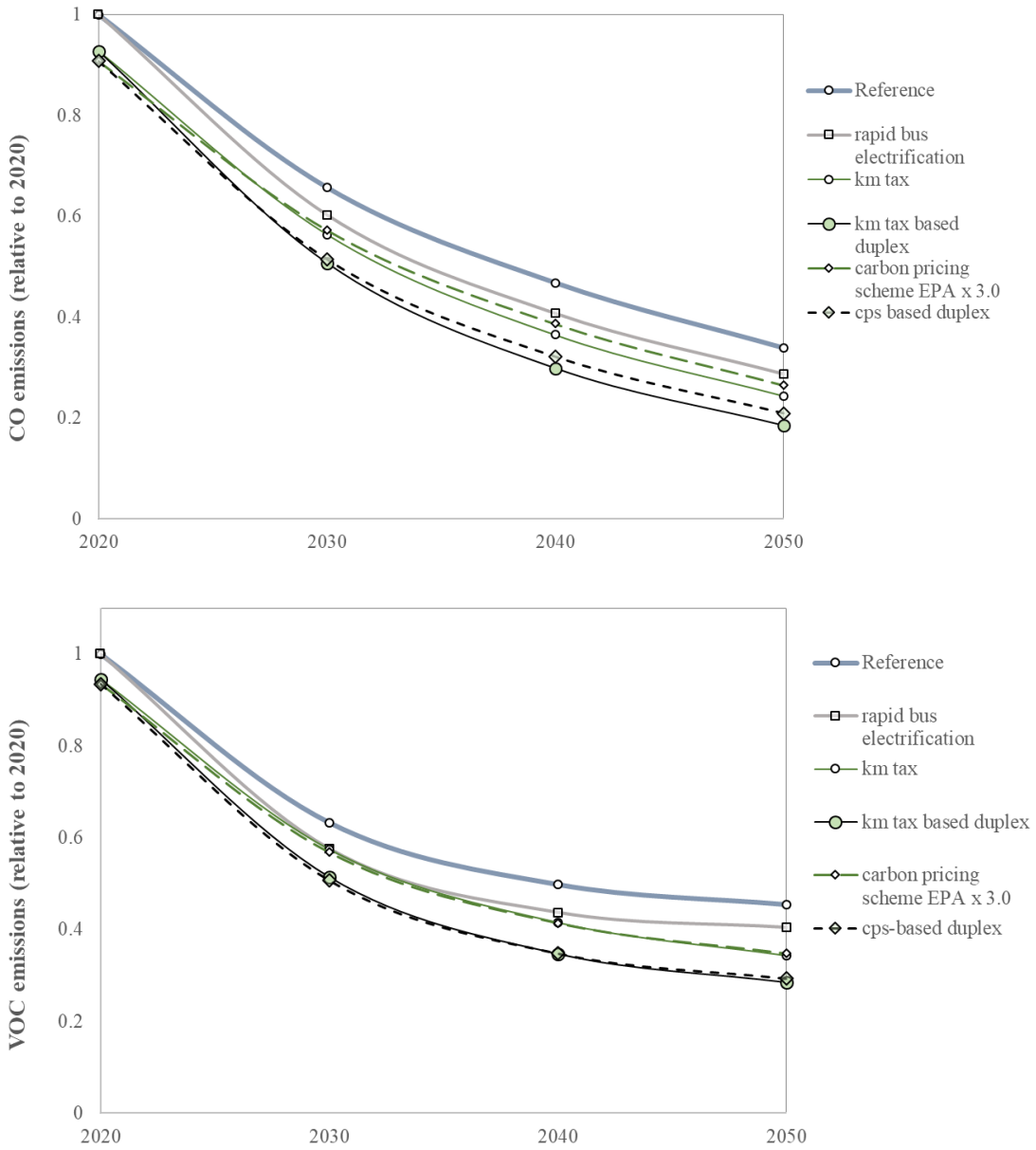

Notes: Graphs generated by the authors. Reference emissions in year t are expressed in relative terms as: $e_t^R = \hat{e}_t^R / \hat{e}_{2020}^R$, where $\hat{e}_t^R$ denotes nominal emissions at year t. Emissions associated with any policy i are also expressed relative to $\hat{e}_{2020}^R$, i.e. $e_t^i = \hat{e}_t^i / \hat{e}_{2020}^R$.Thus $e_t^i / e_t^R = \hat{e}_t^i / \hat{e}_t^R$.

The impact of the various policies on aggregate CO and VOC emissions differs qualitatively and quantitatively from that on aggregate CO_2 emissions. Unlike the rigid trajectory of CO_2 emissions in the reference scenario, CO and VOC are predicted to substantially decrease even in the absence of policy interventions. Therefore, the discussed tax-based policies do not qualitatively alter the trend in these emissions, but rather accelerate their projected decrease.

From a quantitative viewpoint, the effects of policies on CO emissions differ substantially from those regarding CO_2. The rapid electrification of buses is predicted to mitigate 15% of CO emissions by 2050, *vis-à-vis* the reduction of 28% predicted for CO_2 emissions. On the other hand, the two tax schemes have

a much larger mitigating impact on CO than on CO_2. The main driver of this finding is that CO emission factors decrease much faster in buses than in cars. This is diametrically opposite to the evolution of the relative CO_2 intensity between cars and buses. This finding may have important implications, as it indicates that the environmental relevance of policies promoting public transport becomes much greater when their anti-pollution properties are considered. As shown in Figure 4.7, the promotion of public transport through the two tax schemes explored in the study could substantially reduce CO, even without a rapid electrification programme. As the impact of policies on aggregate VOC emissions resembles that of CO, the two graphs are jointly presented in Figure 4.7. The only noticeable difference pertains to the efficiency of the two tax-based schemes, which have an almost identical impact on VOC emissions.

Figure 4.8. Aggregate NOX emissions across different scenarios

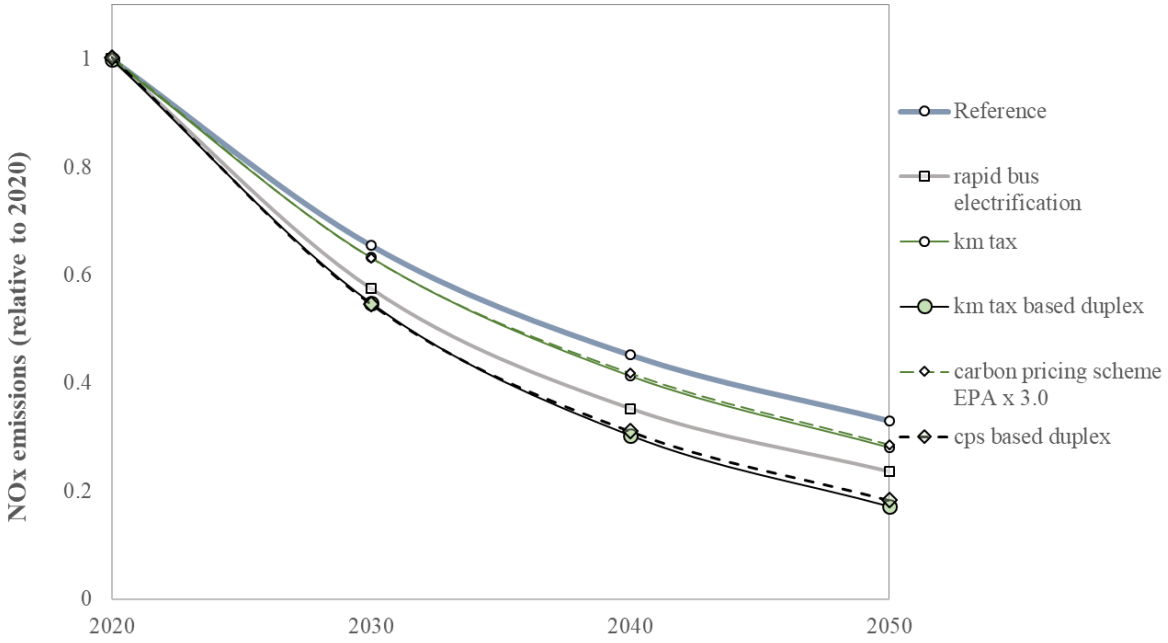

Notes: Graph generated by the authors. Reference emissions in year t are expressed in relative terms as: $e_t^R = \hat{e}_t^R / \hat{e}_{2020}^R$, where $\hat{e}_t^R$ denotes nominal emissions at year t. Emissions associated with any policy i are also expressed relative to $\hat{e}_{2020}^R$, i.e. $e_t^i = \hat{e}_t^i / \hat{e}_{2020}^R$.Thus $e_t^i / e_t^R = \hat{e}_t^i / \hat{e}_t^R$.

The trajectory of NO_X emissions under the various scenarios is similar to that of CO and VOC, but the long-run role of bus electrification in curbing these emissions is more pronounced. The main driver of this difference is the projected evolution of NO_X emission factors, i.e. the amount of NO_X emitted per kilometre driven by future cars and buses. The projections indicate that NO_X filtering technologies in diesel buses will continue improving but not at an increasing rate, while the corresponding technologies in cars seem to have exhausted a considerable part of their potential. These two preconditions imply that policies promoting the use of public bus, such as the two tax schemes, will continue to have a mitigating effect. However, that effect will be smaller compared to the effect of bus electrification initiatives.

Figure 4.9. Aggregate $PM_{2.5}$ emissions across different scenarios

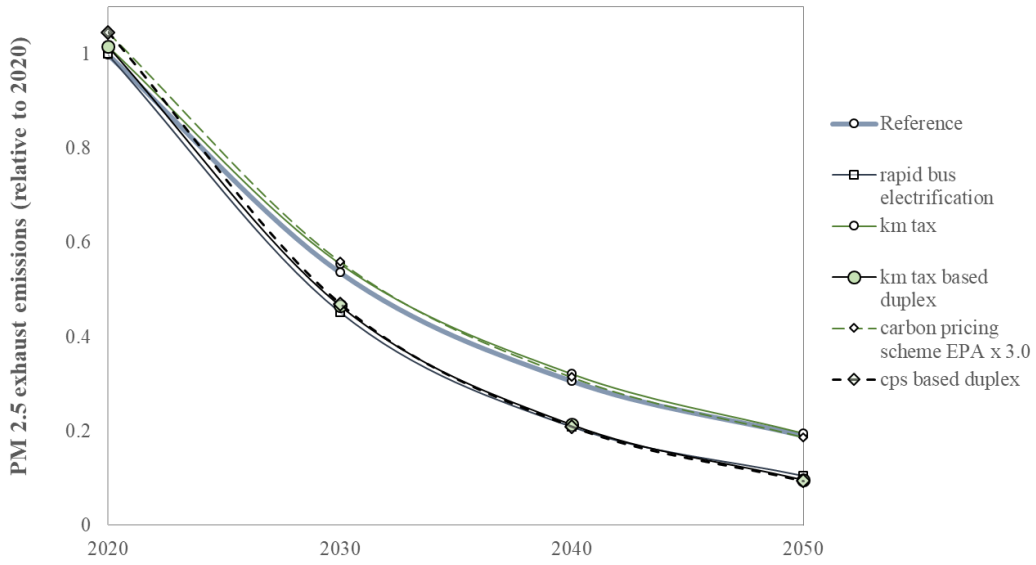

Notes: Graph generated by the authors. Reference emissions in year t are expressed in relative terms as: $e_t^R = \hat{e}_t^R / \hat{e}_{2020}^R$, where $\hat{e}_t^R$ denotes nominal emissions at year t. Emissions associated with any policy i are also expressed relative to $\hat{e}_{2020}^R$, i.e. $e_t^i = \hat{e}_t^i / \hat{e}_{2020}^R$.Thus $e_t^i / e_t^R = \hat{e}_t^i / \hat{e}_t^R$.

Another quantitative variation of the results regards the benefits from the bus electrification programme in in terms of $PM_{2.5}$ emissions reductions. The programme will decrease CO_2, CO, VOC and NO_X, but will cause a larger drop in $PM_{2.5}$ emissions. This occurs because public transport holds a widely different share in the emissions of the various pollutants. Importantly, the bus fleet currently generates the lion's share of transport-related exhaust $PM_{2.5}$, but is responsible for a much smaller portion of the other pollutants. Therefore, accelerating bus electrification is of higher priority for $PM_{2.5}$ emissions. Faster bus electrification is expected to eliminate 50% of the remaining tailpipe $PM_{2.5}$ emissions, while its mitigation impact on other pollutants ranges between 10% and 30%.

Furthermore, the impact of the two tax schemes on tailpipe $PM_{2.5}$ diverges from their impact on other pollutants. In the short run, both policies promote the use of public transport and are expected to increase the number of bus kilometres in the city. Despite reducing the emissions of CO, VOC and NO_X, such a shift to public transport increases $PM_{2.5}$ emissions in the short run. This occurs because the amount of tailpipe $PM_{2.5}$ generated by a bus passenger kilometre is much bigger than the respective amount generated by a car passenger kilometre. Current evidence suggests that this ratio is bound to change. However, that will only occur gradually, as the modernisation of bus fleets is typically far from instant.[23] The slower this change, the weaker the confidence that the two tax-based policies will have a mitigating impact on $PM_{2.5}$ in the long run. This stands in contrast with their considerable potential to curb CO_2 and air pollutants other than $PM_{2.5}$.

[23]It is estimated that in 2050 a diesel bus kilometre will generate 22 to 30 times the amount of $PM_{2.5}$ generated by a random gasoline car.

Figure 4.10. Aggregate $NH_{2.5}$ and N_2O emissions across different scenarios

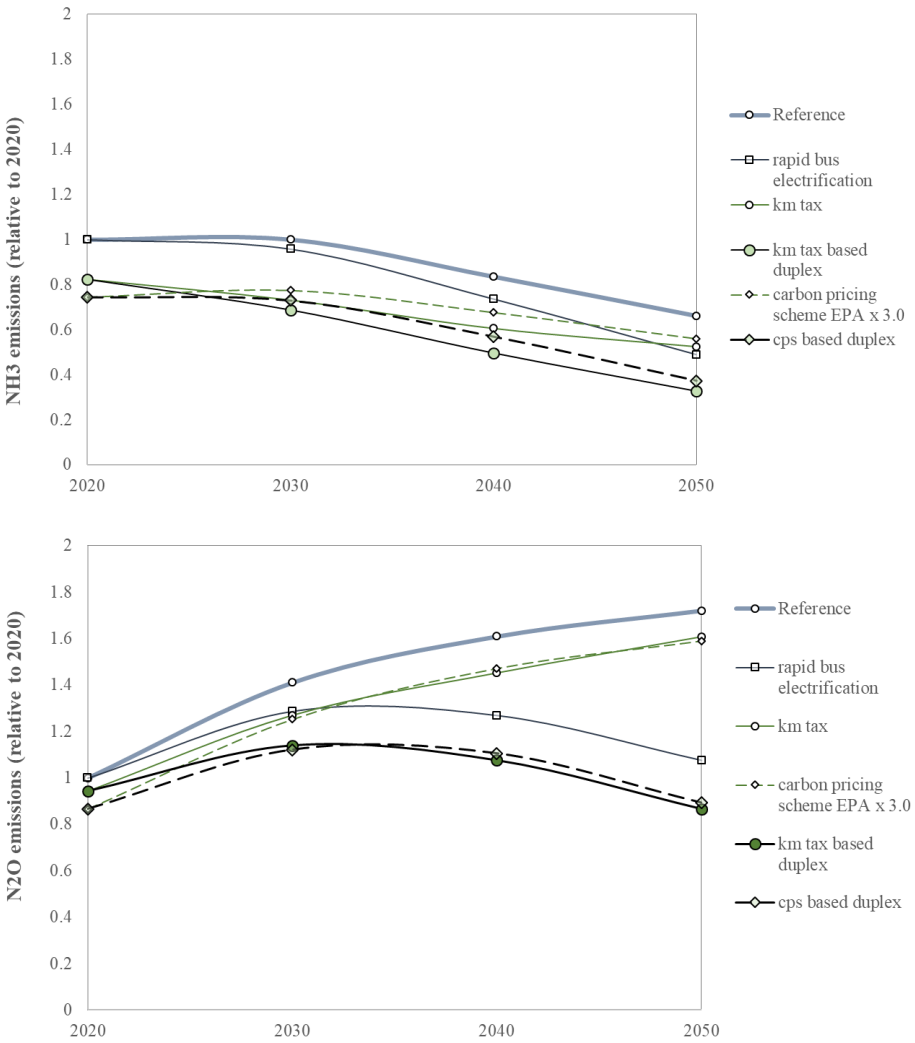

Notes: Graph generated by the authors. Reference emissions in year t are expressed in relative terms as: $e_t^R = \hat{e}_t^R / \hat{e}_{2020}^R$, where $\hat{e}_t^R$ denotes nominal emissions at year t. Emissions associated with any policy i are also expressed relative to $\hat{e}_{2020}^R$, i.e. $e_t^i = \hat{e}_t^i / \hat{e}_{2020}^R$. Thus $e_t^i / e_t^R = \hat{e}_t^i / \hat{e}_t^R$.

Furthermore, the two tax schemes may play an important role in curbing emissions of pollutants whose business-as-usual trajectory is more resistant to technological progress. Emissions of NH_3 and N_2O possibly constitute two such examples, for reasons elaborated in Section 3. In both cases, the proposed tax schemes can be effective in eliminating 5-25% of these emissions. The role of bus electrification is particularly pronounced in the case of N_2O, as current evidence indicates a potential increase in the corresponding emission factors of conventional buses. In this case, rapid bus electrification can prevent a "technological regression" of this kind, independent of its cause.

4.3. First-order welfare effects and distributional impacts

The carbon pricing scheme and the kilometre tax examined in the paper affect different population cohorts in different ways. The total welfare effect of any policy discussed in the paper would incorporate the monetized benefits or losses from the resulting change in CO_2 and air pollutants. In case of a tax-based policy, such a calculation would also account for the interactions that the tax would trigger with the rest of the fiscal system, in particular the labour market.[24] Finally, if that policy pertained to an infrastructure investment, the welfare measure would also incorporate the monetized social cost of raising the necessary funds in order to finance it. However, many of these involved inputs are subjective. For instance, there are no universally accepted marginal social costs corresponding to the emissions of the various air pollutants examined in the study. To avoid relying on highly subjective inputs, the following analysis is based on the calculation of a *partial welfare measure* for the two tax schemes examined earlier. The two components of this measure are detailed below.

Figure 4.11. Monetised gains from travel time savings

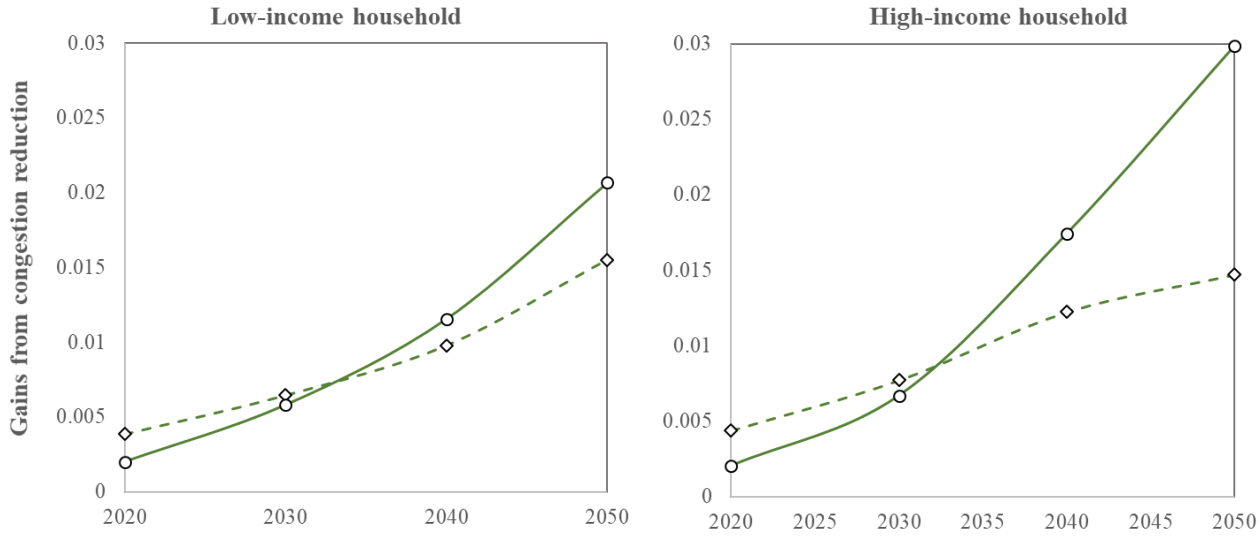

Notes: Solid line: carbon pricing scheme; dashed line: kilometre tax schemes.

The first component of welfare measures the gains from the policy-induced *congestion relief*. Both the carbon pricing scheme and the kilometre tax cause a reduction in traffic congestion, as they discourage the use of private cars and decrease the overall travel demand. This translates into travel time savings, which generate a welfare benefit. Figure 4.11 shows the evolution of the monetised gains from congestion relief for each cohort and policy. These gains are expressed as shares of net total income, i.e. after-tax labour income. The benefit grows over time, as the level of traffic increases and the willingness to pay for time savings, i.e. the value of travel time, grows. This upward trend becomes steeper over time, as congestion increases at a faster rate than the fleet size and travel demand. However, the model overstates the potential time benefits, since it does not account for future investments in road infrastructure that could possibly mitigate part of the increasing congestion. The result is that the monetised gains from congestion

[24] Some contributions focusing on the interaction between an externality tax in the transport system and the labour tax are: Parry and Bento (2001[61]), Tikoudis, Verhoef and van Ommeren (2015[58]), Tikoudis (2020[60]) and Hirte and Tscharaktschiew (2020[62]).

relief range between approximately 0.2% and 0.7% of income in the short run, and between 1% and 3% of income in the long run. Relative welfare gains are similar across the two cohorts examined. However, once these gains are expressed in nominal terms, they are four to five times greater for the high-income group.

The second welfare component is the *change in net tax burden*, i.e. the total change in the private budgets induced by the policy. That is, the net tax burden in year t, for an individual in cohort c, under scenario x is: $N_{x,t,c} = E_{x,t,c} - L_{x,t,c}$. This is the difference between the individual's total tax expenditure, $E_{x,t,c}$, and the received lump-sum transfer, $L_{x,t,c}$. The change in *net tax burden* induced by replacing the reference scenario with policy scenario p in year t is:

$$\Delta N_{p,t,c} = N_{p,t,c} - N_{REF,t,c} = \underbrace{\left(E_{p,t,c} - E_{REF,t,c}\right)}_{\substack{\text{change in tax} \\ \text{expenditure}}} - \underbrace{\left(N_{p,t,c} - N_{REF,t,c}\right)}_{\substack{\text{change in lump-sum} \\ \text{transfer}}}.$$

Figure 4.12. Change in net tax burden induced by the two tax schemes

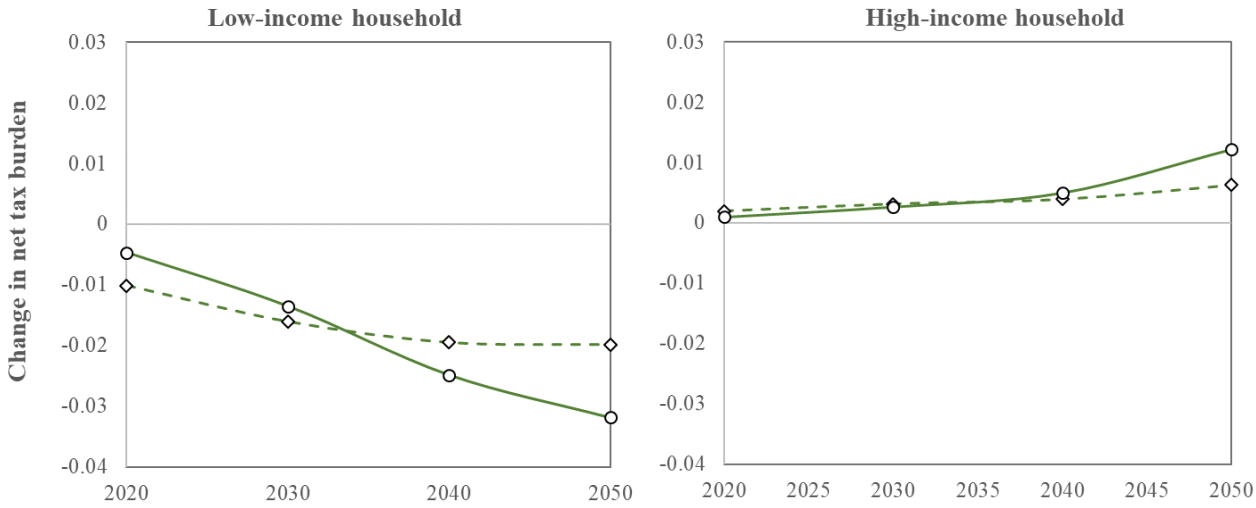

Notes: Solid line: carbon pricing scheme; dashed line: kilometre tax schemes.

The introduction of the policy scenario changes the net tax burden of an individual in cohort c through two channels. Directly, it changes the amount of tax expenditure. In the context of this paper, both the carbon pricing scheme and the kilometre tax tend to increase this expenditure. This occurs because the explored taxes are heavily based on car use, and the latter has limited elasticity with respect to these taxes. Therefore, the first component of $\Delta N_{p,t,c}$ is positive for all cohorts, but is much larger in the high-income cohort. This occurs because cars are predominantly owned by individuals in the high-income group, at least in the benchmark year. Indirectly, the introduction of a tax-based scheme horizontally increases the lump-sum transfer provided to all individuals by the same amount.

The evolution of the net tax burden is depicted in Figure 4.12. In all years of the simulation, both the carbon and the kilometre tax lead to an increase in the net tax burden of higher income individuals, as car ownership is relatively higher in these groups and the revenue recycling mechanism is horizontal. The net tax burden for the high-income cohorts sets out at 0.1% of income in 2020, and reaches values between 0.5% and 1.2% in 2050. This increase occurs because both taxes grow faster than income. In contrast, the net tax burden of low-income group sets out from a negative value and becomes smaller. This occurs because the redistributed tax revenue grows faster than the contribution of the low-income group to the

two tax-schemes. In that sense, both tax-based schemes are *progressive*, and their progressivity increases over time.

Both schemes improve the welfare of both cohorts. Figure 4.13 displays the *first-order monetised welfare gain* of the two tax-based schemes. This is the difference between the monetised gains from managing congestion externalities, displayed in Figure 4.11 and the change in the net tax burden, displayed in Figure 4.12. Each group benefits from the policies for a different reason. The welfare of the high-income group increases due to reduced congestion and the corresponding savings in travel time. In contrast, the low-income cohort benefits primarily from the revenue recycling mechanism and from the fact that its contribution to the two taxes is limited, at least in the short run.

Figure 4.13. First-order welfare gains of cohorts from the two tax schemes

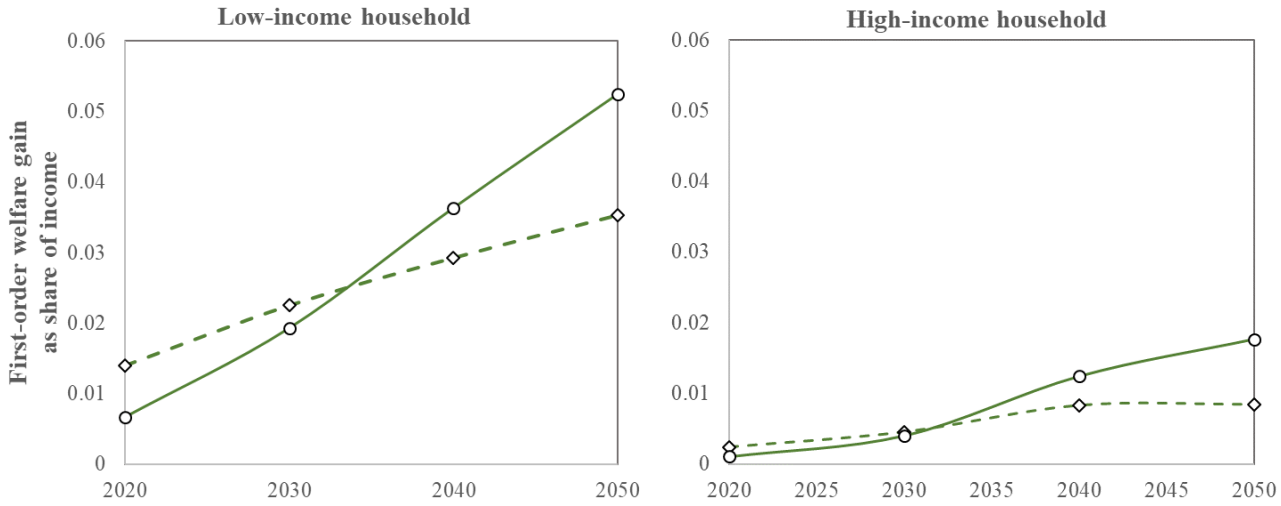

Notes: Solid line: carbon pricing scheme; dashed line: kilometre tax schemes.

The findings from the above analysis have three implications. First, the two tax-based schemes are expected to increase welfare in all population cohorts. This result holds even before the monetized gains from carbon savings and air pollution reduction are factored in. Second, both schemes are progressive, as the bases of the two taxes are determined by the use of cars, which are overwhelmingly owned by the high-income cohort. Finally, the revenue-recycling component is a necessary condition for the aforementioned achievements.

4.4. Policy analysis

The overlap between the causes of climate change and air pollution imply that there is considerable scope to manage these two issues simultaneously. In the case of urban transport, the link between the two is inextricable, as local air pollutants and greenhouse gases are both emitted from the combustion of fossil fuels. To a large extent, the analysis indicates that policy efforts to reduce air pollution could have a substantial synergistic effect in mitigating climate change, and *vice versa*. This does not stem from the dual nature of specific air pollutants, which can behave as or be precursors to greenhouse gases.[25]

[25]For example, air pollutants such as black carbon and methane, a precursor of ground-level ozone, also contribute to global warming (WHO, 2020[41]). Moore (2009[55]) reviews a voluminous literature covering the climatic impacts of two specific air pollutants: tropospheric ozone and black carbon emissions.

Instead, the synergy between these policies originates from the fact that the sources of air pollutant and greenhouse gas emissions are largely overlapping, which means that their management can possibly be achieved with fewer policy instruments.[26] In that sense, the findings corroborate earlier contributions, which highlight the parallel benefits of broader policies targeting any of the two issues.[27]

Importantly, the synergies highlighted in this paper are confined to transport policies, as they are unlikely to extend to policies targeting land-use. The reason is that land-use policies may promote a variety of urban structure configurations with potential trade-offs between climate change mitigation and reducing exposure to air pollutants (Schindler and Caruso, 2014[26]). Dense and compact cities are less car dependent and are characterised by shorter average travel distances. Consequently, they may generate a lower carbon footprint but suffer from greater concentrations of air pollutants in their dense, highly populated cores (OECD, 2018[27]). On the other hand, human exposure to air pollution is likely lower in sprawled cities of low population density, but travel distances are larger and more likely to be covered by car. As a result, there is likely no land-use policy capable of achieving both environmental goals, the same way transport policies could do.[28]

The study reveals several insights regarding the nature of the synergies that urban transport policies can generate. Such policies utilize instruments whose intensity can be refined and adjusted at the local level. The *vehicle-differentiated kilometre tax* proposed in this study is a distance-based charge that can be fine-tuned to align the pecuniary burden it imposes with the emission factors of different vehicles. Furthermore, its overall level can be adjusted within a city and differentiated across cities. That enables the kilometre charge to target the long-run external effects from carbon emissions while also targeting short-run externalities that vary across urban areas. Such externalities go beyond air pollution to include traffic congestion, noise and accidents. The results provide evidence that carefully designed policy instruments will not only accelerate relief from most air pollutants, but will also substantially curb CO_2 emissions. The key mechanism behind this potential is that vehicle technology strongly correlates with emission factors and fuel efficiency. Imposing a higher charge on a kilometre generated by an older vehicle is an indirect, but efficient way to put a higher price on emission intensity and fossil fuel consumption.

The *vehicle-differentiated kilometre tax* can partially offset the adverse effects of annual vehicle circulation taxes or registration fees, when the latter are misaligned with environmental objectives. In Chile, the annual circulation tax increases steeply for newer vehicles possessing superior filtering technologies and consuming less fuel, while it is substantially lower for their older counterparts.[29] Furthermore, it favours the ownership of conventional cars *vis-à-vis* low emission vehicles.[30] Although the structure of the annual circulation tax could be somewhat justified from a distributional viewpoint, it creates long-run incentives

[26]The literature has highlighted some potential trade-offs, which however do not alter the qualitative conclusions of the study. For example, fitting $PM_{2.5}$ filters to diesel vehicles can reduce the emissions of air pollutants but may increase fuel consumption and CO_2 emissions (Williams, 2012[40]). Outside of the transport sector, wood stoves have sometimes been considered a net-zero GHG heating source but contribute significantly to air quality problems through the emissions of black carbon and nitrous oxide (EU, 2003[38]; Sterman, Siegel and Rooney-Varga, 2018[36]; WHO, 2018[37]).

[27]Some notable references include ApSimon et al. (2009[56]), Lanzi and Dellink (2019[6]), von Schneidemesser and Monks (2013[39]) and IASS Potsdam (2019[30]).

[28]An exception could be a land use policy that contains a considerable degree of spatial resolution. However, identifying such a policy goes beyond the scope and capacity of this study.

[29]The median annual circulation fee for new vehicles (0-10 years) is estimated to be between 2 and 4 times the corresponding median fee for vehicles of medium vintage (10-20 years) and multiple times that of older cars.

[30]The median annual circulation fee for gasoline, diesel and electric vehicles is estimated to be: 25, 105, 569 kCLP respectively. The data used in the calculation are available online by the Chilean Ministry of Finance (Servicio de Impuestos Internos) at: https://www.sii.cl//servicios_online/1049-2612.html.

towards owning vehicles of higher emission intensity. The introduction of a scheme like the vehicle-differentiated kilometre tax can contribute to weakening these incentives in a non-regressive way.

The study also highlights the synergetic benefits of a *carbon tax applied to urban transport*. This scheme introduces a tax on all energy sources used in the transport system. An environmental tax per litre of gasoline and diesel is introduced simultaneously with a tax per kilowatt-hour of electricity. All tax levels adjust with the assumed marginal social cost of carbon and the amount of CO_2 released during the generation and combustion of final fuel. Thus, carbon capture technologies and a cleaner electricity grid lower the tax, while increases in the estimated damages from climate change adjust it upwards. The results indicate that such a tax could also function as an air-pollution mitigating instrument. This holds particularly true as long as carbon capture technologies remain at an infant stage and the generation of electricity contributes to air pollution.

Another policy implication emerging from the analysis is that national and local policy instruments could possibly substitute each other, apart from being complements. In the context of the study, a significant decrease in the carbon footprint and air pollution generated by the existing transport system can be achieved with the use of instruments controlled by different levels of government.

The analysis also finds that the composition of the bus fleet plays a central role in delivering environmental benefits. Cities with a relatively old bus fleet, i.e. one composed predominantly by diesel buses, tend to have lower air quality. Delaying the deployment of bus electrification keeps the emissions generated by public transport higher than they otherwise would be. Importantly, it also reduces the potential of several environmentally related policies that induce a switch from the use of private vehicles to public transport. This additional effect occurs because the success of such a switch ultimately depends on the difference between the emission intensity of passenger kilometres generated with the two modes. Therefore, obtaining high occupancy rates in public transport modes and reducing the polluting footprint of buses are both of high importance.

Specifically for Santiago, the study highlights how bus electrification can contribute to improving air quality and curbing CO_2 emissions. For many pollutants, the relative contribution of rapid bus electrification as a stand-alone policy, is higher than that achieved by the tax-based instruments examined in the study. This occurs largely because the city has already a modal split that favours the use of public transport. In this context, any initiative that reduces the emission intensity of a passenger kilometres travelled *via* public transport modes will result in considerable environmental benefits. Furthermore, the study finds that electrifying the bus fleet can be a prerequisite in order for the two tax-based policies to deliver the aimed environmental benefits. The most characteristic example regards the emissions of $PM_{2.5}$, upon which the two examined tax-based schemes –when used as stand-alone policies – have a reinforcing, rather than a mitigating effect. Possibly, that adverse effect can be generated by any measure that discourages the use of private cars in favour of public transport. However, once a substantial fraction of the bus fleet electrifies, tax-based instruments will also become more effective *per se* in reducing pollutants like $PM_{2.5}$.

Apart from the various cross-instrument synergies, the combined implementation of a bus electrification programme with at least one tax-based scheme can ensure fiscal balance. The latter is key, as policies that avoid generating a fiscal deficit are more sustainable (OECD, 2006[28]).[31] At the same time, fiscal consolidation initiatives may enjoy limited acceptance by the public. The study does not offer a detailed analysis for the cost of accelerating the replacement of diesel with electric buses. However, the tax revenue from the two proposed schemes is expected to be substantial and is highly likely to cover the costs of the

[31]Both the current and the previous Chilean governments have raised public transport fares in Santiago to address public transport budget deficits (Font, 2015[42]).

rapid electrification program.[32] Tax levels and the speed of the electrification programme can both be adjusted to eliminate budget deficits.

Finally, the analysis shows that the combined use of the two policies achieves important environmental objectives without adverse distributional consequences. The main reason for expecting the proposed policies to be relatively neutral from a distributional viewpoint is that their direct impacts pertain almost exclusively to the upper two quartiles of the income distribution.[33] The instruments examined in the analysis tax the use of cars, which are disproportionately owned by higher income groups. In return, these groups benefit greatly from congestion relief, since they display a much higher willingness-to-pay for travel time savings. Furthermore, the simulations assume that all tax revenue returns in the form of a lump-sum transfer to the economy.[34] Factoring in the benefits from tax revenue return, the analysis shows that high-income groups will be made better off by the combined implementation of these policies, even before accounting for the benefits from air pollution reduction. At the same time, the vast majority of low-income households will also benefit from the reform. Although the policies do not directly affect them, they ensure better public transport and access to additional lump-sum transfers or public goods. In fact, the analysis shows that the proposed policies reduce the net tax burden of low-income households and create welfare gains that, at least in percentage terms, are greater than those estimated for the high-income groups.

[32]Furthermore, the analysis in the study does not account for public transport revenue increases that could possibly be generated by those switching to public transport due to the characteristics of electric buses.

[33]At first sight this finding may appear to contradict earlier proposals suggesting that such a policy is in general regressive. The argument is that less affluent households are hurt more by price increases than richer ones, as they generally spend a greater share of their budgets on food and transport than high-income households (Claeys, Fredriksson and Zachman, 2018[35]). Such an argument would also fit in the context of this paper in case the examined policies caused an overall increase in public transport prices.

[34]In real world terms, this implies that once some part of the tax revenue is used to subsidize bus electrification, part of that will also return as a compensatory mechanism.

5 Concluding remarks

Reducing air pollution and greenhouse gas emissions from urban transport is a timely policy challenge. Finding a socially desirable remedy can be complicated, as the ideal policy mix has to ensure economic efficiency and satisfy fiscal constraints. At the same time, it should not interfere with long-run economic growth or exacerbate existing inequalities. To jointly satisfy these requirements, policy making should be supported by evidence-based analysis that utilises the maximum amount of available information and state-of-the-art modelling techniques.

This paper presented the methods and findings of a study focusing on the case of Santiago, Chile. The conducted study explored a reference scenario for the evolution of CO_2 and seven air pollutants (CO, VOC, NO_X, $PM_{2.5}$, SO_2, N_2O, NH_3). It also examined, in an *ex-ante* way, a series of counterfactual scenarios based on three policies: a rapid bus electrification programme, a vehicle-differentiated kilometre tax and a carbon tax scheme applied in urban transport. These tax-based policies were examined in conjunction with a horizontal lump-sum revenue-recycling programme. The scenarios were simulated using the OECD's urban land-use and transport model, MOLES, which was tailored for the case study and calibrated upon several data sources from Santiago and Chile.

The methodology of the study enabled a series of policy relevant findings. First, in the absence of drastic policy changes, emissions of CO_2 and air pollutants from urban transport are likely to follow very different paths. Without rapid progress in carbon capture technologies in transport, the former is likely to remain close to today's levels. Improvements in fuel efficiency and a partial penetration of electric vehicles are offset by increases in population, income, car ownership and travel demand. In contrast, the emissions of air pollutants will drastically decrease. This finding is based on conservative expectations about progress in the filtering technologies of future diesel and gasoline vehicles.

The study highlighted the role of policy as a lever to obtain a multifaceted socioeconomic and environmental objective. Overall, all proposed policy interventions are found to induce a substantial decrease in the carbon footprint of urban transport and to accelerate a transition to a city with cleaner air. Importantly, the two tax-based schemes simulated in the paper were shown to be capable of achieving comparable results. Once their tax levels are aligned, each scheme can target both issues, despite the fact that they focus on air pollution and climate change respectively, and that they are likely to be administered by different governmental authorities. In that sense, the study has corroborated −this time from the viewpoint of urban transport− earlier work highlighting the strong linkages between policies combating air pollution and curbing climate change.

The findings indicate that accelerating the electrification of the public bus fleet plays a pivotal role in delivering environmental benefits. Cities where the bus fleet is relatively old but public transport possesses a large part of the modal share will largely benefit from such a programme. In fact, the analysis reveals that bus electrification could have a multiplicative effect when used in conjunction with one of the tax policies. Ideally, bus electrification would precede the implementation of stringent policies promoting the increase of public transport use, as the effect of the latter would be limited or even negative in absence of a greener bus fleet.

At the same time, the findings have also brought attention to some limitations of the examined policy instruments. Such limitations include their efficacy in achieving their primary environmental goal without

obtaining stringent values, the optimal sequence at which some of them have to be applied and the asymmetric reductions they may cause in some of the air pollutants.

The environmental effects reported in the study should be assessed in conjunction with the fiscal and distributional consequences of the examined policies. Policies that generate emission reductions through generous subsidies, without proportional increases in public revenue, generate deficits. As the fiscal cost of a policy is an important component of any associated reform, policies should also be assessed in terms of their impacts on fiscal balance (OECD, 2006[28]). The distributional consequences, as well as the wider social welfare implications of a policy, are of particular importance in determining the likelihood that a policy will be successfully implemented. Recent protests in Chile in response to the raising of metro fares have underlined the significance of political acceptability. Therefore, the policy impacts in this analysis were evaluated for households of different income levels, providing a measure of their social acceptability.

Despite the fact that this study focused on Santiago, its findings possess a considerable degree of external validity for similar cities. Some of the key characteristics are the relatively low, but rapidly growing rate of private vehicle ownership and the considerable share of travel demand served by public transport. The relatively old, emission-intensive bus fleet and the relatively new fleet of private vehicles are also important elements that partially drive the study's findings. The above characteristics are common to many emerging economies in which income and travel demand are expected to continue growing in the years to come. However, any extrapolation of the present findings to resembling contexts should be made with caution, accounting for the various idiosyncratic characteristics of Santiago and Chile incorporated in the analysis.

6 Technical Appendix

6.1. MOLES version 1.2: Model specification for Santiago

6.1.1. Populations, incomes and representative agents

The model exhibited in the following sections builds upon an evolving population of individuals that grows at a steady annual rate equal to r_P. At year t, that population amounts to $N_t = (1 + r_P)^t N_0$, where N_0 is the population at the benchmark year of the simulation. The model approximates the aggregate behaviour of population N_t by focusing on the corresponding behaviour of two representative individuals, of low and high income respectively. The threshold income that distinguishes the two cohorts is the median income, implying that the two cohorts possess an equal share in the population. Consequently, any arbitrary behavioural variable y_t is aggregated using the weighted sum:

$$y_t \approx 0.5\, N_t \sum_{n=1}^{2} y_{nt}(x_{nt}), \qquad (6.1)$$

where x_{nt} are the factors that determine y_{nt}, the individual contribution of the representative agent from cohort n at year t.

One such factor is income. The daily after-tax real wage of the representative individual from cohort n depends on her working location j:

$$w_{njt} = (1 + r_W)^t\, w_{nj0}. \qquad (6.2)$$

In equation (**6.2**), w_{nj0} is the corresponding wage offered to her at the same location in the benchmark year and r_W is the annual growth rate of real wages, which is assumed to be constant across space, cohorts and time.

6.1.2. Time

The model considers two different time scales. The first is the calendar year at which simulation is carried out, and is denoted by t. Within each year, the behaviour of agents in the model is also examined at four distinct periods: i) the on-peak hours of working days, ii) the off-peak hours of working days, iii) Saturdays, and iv) Sundays. The period to which an output refers is denoted by p.[35] The simulation is repeated for years 2020, 2030, 2040 and 2050. Year 2020 is referred to as the benchmark year and is represented by $t = 0$. The rest of the years are expressed in terms of years from the benchmark year, i.e. $t = 10, 20, 30$.

[35]Assuming that the on-peak period on working days lasts for 6.5 hours, the allocation of within-year time across the four periods is $\left(\frac{5}{7}\cdot\frac{6.5}{24}, \frac{5}{7}\cdot\frac{17.5}{24}, \frac{1}{7}, \frac{1}{7}\right)$.

6.1.3. Networks, traffic and spatial configuration

Economic activity in the model takes place in a set of residential zones, $\mathcal{R}$, a set of job hubs, $\mathcal{J}$, and a set of non-commuting trip attraction points, $\mathcal{A}$. Arbitrary points in these sets are indexed by i, j and r respectively. That is, agents travel from any home location i to their job location j for commuting trips (L-trips) and to any trip attractor r for shopping and leisure purposes (O-trips).

Trips materialize with private vehicles, buses, metro and soft mobility modes. They take place in a transport network characterised by a set of nodes (edges), $\mathcal{P}$, and sets $\mathcal{L}_R$, $\mathcal{L}_{Mt}$ and $\mathcal{L}_S$ containing road (R), metro (M) and soft mobility (S) links (vertexes) respectively.[36] An arbitrary link of type q, l_{se}^{q}, connects nodes s and e and has length ℓ_{se} equal to the Euclidean distance between these points. Links are unidirectional, i.e. $l_{se}^{q} \neq l_{es}^{q}$. Links of different sets (i.e. road, metro, soft mobility) spatially overlap if they connect the same pair of nodes (s,e). However, the traffic flows within them do not interact with each other, thus $l_{se}^{R} \neq l_{se}^{S} \neq l_{se}^{M}$.

Travel decisions depend on expected travel times, denoted by $\hat{\mathrm{t}}$. The time that a road mode w, i.e. car or bus, requires in order to traverse the road link l_{se}^{R} is given by:

$$\hat{\mathrm{t}}_{s,e,C}^{R,p,t} = \ell_{se} / \hat{s}_{s,e,w}^{R,p,t} . \tag{6.3}$$

Forming an expectation about road travel times is necessary due to the uncertainty in traffic conditions. The level of congestion in road link l_{se}^{R} during $\mathbf{t} = (p,t)$ is unknown, therefore the resulting travel speed $s_{s,e,w}^{R,p,t}$ cannot be known *ex-ante* with certainty. Equation (6.3) states that individuals form an expectation ($\hat{s}_{s,e,w}^{R,p,t}$) about the average speed at which they will travel in the link l_{se}^{R} if they choose mode w during $\mathbf{t}$. This is equivalent to an expectation about the time required to travel from s to e with mode w ($\hat{\mathrm{t}}_{s,e,C}^{R,p,t}$). In contrast to roads, travelling with metro or soft mobility modes (i.e. bike or walk) is assumed to be congestion free. Thus, expected travel times equal actual travel times for these modes. Travel times for metro and soft mobility are given by:

$$\mathrm{t}_{s,e}^{M,p,t} = \ell_{se} / s_{s,e}^{M,p,t} , \tag{6.4}$$

and

$$\mathrm{t}_{s,e}^{S,p,t} = \ell_{se} / s_{s,e}^{S,p,t} , \tag{6.5}$$

respectively.

A route q is a sequence of S_q nodes and a sequence of $S_q - 1$ links. Letting $s(i)$ and $s(i+1)$ denote the (i)-th and $(i+1)$-th entries in S_q, the expected time to traverse a road (R) route during time period p of year t with car is:

$$\hat{\mathrm{t}}_{q,C}^{R,p,t} = \sum_{i=1}^{S_q - 1} \hat{\mathrm{t}}_{s(i),s(i+1),C}^{R,p,t} . \tag{6.6}$$

[36] Sets are $\mathcal{L}_R$ and $\mathcal{L}_S$ are constant over time. In contrast, the set $\mathcal{L}_{Mt}$ is subscripted by t to account for an expanding metro network considered in this study.

The expected time to traverse route q with public transport, i.e. bus and metro, is:

$$\hat{\mathrm{t}}_{q,B}^{R,p,t} = \underbrace{\left(N_q^T\, \mathrm{t}_{p,t}^T\right)}_{\substack{\text{transit time}\\(\text{total})}} + \sum_{i=1}^{S_q-1}\left(I_{q,i}^B \underbrace{\hat{\mathrm{t}}_{s(i),s(i+1),B}^{R,p,t}}_{\substack{\text{on-bus time}\\(\text{from } i \text{ to } i+1)}} + I_{q,i}^M \underbrace{\mathrm{t}_{s(i),s(i+1)}^{M,p,t}}_{\substack{\text{on-metro time}\\(\text{from } i \text{ to } i+1)}} \right), \tag{6.7}$$

where N_q^T is the minimum number of public transport transits[37] required to traverse q with the sequence of links it contains; $\mathrm{t}_{p,t}^T$ is the average waiting time during a public transport transit in time period p and year t; $I_{q,i}^B$ is an indicator function that equals one if route q uses a bus (i.e. $w = B$) to move the passenger from node $s(i)$ to $s(i+1)$, and zero otherwise; $I_{q,i}^M$ is the corresponding indicator for metro; $\mathrm{t}_{s(i),s(i+1),B}^{R,p,t}$ and $\mathrm{t}_{s(i),s(i+1)}^{M,p,t}$ are the in-vehicle travel times for the transition from $s(i)$ to $s(i+1)$, if this transition takes place with bus and metro, respectively. Finally, when route q is traversed by soft mobility, the expected travel time becomes:

$$\mathrm{t}_{q,B}^{R,p,t} = \sum_{i=1}^{S_q-1} \mathrm{t}_{s(i),s(i+1)}^{S,p,t}. \tag{6.8}$$

From the above it follows that if the expected speeds of cars and buses, $\hat{s}_{s,e,C}^{R,p,t}$ and $\hat{s}_{s,e,B}^{R,p,t}$ equal their actual counterparts $s_{s,e,C}^{R,p,t}$ and $s_{s,e,B}^{R,p,t}$, which are derived in (6.71), then the micro-expectations are correct. The subsequent section details how this is achieved. The algorithm used to generate each route in the network is provided below.[38]

6.1.4. Individual consumer behaviour

Consider an individual from socioeconomic cohort n that during year t chooses alternative $\mathbf{a} = (i,j)$, i.e. she chooses to reside in zone i and work in zone j. The individual works $L_{tn\mathbf{a}}$ days per year, earns an income of w_{tnj} per day and has a non-labour annual income, Θ_{tn}. Each working day implies a commuting trip with an average cost of $p_{Lt\mathbf{a}}^{\mathrm{e}}$, where the superscript e denotes expectation; subscript $\mathbf{a}$ indicates that the daily commuting cost varies across combinations of residential and job location pairs (i,j); and t implies that the cost evolves across years. The individual spends part of her total income on generic consumption, whose price is fixed to 1.0 in every year t, so that all prices are expressed in real terms. The remainder of income is spent on housing, which is (annually) priced at p_{Hit} per m^2, and on non-commuting trips (O-trips), which have an average cost of $p_{Ot\mathbf{a}}^{\mathrm{e}}$.Therefore, the annual budget constraint can be written as:

$$C_{tn\mathbf{a}} + p_{Hit}H_{tn\mathbf{a}} + p_{Ot\mathbf{a}}^{\mathrm{e}}T_{tn\mathbf{a}}^O = \left(w_{tnj} - p_{Lt\mathbf{a}}^{\mathrm{e}}\right)L_{tn\mathbf{a}} + \Theta_{tn}. \tag{6.9}$$

In equation (6.9), housing consumption, $H_{tn\mathbf{a}}$, the number of non-commuting trips, $T_{tn\mathbf{a}}^O$, and labour supply, $L_{tn\mathbf{a}}$, are all subscripted by t, n and $\mathbf{a}$, as their optimal values vary by year, cohort and alternative. This will become apparent upon their derivation, below.

The individual faces the time constraint:

[37] A transit is defined as a change between two bus lines, between two metro lines or a change from a metro line to a bus line or *vice versa*.

[38] On top of the network routes, the model generates off-network kilometres. These serve the entry to and exit from the network, as well as local non-commuting trips of short distance.

$$\ell_{tn\mathbf{a}} + (d_{Wn} + \mathrm{t}^{\mathrm{e}}_{Lt\mathbf{a}})\, L_{tn\mathbf{a}} + \mathrm{t}^{\mathrm{e}}_{Ot\mathbf{a}} T^{O}_{tn\mathbf{a}} = \bar{T}, \tag{6.10}$$

where d_{Wn} is the average duration of a working day, which is assumed to be different across cohorts but fixed across years; $\mathrm{t}^{\mathrm{e}}_{Lt\mathbf{a}}$ and $\mathrm{t}^{\mathrm{e}}_{Ot\mathbf{a}}$ denote the average time needed for a commuting and non-commuting trip, respectively; $\bar{T}$ is the total time endowment and $\ell_{tn\mathbf{a}}$ the total leisure, both expressed in hours per year.

The two constraints can be combined into a single, full-time constraint:

$$C_{tn\mathbf{a}} + p_{Hit} H_{tn\mathbf{a}} + \underbrace{(p^{\mathrm{e}}_{Ot\mathbf{a}} + v_{tn\mathbf{a}} \mathrm{t}^{\mathrm{e}}_{Ot\mathbf{a}})}_{\tilde{p}^{O}_{tn\mathbf{a}}} T^{O}_{tn\mathbf{a}} + v_{tn\mathbf{a}} \ell_{tn\mathbf{a}} = \underbrace{\Theta_{tn} + v_{tn\mathbf{a}} \bar{T}}_{\Omega_{tn\mathbf{a}}}, \tag{6.11}$$

where:

$$v_{tn\mathbf{a}} = \frac{w_{tnj} - p^{\mathrm{e}}_{Lt\mathbf{a}}}{d_{Wn} + \mathrm{t}^{\mathrm{e}}_{Lt\mathbf{a}}}, \tag{6.12}$$

is the shadow value of time for cohort n in year t under the choice of alternative $\mathbf{a}$; $\tilde{p}^{O}_{tn\mathbf{a}}$ is the generalised value of a non-commuting trip. The latter encompasses the pecuniary cost of such a trip and the monetised value of the time spent on it.

The four utility-generating goods are assumed to be inputs in two baskets. The first basket, denoted by B, combines generic goods and housing, it can therefore be seen as a "real consumption" basket. Its real price in zone i and year t is denoted by p^{B}_{it}. The second basket, denoted by G, is a basket comprising leisure time and non-working trips. The reader can interpret that as a "generic leisure basket", which has a (shadow) composite price $p^{G}_{tn\mathbf{a}}$. The two composite prices, p^{B}_{it} and $p^{G}_{tn\mathbf{a}}$, are functions of the input prices, the exogenous variables, as well as of the parameters appearing in equations (6.9)-(6.11). They are the monetary cost of obtaining one unit of utility through generic consumption or leisure. The closed forms for the two basket prices are derived by minimizing the cost of obtaining the fixed levels of utility $\bar{B}$ and $\bar{G}$. The corresponding minimization problems are:

$$\min \quad p^{C}\, C_{tn\mathbf{a}} + p_{Hit}\, H_{tn\mathbf{a}} \quad \text{s.t.} \left(\omega_C\, C_{tn\mathbf{a}}^{\frac{\sigma_B - 1}{\sigma_B}} + \omega_H\, H_{tn\mathbf{a}}^{\frac{\sigma_B - 1}{\sigma_B}} \right)^{\frac{\sigma_B}{\sigma_B - 1}} = B_{tn\mathbf{a}} \tag{6.13}$$

and:

$$\min \quad \tilde{p}^{O}_{tn\mathbf{a}}\, T^{O}_{tn\mathbf{a}} + v_{tn\mathbf{a}} \ell_{tn\mathbf{a}} \quad \text{s.t.} \left(\omega_O (T^{O}_{tn\mathbf{a}})^{\frac{\sigma_G - 1}{\sigma_G}} + \omega_\ell\, (\ell_{tn\mathbf{a}})^{\frac{\sigma_G - 1}{\sigma_G}} \right)^{\frac{\sigma_G}{\sigma_G - 1}} = G_{tn\mathbf{a}} \tag{6.14}$$

where σ_B is the elasticity of substitution between consumption and housing and σ_G is the elasticity of substitution between non-commuting trips and leisure time.

Solving the two problems yields the Hicksian demands for consumption, housing, leisure and O-trips. These are respectively:

$$C_{tn\mathbf{a}} = B_{tn\mathbf{a}} \left(\left(\frac{p^C}{\omega_C} \right)^{-\sigma_B} + \left(\frac{p_{Hit}}{\omega_H} \right)^{-\sigma_B} \right)^{-\frac{1}{\sigma_B}} \left(\frac{\omega_C}{p^C} \right)^{\sigma_B}, \tag{6.15}$$

$$H_{tn\mathbf{a}} = B_{tn\mathbf{a}} \left(\left(\frac{p^C}{\omega_C} \right)^{-\sigma_B} + \left(\frac{p_{Hit}}{\omega_H} \right)^{-\sigma_B} \right)^{-\frac{1}{\sigma_B}} \left(\frac{\omega_H}{p_{Hit}} \right)^{\sigma_B}, \tag{6.16}$$

$$\ell_{tn\mathbf{a}} = G_{tn\mathbf{a}}\left(\left(\frac{v_{t\mathbf{a}}}{\omega_\ell}\right)^{-\sigma_G} + \left(\frac{\tilde{p}^O_{nt\mathbf{a}}}{\omega_O}\right)^{-\sigma_G}\right)^{-\frac{1}{\sigma_G}}\left(\frac{\omega_\ell}{v_{t\mathbf{a}}}\right)^{\sigma_G}, \tag{6.17}$$

$$T^O_{tn\mathbf{a}} = G_{tn\mathbf{a}}\left(\left(\frac{v_{t\mathbf{a}}}{\omega_\ell}\right)^{-\sigma_G} + \left(\frac{\tilde{p}^O_{nt\mathbf{a}}}{\omega_O}\right)^{-\sigma_G}\right)^{-\frac{1}{\sigma_G}}\left(\frac{\omega_O}{\tilde{p}^O_{nt\mathbf{a}}}\right)^{\sigma_G}. \tag{6.18}$$

Inserting these optimal quantities in the objective functions in (6.13) and (6.14) yields the minimum cost of obtaining a unit of utility through baskets B and G:

$$p^B_{it} = \left(\left(\frac{p^C}{\omega_C}\right)^{-\sigma_B} + \left(\frac{p_{Hit}}{\omega_H}\right)^{-\sigma_B}\right)^{-\frac{1}{\sigma_B}}, \tag{6.19}$$

$$p^G_{tn\mathbf{a}} = \left(\left(\frac{v_{tn\mathbf{a}}}{\omega_\ell}\right)^{-\sigma_G} + \left(\frac{\tilde{p}^O_{tn\mathbf{a}}}{\omega_O}\right)^{-\sigma_G}\right)^{-\frac{1}{\sigma_G}}. \tag{6.20}$$

The combined budget constraint in (6.11) can now be written more simply as:

$$p^B_{it}\, B_{tn\mathbf{a}} + p^G_{tn\mathbf{a}}\, G_{tn\mathbf{a}} = \Omega_{tn\mathbf{a}}. \tag{6.21}$$

The Constant Elasticity of Substitution (CES) utility to be maximised subject to (6.21) through an optimal allocation of resources between baskets B and G is:

$$U_{tn\mathbf{a}} = \underbrace{\left(\omega_B\, B_{tn\mathbf{a}}^{\frac{\sigma_{BG}-1}{\sigma_{BG}}} + \omega_G\, G_{tn\mathbf{a}}^{\frac{\sigma_{BG}-1}{\sigma_{BG}}}\right)^{\frac{\sigma_{BG}}{\sigma_{BG}-1}}}_{\text{systematic utility}} + \varepsilon_{tn\mathbf{a}}. \tag{6.22}$$

In equation (6.22), σ_{BG} denotes the elasticity of substitution between the two baskets; ω_B and ω_G are parameters of the CES function and $\varepsilon_{tn\mathbf{a}}$ is a stochastic term that varies under cohorts, alternatives and years.

The Marshallian demand for basket B is equal to:

$$B_{tn\mathbf{a}} = \frac{\Omega_{tn\mathbf{a}}}{p^B_{it}}\underbrace{\left(\frac{\left(\frac{p^B_{it}}{p^G_{tn\mathbf{a}}}\right)^{1-\sigma_{BG}}\left(\frac{\omega_B}{\omega_G}\right)^{\sigma_{BG}}}{1+\left(\frac{p^B_{it}}{p^G_{tn\mathbf{a}}}\right)^{1-\sigma_{BG}}\left(\frac{\omega_B}{\omega_G}\right)^{\sigma_{BG}}}\right)}_{\text{share of income spent on basket B}}. \tag{6.23}$$

The corresponding demand for basket G is:

$$G_{tn\mathbf{a}} = \frac{\Omega_{tn\mathbf{a}}}{p^G_{tn\mathbf{a}}} \underbrace{\left(\frac{1}{1 + \left(\frac{p^B_{it}}{p^G_{tn\mathbf{a}}} \right)^{1-\sigma_{BG}} \left(\frac{\omega_B}{\omega_G} \right)^{\sigma_{BG}}} \right)}_{\text{share of income spent on basket G}}, \tag{6.24}$$

respectively. Inserting equations (6.23) and (6.24) into equations (6.15)-(6.18) yields the Marshallian demands for consumption, housing, leisure and O-trips. The labour supply of each cohort, $L_{tn\mathbf{a}}$, can then be retrieved by inserting $\ell_{tn\mathbf{a}}$ and $T^O_{tn\mathbf{a}}$ in (6.10).

Equations (6.23) and (6.24) indicate that the demand for the two baskets evolves over time, varies across space (i.e. depends on home location i and job location j incorporated in $\mathbf{a}$) and depends on the population cohort n. Inserting them in equation (6.22) yields the maximum utility that can be achieved by an individual in cohort n if she selects $\mathbf{a}$ in year t. This utility is given by:

$$U^*_{nt\mathbf{a}} = V^*_{nt\mathbf{a}} + \varepsilon_{\mathbf{a}tn}, \tag{6.25}$$

where:

$$V^*_{nt\mathbf{a}} = \left(\frac{\Omega_{nt\mathbf{a}}}{1 + \left(\frac{p^B_{it}}{p^G_{nt\mathbf{a}}} \right)^{1-\sigma_{BG}} \left(\frac{\omega_B}{\omega_G} \right)^{\sigma_{BG}}} \right) \left(\omega_B \left(\frac{\left(\frac{p^B_{it}}{p^G_{nt\mathbf{a}}} \right)^{1-\sigma_{BG}} \left(\frac{\omega_B}{\omega_G} \right)^{\sigma_{BG}}}{p^B_{it}} \right)^{\frac{\sigma_{BG}-1}{\sigma_{BG}}} + \omega_G \left(\frac{1}{p^G_{nt\mathbf{a}}} \right)^{\frac{\sigma_{BG}-1}{\sigma_{BG}}} \right)^{\frac{\sigma_{BG}}{\sigma_{BG}-1}}, \tag{6.26}$$

is the indirect utility corresponding to the tuple $n, t, \mathbf{a}$. It is assumed that the $\varepsilon_{tn\mathbf{a}}$ terms are independently and identically drawn from an extreme value type I distribution with scale parameter λ_A. Then, the expected maximum utility that an individual n can achieve when faced with the set of alternatives $\mathcal{C}_{nt}$ at year t is the well-known log-sum expression:

$$\text{Emax}_{nt} = \lambda_A \left(E + log \sum_{\mathbf{a} \in \mathcal{C}_{nt}} \exp\left(\frac{V^*_{nt\mathbf{a}}}{\lambda_A} \right) \right), \tag{6.27}$$

where E is the Euler's constant. Finally, the probability that an individual from cohort n chooses $\mathbf{a}$ in year t given by the logit formula:

$$\text{P}_{nt\mathbf{a}} = \frac{\exp(V^*_{nt\mathbf{a}}/\lambda_A)}{\sum_{\mathbf{b} \in \mathcal{C}_{nt}} \left(\exp(V^*_{nt\mathbf{b}}/\lambda_A) \right)}. \tag{6.28}$$

6.1.5. Spatial equilibrium

The housing market equilibrium condition in zone i and year t is:

$$\mathrm{E}_{it}^{H} = \underbrace{\sum_{n}\left(N_t \sum_{\mathbf{a}\in\mathcal{C}_{nt}} (\mathrm{P}_{nt\mathbf{a}}\, I_{\mathbf{a}i}\, H_{tn\mathbf{a}})\right)}_{\text{aggregate demand for housing}} - \mathrm{S}_{it}^{H} = 0, \tag{6.29}$$

where E_{it}^{H} is the excess demand for residential floor space; S_{it}^{H} is the supply of floor space; and $I_{\mathbf{a}i}$ is an indicator function that equals one if alternative $\mathbf{a}$ implies the choice of zone i and zero otherwise.

On the supply side, the construction sector is assumed to operate competitively. The production function of residential space is assumed to have a constant elasticity of substitution between land and capital, σ_{KX}. The zero profit condition for the provision of residential floor space is:

$$\Pi_{it}^{H} = \underbrace{\left(\left(\frac{p_{Xit}}{\gamma_X}\right)^{1-\sigma_{KX}} + \left(\frac{p_K}{\gamma_K}\right)^{1-\sigma_{KX}}\right)^{\frac{1}{1-\sigma_{KX}}}}_{\text{housing provision cost}} - p_{Hit} = 0, \tag{6.30}$$

where p_{Xit} is the annual rental rate of land; p_K is the exogenous price of capital; γ_X, γ_K are parameters of the production function. The equilibrium condition for land demand in zone i and year t is:

$$E_{it}^{X} = \mathrm{S}_{it}^{H} \underbrace{\left(\left(\frac{p_{Xit}}{\gamma_X}\right)^{1-\sigma_{KX}} + \left(\frac{p_K}{\gamma_K}\right)^{1-\sigma_{KX}}\right)^{\frac{\sigma_{KX}}{1-\sigma_{KX}}} \left(\frac{p_{Xit}}{\gamma_X}\right)^{-\sigma_{KX}} \left(\frac{1}{\gamma_X}\right)}_{\text{land per m2 of residential space supplied}} - X_{it} = 0, \tag{6.31}$$

where E_{it}^{X} is the excess demand for land; X_{it} is the land supply in zone i in year t. Solving the system of equations (6.28), (6.29), (6.30) and (6.31) for $\mathrm{P}_{nt\mathbf{a}}$, p_{Hit}, p_{Xit} and S_{it}^{H} yields the spatial equilibrium that jointly determines the locational patterns in the city.

6.1.6. Individual travel behaviour

Construction of input matrices and vectors

Using the equilibrium labour supply, $L_{tn\mathbf{a}}$, it is possible to construct the origin-destination matrix of commuting trips for cohort n in year t, $\mathbf{L}_{npt}^{OD}$. The element in the i-th row and j-th column of $\mathbf{L}_{npt}^{OD}$ is the number of commuting trips that depart from residential location i and terminate at job hub j, made by individuals in cohort n during period p in year t:

$$\mathbf{L}_{npt}^{OD}(i,j|\mathbf{e}) = N_{nt}\, \mathrm{P}_{Lpt} \sum_{\mathbf{a}\in\mathcal{C}_{nt}} \left(I_{\mathbf{a}ij}\, \mathrm{P}_{tn\mathbf{a}}\, L_{tn\mathbf{a}}(\mathbf{e}_{\mathbf{a}})\right). \tag{6.32}$$

In (6.32), the indicator function $I_{\mathbf{a}ij}$ equals one if the alternative $\mathbf{a}$ implies living in i and working in j; P_{Lpt} is the exogenous probability that a random commuting trip in year t takes place in period p; vector $\mathbf{e}_{\mathbf{a}}$ encompasses the *macro-expectations* regarding travel times and costs, i.e. $p_{Lt\mathbf{a}}^{\mathrm{e}}, p_{Ot\mathbf{a}}^{\mathrm{e}}, \mathrm{t}_{Lt\mathbf{a}}^{\mathrm{e}}, \mathrm{t}_{Ot\mathbf{a}}^{\mathrm{e}}$; and vector $\mathbf{e}$ concatenates expectations across all alternatives.[39] The formula indicates that the matrix is conditional on these expectations. Should these expectations change, alternative-specific labour supply levels change, the indirect utility of each alternative adjusts, and locational patterns are affected. The spatial model does not yield a similar matrix for generic trips, i.e. O-trips. Assuming that these trips initiate from

[39]The reason for this is that labour supply and the number of non-commuting trips are jointly determined. For instance, a change in commuting travel time expectations in an origin-destination pair (i,j) does not only affect labour supply of every alternative $\mathbf{a}$ for which it holds that $I_{\mathbf{a}ij} = 1$. It also affects the optimal number of generic trips (O-trips) in the same alternatives.

home locations enables the construction of an origin vector, $\mathbf{o}_{nt}^{O}$. The element in the i-th row of this vector denotes the number of O-trips departing from residential location i by individuals in cohort n during year t:

$$\mathbf{o}_{nt}^{O}(i|\mathbf{e}) = N_{nt}\, \mathrm{P}_{Opt} \sum_{\mathbf{a} \in \mathcal{C}_{nt}} \left(I_{\mathbf{a}ij}\, \mathrm{P}_{tn\mathbf{a}}\, T_{tn\mathbf{a}}^{O}(\mathbf{e}_{\mathbf{a}}) \right). \tag{6.33}$$

Structure and micro-expectations

The model assumes that choosing the route of a trip is the final link in a chain of sequential decisions. In every year t of the simulation, these decisions begin with each individual choosing whether to own a vehicle ($c = 1$) or not ($c = 0$). The choice sequence continues with the type of vehicle (v), the choice of transport mode (m) and the destination of an O-trip (x). The final behavioural steps are the choice of commuting route q_L between the chosen residential and job locations, i and j, and a non-commuting route q_O between i and x. The following index tuples keep the notation concise:

$$\mathbf{t} = (p, t);\ \boldsymbol{\mu} = (c, v, m);\ \boldsymbol{\mu}' = (c, v, m, x) = (\boldsymbol{\mu}, x). \tag{6.34}$$

The pecuniary cost of a two-way trip that uses route q characterised by $\boldsymbol{\mu}$ = (c, v, m) is:[40]

$$\mathrm{c}_{qt\boldsymbol{\mu}} = \begin{cases} 2.0 \left(p_{ft}^{T} \underbrace{\sum_{k \in \mathbb{S}(q)} \left(\ell_k (I_{kU}\, f_{Uv} + (1 - I_{kU}) f_{Hv}) \right)}_{\text{fuel consumption: route } q \text{ with vehicle } v} + \ell_q \underbrace{(V_v + \tau_{vt}^{KM})}_{\substack{\text{kilometric} \\ \text{depreciation} \\ \text{and charges}}} \right) & \text{if } c = 1, v \neq 0, m = PV \\ 2.0\, p_{PT} & \text{if } m = PT \\ 0 & \text{if } m = SM \\ +\infty & \text{otherwise} \end{cases}, \tag{6.35}$$

where $p_{f(v)t}^{T}$ is the after-tax price per unit (litre, kWh) of fuel type f compatible with vehicle v, i.e. $f(v)$, in year t; $\mathbb{S}(q) = \{l_0, l_1, .., l_K\}$ is the sequence of road links making up route q; ℓ_k is the length of the road link k in $\mathbb{S}(q)$; I_{kU} is an indicator that equals one if l_k is an urban road link and zero if it is a highway link; f_{Uv} and f_{Hv} denote the amount of fuel consumed per kilometre under urban and highway driving, respectively; ℓ_q is the length of the route;[41] V_v is the kilometric depreciation of vehicle v;[42] τ_{vt}^{KM} encapsulates all kilometric charges that may apply, possibly varying across vehicle types and years; and scripts PV, PT and SM refer to the three mode choices the model covers: private vehicle, public transport and soft mobility. For simplicity, it is assumed that the above cost function does not vary across periods within a given year, i.e. it is not a function of p, and it is known with certainty by individual n. Thus, individuals form no *micro-expectations* regarding the cost of a trip.

Route choice

The utility derived from selecting route q for a commuting trip during **t**, conditional on all expectations in vector **ξ** and the information in tuple **μ** is:

[40]This is a trip generated in year t using vehicle v, transport mode m and route r.

[41]That is, $l_q = \sum_{k \in \mathbb{S}(q)} (l_k)$.

[42]Here, it is implicitly assumed that vehicles have an initial value which diminishes by the same amount per kilometre, i.e. V_v, with a rate that does not depend on the year in which the kilometres are materialized. Any cross-vehicle variation in this value can be attributed to a different purchase price or kilometric lifetime.

$$\mathrm{u}_{nt}(q|\boldsymbol{\xi},\mathbf{a},\boldsymbol{\mu}) = \underbrace{-\left[\mathrm{c}_{qt\boldsymbol{\mu}} + v_{tn\mathbf{a}}\,\mathrm{t}^{\mathrm{e}}_{\mathbf{t}\boldsymbol{\mu}q}\right]}_{\mathrm{v}_{nt}(q|\boldsymbol{\xi},\mathbf{a},\boldsymbol{\mu})} + \varepsilon_{\mathbf{a}nt\boldsymbol{\mu}q}. \tag{6.36}$$

where $\mathrm{c}_{qt\boldsymbol{\mu}}$ is the pecuniary cost of the trip, defined earlier; $v_{tn\mathbf{a}}$ is the value of time imported from the spatial model; $\mathrm{t}^{\mathrm{e}}_{\mathbf{t}\boldsymbol{\mu}q}$ is the expected travel time for a trip using route q that is characterised by $\boldsymbol{\mu}$ in period p and year t; $\mathrm{v}_{nt}(q|\boldsymbol{\xi},\mathbf{a},\boldsymbol{\mu})$ is the systematic utility captured by the travel time and cost; $\varepsilon_{\mathbf{a}nt\boldsymbol{\mu}q}$ is a random component which is identically and independently distributed with scale parameter λ_Q across all elements in its subscript. The conditional choice probability of route q is:

$$\mathrm{P}_{Lnt}(q|\boldsymbol{\xi},\mathbf{a},\boldsymbol{\mu}) = \frac{\exp(\mathrm{v}_{nt}(q|\boldsymbol{\xi},\mathbf{a},\boldsymbol{\mu})/\lambda_Q)}{\sum_{\hat{q}\in\mathcal{C}_q(m,t,i,j)}\left(\exp(\mathrm{v}_{nt}(\hat{q}|\boldsymbol{\xi},\mathbf{a},\boldsymbol{\mu})/\lambda_Q)\right)}, \tag{6.37}$$

where $\mathcal{C}_q(m,t,i,j)$ is the set containing all travel routes that lead from i to j with mode m in year t and $\hat{q}$ is an arbitrary route in this set. The expected maximum utility from a commuting trip is:

$$\Omega_{Lnt}(\boldsymbol{\xi},\mathbf{a},\boldsymbol{\mu}) = \Omega_{Lnt}(\boldsymbol{\xi},\mathbf{a},v,m) = \lambda_Q\left(E + log\sum_{\hat{q}\in\mathcal{C}_q(m,t,i,j)}\exp\left(\frac{\mathrm{v}_{nt}(\hat{q}|\boldsymbol{\xi},\mathbf{a},\boldsymbol{\mu})}{\lambda_Q}\right)\right). \tag{6.38}$$

The utility from selecting route q for an O-trip to location x during $\mathbf{t}$, conditional on all expectations in vector $\boldsymbol{\xi}$ and the information in tuple $\boldsymbol{\mu}$ is:

$$\mathrm{u}_{nt}(q|\boldsymbol{\xi},\mathbf{a},\boldsymbol{\mu},x) = \underbrace{\bar{\omega}_{\mathbf{t}} - \left[\mathrm{c}_{qt\boldsymbol{\mu}} + v_{tn\mathbf{a}}\,\mathrm{t}^{\mathrm{e}}_{\mathbf{t}\boldsymbol{\mu}q}\right]}_{\mathrm{v}_{nt}(q|\boldsymbol{\xi},\mathbf{a},\boldsymbol{\mu},x)} + \varepsilon_{\mathbf{a}nt\boldsymbol{\mu}xq}. \tag{6.39}$$

where $\bar{\omega}_{\mathbf{t}}$ is the *average* monetized benefit from taking the O-trip at $\mathbf{t}$. If no trip is taken during p in year t, the systematic utility is set to zero. The choice probability of selecting route q for a trip from i to x that corresponds to (6.37) is:

$$\mathrm{P}_{Ont}(q|\boldsymbol{\xi},\mathbf{a},\boldsymbol{\mu},x) = \frac{\exp(\mathrm{v}_{nt}(q|\boldsymbol{\xi},\mathbf{a},\boldsymbol{\mu},x)/\lambda_Q)}{1+\sum_{\hat{q}\in\mathcal{C}_q(m,t,i,j)}\left(\exp(\mathrm{v}_{nt}(\hat{q}|\boldsymbol{\xi},\mathbf{a},\boldsymbol{\mu},x)/\lambda_Q)\right)}, \tag{6.40}$$

and the log-sum formula that corresponds to (6.38) is:

$$\Omega_{Ont}(\boldsymbol{\xi},\mathbf{a},\boldsymbol{\mu},x) = \Omega_{Ont}(\boldsymbol{\xi},\mathbf{a},v,m,x) = \lambda_Q\left(E + log\sum_{\hat{q}\in\mathcal{C}_q(m,t,i,x)}\exp\left(\frac{\mathrm{v}_{nt}(\hat{q}|\boldsymbol{\xi},\mathbf{a},\boldsymbol{\mu},x)}{\lambda_Q}\right)\right). \tag{6.41}$$

Choice of destination for O-trips

The spatial model does not predict where generic trips terminate. The following module handles the issue. The utility from a generic trip to location x is:

$$\mathrm{u}_{nt}(x|\boldsymbol{\xi},\mathbf{a},\boldsymbol{\mu}) = \underbrace{\omega_{tx} + \Omega_{Ont}(\boldsymbol{\xi},\mathbf{a},v,m,x)}_{\mathrm{v}_{nt}(x|\boldsymbol{\xi},\mathbf{a},\boldsymbol{\mu})} + \varepsilon_{\mathbf{a}nt\boldsymbol{\mu}x}. \tag{6.42}$$

The new term in (6.42), ω_{tx}, is the utility derived from making a trip to location x. That location-specific utility varies across years. The rest of the systematic utility is the expected maximum utility derived by the traveller who faces the choice set $\mathcal{C}_q(m,t,i,x)$ containing all routes connecting home location i to destination location x. The stochastic term is i.i.d. extreme value type I with scale parameter λ_X across all elements in its subscript. The probability of selecting destination x is:

$$\mathrm{P}_{Ont}(x|\boldsymbol{\xi},\mathbf{a},\boldsymbol{\mu}) = \frac{\exp(\mathrm{v}_{nt}(x|\boldsymbol{\xi},\mathbf{a},\boldsymbol{\mu})/\lambda_X)}{\sum_{\hat{x}\in\mathcal{C}_x}(\exp(\mathrm{v}_{nt}(\hat{x}|\boldsymbol{\xi},\mathbf{a},\boldsymbol{\mu})/\lambda_X))}, \tag{6.43}$$

where $\mathcal{C}_x$ is the time-invariant set of all possible O-trip destinations. The log-sum formula for the destination choice model is:

$$\Omega_{Ont}(\boldsymbol{\xi},\mathbf{a},\boldsymbol{\mu}) = \Omega_{Ont}(\boldsymbol{\xi},\mathbf{a},v,m) = \lambda_X\left(E + log\sum_{\hat{x}\in\mathcal{C}_x}\exp\left(\frac{\mathrm{v}_{nt}(\hat{x}|\boldsymbol{\xi},\mathbf{a},\boldsymbol{\mu})}{\lambda_X}\right)\right). \tag{6.44}$$

The expression in (6.44) encapsulates all the lower-level log-sum components that appear in equation (6.41).

Mode choice

The utilities derived from a commuting and a generic trip using transport mode m are:

$$\begin{aligned}\mathrm{u}_{Lnt}(m|\boldsymbol{\xi},\mathbf{a},v) &= \underbrace{\omega_{Ltm} + \Omega_{Lnt}(\boldsymbol{\xi},\mathbf{a},v,m)}_{\mathrm{v}_{Lnt}(m|\boldsymbol{\xi},\mathbf{a},v)} + \varepsilon_{\mathbf{a}nt\boldsymbol{\mu}},\\ \mathrm{u}_{Ont}(m|\boldsymbol{\xi},\mathbf{a},v) &= \underbrace{\omega_{Otm} + \Omega_{Ont}(\boldsymbol{\xi},\mathbf{a},v,m)}_{\mathrm{v}_{Ont}(m|\boldsymbol{\xi},\mathbf{a},v)} + \varepsilon_{\mathbf{a}nt\boldsymbol{\mu}},\end{aligned} \tag{6.45}$$

where ω_{Ltm} and ω_{Otm} are mode-specific terms that evolve with time and are differentiated by trip purpose; $\Omega_{Lnt}(\boldsymbol{\xi},\mathbf{a},v,m)$ and $\Omega_{Ont}(\boldsymbol{\xi},\mathbf{a},v,m)$ are the expected maximum utilities in (6.38) and (6.44). The probability of choosing mode m in the two types of trips is:

$$\mathrm{P}_{Lnt}(m|\boldsymbol{\xi},\mathbf{a},v) = \frac{\exp(\mathrm{v}_{Lnt}(m|\boldsymbol{\xi},\mathbf{a},v)/\lambda_M)}{\sum_{\hat{m}\in\mathcal{C}_m}(\exp(\mathrm{v}_{Lnt}(\hat{m}|\boldsymbol{\xi},\mathbf{a},v)/\lambda_M))}, \tag{6.46}$$

and:

$$\mathrm{P}_{Ont}(m|\boldsymbol{\xi},\mathbf{a},v) = \frac{\exp(\mathrm{v}_{Ont}(m|\boldsymbol{\xi},\mathbf{a},v)/\lambda_M)}{\sum_{\hat{m}\in\mathcal{C}_m}(\exp(\mathrm{v}_{Ont}(\hat{m}|\boldsymbol{\xi},\mathbf{a},v)/\lambda_M))}, \tag{6.47}$$

respectively. Finally, the expected maximum utility that can be obtained from facing the choice set $\mathcal{C}_m(v)$ in the two types of trips is:

$$\Omega_{Lnt}(\boldsymbol{\xi}, \mathbf{a}, v) = \lambda_M \left(E + log \sum_{\hat{m} \in \mathcal{C}_m(v)} \exp\left(\frac{\mathrm{v}_{Lnt}(\hat{m}|\boldsymbol{\xi}, \mathbf{a}, v)}{\lambda_M} \right) \right), \tag{6.48}$$

and:

$$\Omega_{Ont}(\boldsymbol{\xi}, \mathbf{a}, v) = \lambda_M \left(E + log \sum_{\hat{m} \in \mathcal{C}_m(v)} \exp\left(\frac{\mathrm{v}_{Ont}(\hat{m}|\boldsymbol{\xi}, \mathbf{a}, v)}{\lambda_M} \right) \right), \tag{6.49}$$

respectively. Weighting trips by trip purpose and time period yields a measure of the overall maximum utility expected for a random trip, once an individual chooses vehicle type v. This is:

$$\Omega_{nt}(\boldsymbol{\xi}, \mathbf{a}, v) = \sum_p \left(\mathrm{P}_{Lpt} \left(\frac{L_{tna}}{L_{tna} + T^O_{tna}} \right) \Omega_{Lnt}(\boldsymbol{\xi}, \mathbf{a}, v) + \mathrm{P}_{Opt} \left(\frac{T^O_{tna}}{L_{tna} + T^O_{tna}} \right) \Omega_{Ont}(\boldsymbol{\xi}, \mathbf{a}, v) \right). \tag{6.50}$$

where:

$$\sum_p \mathrm{P}_{Lpt} = \sum_p \mathrm{P}_{Opt} = 1.0. \tag{6.51}$$

Vehicle choice

The utility derived from choosing vehicle v from the choice set of vehicles available at year t, $\mathcal{V}_t$, is:

$$\mathrm{u}_{nt}(v \neq \emptyset|\boldsymbol{\xi}, \mathbf{a}) = \underbrace{\omega_{tv} + \Omega_{nt}(\boldsymbol{\xi}, \mathbf{a}, v)}_{\mathrm{v}_{nt}(v|\boldsymbol{\xi}, \mathbf{a})} + \varepsilon_{ant}, \tag{6.52}$$

where ω_{tv} is a vehicle-specific term that evolves with time; and $\Omega_{nt}(\boldsymbol{\xi}, \mathbf{a}, v)$ is the expected maximum utility that follows from choosing vehicle v. The probability of choosing vehicle v is then:

$$\mathrm{P}_{nt}(v \neq \emptyset|\boldsymbol{\xi}, \mathbf{a}) = \frac{\exp(\mathrm{v}_{nt}(v \neq \emptyset|\boldsymbol{\xi}, \mathbf{a})/\lambda_V)}{\sum_{\hat{v} \in \mathcal{C}_t(v)} (\exp(\mathrm{v}_{nt}(\hat{v} \neq \emptyset|\boldsymbol{\xi}, \mathbf{a})/\lambda_V))}. \tag{6.53}$$

The expected maximum utility from choosing to own a private vehicle is:

$$\Omega^{\mathrm{o}}_{nt}(\boldsymbol{\xi}, \mathbf{a}) = \lambda_V \left(E + log \sum_{\hat{v} \in \mathcal{C}_t(v)} \exp\left(\frac{\mathrm{v}_{nt}(v \neq \emptyset|\boldsymbol{\xi}, \mathbf{a})}{\lambda_V} \right) \right), \tag{6.54}$$

and the corresponding utility of not owning a vehicle is:

$$\Omega^{\mathrm{n}}_{nt}(\boldsymbol{\xi}, \mathbf{a}) = \mathrm{v}_{nt}(v = \emptyset|\boldsymbol{\xi}, \mathbf{a}). \tag{6.55}$$

Ownership decision

The decision regarding whether to own a vehicle ($c = 1$) or not ($c = 0$) is binary, with the following choice probabilities:

$$\mathrm{P}_{nt}(c=1|\boldsymbol{\xi},\mathbf{a})=\frac{\exp\big(\big(\omega_{c1}+\Omega^{\mathrm{o}}_{nt}(\boldsymbol{\xi},\mathbf{a})\big)/\lambda_c\big)}{\exp\big(\big(\omega_{c1}+\Omega^{\mathrm{o}}_{nt}(\boldsymbol{\xi},\mathbf{a})\big)/\lambda_c\big)+\exp(\Omega^{\mathrm{n}}_{nt}(\boldsymbol{\xi},\mathbf{a})/\lambda_c)}, \tag{6.56}$$

and:

$$\mathrm{P}_{nt}(c=0|\boldsymbol{\xi},\mathbf{a})=\frac{\exp(\Omega^{\mathrm{n}}_{nt}(\boldsymbol{\xi},\mathbf{a})/\lambda_c)}{\exp\big(\big(\omega_{c1}+\Omega^{\mathrm{o}}_{nt}(\boldsymbol{\xi},\mathbf{a})\big)/\lambda_c\big)+\exp(\Omega^{\mathrm{n}}_{nt}(\boldsymbol{\xi},\mathbf{a})/\lambda_c)}. \tag{6.57}$$

Chain rule

With the conditional choice probabilities of the previous sections, chain rule formulas can be used to calculate the joint probability that a trip of a certain purpose, undertaken by individual n during period p in year t will be taken with transport mode m, will end up at location x and will use route q. That is:

$$\begin{aligned}&\mathrm{P}_{Ln\mathbf{t}}(c,v,m,q|\boldsymbol{\xi},\mathbf{a})=\mathrm{P}_{Ln\mathbf{t}}(\boldsymbol{\mu},q|\boldsymbol{\xi},\mathbf{a})=\\&\mathrm{P}_{nt}(c|\boldsymbol{\xi},\mathbf{a})\;\mathrm{P}_{nt}(v|\boldsymbol{\xi},\mathbf{a},c)\;\mathrm{P}_{Lpt}\;\mathrm{P}_{Ln\mathbf{t}}(m|\boldsymbol{\xi},\mathbf{a},c,v)\;\mathrm{P}_{Ln\mathbf{t}}(q|\boldsymbol{\xi},\mathbf{a},\boldsymbol{\mu})\end{aligned} \tag{6.58}$$

$$\begin{aligned}&\mathrm{P}_{On\mathbf{t}}(\mathrm{c},v,m,x,q|\boldsymbol{\xi},\mathbf{a})=\mathrm{P}_{On\mathbf{t}}(\boldsymbol{\mu}',q|\boldsymbol{\xi},\mathbf{a})=\\&\mathrm{P}_{nt}(c|\boldsymbol{\xi},\mathbf{a})\;\mathrm{P}_{nt}(v|\boldsymbol{\xi},\mathbf{a},c)\;\mathrm{P}_{Opt}\;\mathrm{P}_{On\mathbf{t}}(m|\boldsymbol{\xi},\mathbf{a},v,c)\;\mathrm{P}_{On\mathbf{t}}(x|\boldsymbol{\xi},\mathbf{a},\boldsymbol{\mu})\;\mathrm{P}_{On\mathbf{t}}(q|\boldsymbol{\xi},\mathbf{a},\boldsymbol{\mu}')\end{aligned} \tag{6.59}$$

All systematic utility expressions v_{nt} in the previous sections attain the value of minus infinity ($-\infty$) when the joint choice they refer to is internally inconsistent. Then, the associated conditional probability, and thus of the entire chain in (6.58) and (6.59) becomes zero. For instance, choosing not to own a private vehicle ($c=0$) is incompatible with the choice of any vehicle ($v\neq\emptyset$) and the use of private car as a mode of transport. This implies that the probability $\mathrm{P}_{nt}(v\neq\emptyset|\boldsymbol{\xi},\mathbf{a},c=0)$ is zero and thus $\mathrm{P}_{Ln\mathbf{t}}(c=0,v\neq\emptyset,m,q|\boldsymbol{\xi},\mathbf{a})$ is zero too.

Traffic assignment

The joint choice probabilities in (6.58) and (6.59) can be used to calculate the traffic volume in an area k of the transport network during period p in year t. The number of passengers using road link k for commuting trips with vehicles of type v during $\mathbf{t}=(p,t)$ is:

$$\hat{V}_{Lkptv}=\hat{V}_{Lkv\mathbf{t}}=\sum_n N_{nt}\left(\sum_{\mathbf{a}\in\mathcal{C}_{nt}}\left(L_{tn\mathbf{a}}\sum_{\boldsymbol{\mu}\in\mathcal{C}_t(\mu)}\left(I_{vC\boldsymbol{\mu}}\sum_{q\in\mathcal{Q}_{tC}}\left(\mathrm{P}_{Ln\mathbf{t}}(\boldsymbol{\mu},q|\boldsymbol{\xi},\mathbf{a})\;I_{ijq}\;I_{qk}\right)\right)\right)\right). \tag{6.60}$$

The corresponding volume of passengers making O-trips is:

$$\begin{aligned}\hat{V}_{Okptv}&=\hat{V}_{Okv\mathbf{t}}\\&=\sum_n N_{nt}\left(\sum_{\mathbf{a}\in\mathcal{C}_{nt}}\left(T^{O}_{tn\mathbf{a}}\sum_{\boldsymbol{\mu}'\in\mathcal{C}_t(\mu)}\left(I_{vC\boldsymbol{\mu}'}\sum_{q\in\mathcal{Q}_{tC}}\left(\mathrm{P}_{On\mathbf{t}}(\boldsymbol{\mu}',q|\boldsymbol{\xi},\mathbf{a})\;I_{iq}\;I_{qk}\;\right)\right)\right)\right).\end{aligned} \tag{6.61}$$

In equations (6.60) and (6.61), subscript C denotes car and $\mathcal{Q}_{tC}$ denotes the set of possible car trips in year t. The mode compatibility indicator $I_{vC\boldsymbol{\mu}}$ in (6.60) obtains the value of one if joint choice $\boldsymbol{\mu}$ implies the ownership of vehicle v and the use of a car for commuting trips, and the value of zero otherwise. Similarly, indicator $I_{vC\boldsymbol{\mu}'}$ in (6.61) obtains the value of one if joint choice $\boldsymbol{\mu}'$ implies the ownership of vehicle v and the use of car for non-commuting trips, and the value of zero otherwise. The spatial compatibility indicator I_{ijq} appearing in equation (6.60) equals one if the commuting trip's route q, the residential location i and job location j implied by $\mathbf{a}=(i,j)$ are mutually consistent, and zero otherwise. For non-commuting trips, the

corresponding compatibility indicator is I_{iq} in equation (6.61). It equals one if the O-trip's route q and the residential location i implied by $\mathbf{a} = (i, j)$ are mutually consistent, and zero otherwise. The route-link indicator I_{qk}, which appears in both (6.60) and (6.61) equals one if network link k is part of route q.

1. The number of bus passengers using road link k for commuting trips during $\mathbf{t} = (p, t)$ is:

$$\hat{V}_{LkptB} = \hat{V}_{LkB\mathbf{t}} = \sum_{n} N_{nt} \left(\sum_{\mathbf{a} \in \mathcal{C}_{nt}} \left(L_{tn\mathbf{a}} \sum_{\boldsymbol{\mu} \in \mathcal{C}_t(\mu)} \left(I_{P\boldsymbol{\mu}} \sum_{q \in \mathcal{Q}_{t,PT}} \left(\mathrm{P}_{Ln\mathbf{t}}(\boldsymbol{\mu}, q | \boldsymbol{\xi}, \mathbf{a}) \, I_{ijq} \, I_{qk} \right) \right) \right) \right). \tag{6.62}$$

The corresponding passenger volume making O-trips is:

$$\hat{V}_{OkptB} = \hat{V}_{OkB\mathbf{t}} = \sum_{n} N_{nt} \left(\sum_{\mathbf{a} \in \mathcal{C}_{nt}} \left(T^{O}_{tn\mathbf{a}} \sum_{\boldsymbol{\mu}' \in \mathcal{C}_t(\mu)} \left(I_{P\boldsymbol{\mu}'} \sum_{q \in \mathcal{Q}_{t,PT}} \left(\mathrm{P}_{On\mathbf{t}}(\boldsymbol{\mu}', q | \boldsymbol{\xi}, \mathbf{a}) \, I_{iq} \, I_{qk} \right) \right) \right) \right). \tag{6.63}$$

In equations (6.62) and (6.63), subscript B denotes bus and $\mathcal{Q}_{t,PT}$ denotes a set containing available routes with public transport in year t. The indicators I_{ijq}, I_{iq} and I_{qk} perform the same functions as in (6.60) and (6.61). The mode compatibility indicators $I_{P\boldsymbol{\mu}}$ in (6.62) and $I_{P\boldsymbol{\mu}'}$ (6.63) obtain the value of one if joint choice $\boldsymbol{\mu}$ and $\boldsymbol{\mu}'$ implies the use of public transport for commuting and O-trips, and the value of zero otherwise.

Finally, the number of metro (subscript M) passengers using metro link k' for the two types of trips during $\mathbf{t} = (p, t)$ is:

$$\hat{V}_{Lk'ptM} = \hat{V}_{Lk'M\mathbf{t}} = \sum_{n} N_{nt} \left(\sum_{\mathbf{a} \in \mathcal{C}_{nt}} \left(L_{tn\mathbf{a}} \sum_{\boldsymbol{\mu} \in \mathcal{C}_t(\mu)} \left(I_{P\boldsymbol{\mu}} \sum_{q \in \mathcal{Q}_{t,PT}} \left(\mathrm{P}_{Ln\mathbf{t}}(\boldsymbol{\mu}, q | \boldsymbol{\xi}, \mathbf{a}) \, I_{ijq} \, I_{qk'} \right) \right) \right) \right), \tag{6.64}$$

and:

$$\hat{V}_{Ok'ptM} = \hat{V}_{Ok'M\mathbf{t}} = \sum_{n} N_{nt} \left(\sum_{\mathbf{a} \in \mathcal{C}_{nt}} \left(T^{O}_{tn\mathbf{a}} \sum_{\boldsymbol{\mu}' \in \mathcal{C}_t(\mu)} \left(I_{P\boldsymbol{\mu}'} \sum_{q \in \mathcal{Q}_{t,PT}} \left(\mathrm{P}_{On\mathbf{t}}(\boldsymbol{\mu}', q | \boldsymbol{\xi}, \mathbf{a}) \, I_{iq} \, I_{qk'} \right) \right) \right) \right), \tag{6.65}$$

respectively. The algorithms used to iterate across elements of the choice sets and calculate the sums appearing in equations (6.60)-(6.65) are presented in the following subsection.

Conversion of passenger kilometres to vehicle kilometres

MOLES converts the predicted passenger flows in equations (6.60)-(6.65) to vehicle volumes. For road transport, i.e. cars and buses, vehicle volumes are expressed in passenger car equivalent (PCE) units. For car passenger transport, the conversion is proportional:

$$V_{kv\mathbf{t}} = \frac{\left(\hat{V}_{Lkv\mathbf{t}} + \hat{V}_{Okv\mathbf{t}} \right)}{1.3}. \tag{6.66}$$

In (6.66), $V_{kv\mathbf{t}}$ is the volume of passenger cars using road link k. The conversion makes the simplifying assumption that the average size of a car does not substantially vary across vehicle types and years. The denominator is a proxy for the average number of passengers in each car. Thus, the model implicitly assumes that carpooling rates are fixed over time. The ridership rate of buses, i.e. the percentage of a bus's capacity utilized on average during period p of year t, is:

$$A_{Bpt} = \min\left\{1.00, 0.05\left(\log\left(1.00 + a_{PVB}\left(\frac{Q_{Bpt}}{Q_{B00}} / \frac{\mathrm{d}_p}{\mathrm{d}_0}\right)^{b_{PVB}}\right)\right)\right\}, \tag{6.67}$$

where Q_{Btp} is the total number of bus trips during period p of year t; Q_{B00} is the total number of bus trips during the on-peak time of weekdays ($p = 0$) in the benchmark year of the simulation ($t = 0$); the fraction $\mathrm{d}_p/\mathrm{d}_0$ is the duration of period p relative to that of the on-peak in a weekday. Equation (6.67) ensures that the maximum ridership rate ranges between 0.00 and 1.00.[43] The conversion relationship that corresponds to (6.66) for buses is:

$$V_{kB\mathbf{t}} = \frac{\left(\hat{V}_{LkB\mathbf{t}} + \hat{V}_{OkB\mathbf{t}}\right)}{A_{Bpt}}\left(\frac{8.00}{60.0}\right), \tag{6.68}$$

where the numerator of the numerical fraction is the assumed size that a bus occupies on the road relative to a car, and the denominator is the assumed maximum passenger capacity of a bus. The study's findings display limited sensitivity to this fraction, since the explored policies leave it intact while affecting $\hat{V}_{LkB\mathbf{t}}$ and A_{Bpt}.[44] To convert metro passenger kilometres to metro wagon kilometres, $V_{kM\mathbf{t}}$, MOLES uses the equation:

$$V_{kM\mathbf{t}} = \frac{\left(\hat{V}_{LkM\mathbf{t}} + \hat{V}_{OkM\mathbf{t}}\right)}{A_{Mpt}}\left(\frac{1}{166.0}\right), \tag{6.69}$$

which assumes a maximum capacity of 166 passengers per wagon. To compute A_{Mpt}, MOLES uses formula (6.67), replacing Q_{Bpt} with the number of metro trips the model predicts during period p in year t, i.e. Q_{Mpt}, and Q_{B00} with the number of metro trips predicted by the model for the on-peak period of the benchmark year, i.e. Q_{M00}.

Network loading

Using the aggregate vehicle volume in road link k during period p in year t, i.e.:

$$V_{kpt} = V_{kB\mathbf{t}} + \sum_{v \in C_t(v)} (V_{kv\mathbf{t}}), \tag{6.70}$$

MOLES computes the average vehicle speed in the link:

$$s_{k,w}^{R,p,t} = \frac{s_{wk}^{F}}{\left(1 + a_{S,p}\left(\frac{V_{kpt}}{\mathrm{d}_p \mathrm{K}_k}\right)^{b_S}\right)}, \tag{6.71}$$

[43] To see that its minimum value equals 0.0, set $Q_{Btp} = 0.0$. It follows that $A_{pt} = 0.0$.

[44] This is particularly true for simulations that focus on the evolution of $V_{LkB\mathbf{t}} = V_{LkBpt}$ as a fraction of its value in the benchmark year, i.e. V_{LkBp0}. From (6.68) it follows that $\frac{V_{kBpt}}{V_{kBp0}} = \frac{\left(\hat{V}_{LkBpt} + \hat{V}_{LkBpt}\right)}{A_{Bpt}} \frac{A_{Bp0}}{\left(\hat{V}_{LkBp0} + \hat{V}_{LkBp0}\right)}$, which is completely independent of the assumptions made for the size and maximum capacity of a bus.

where s_{wk}^{F} is the free-flow speed of road mode w; K_k is the serving capacity of link k, measured in passenger car equivalent (PCE) units per hour; d_p is the duration of period p, measured in hours per year, thus $\mathrm{d}_p\mathrm{K}_k$ is the maximum traffic flow link k can serve annually; $a_{S,p}$ is a parameter controlling for the impact of congestion on the resulting speed;[45] and b_S is a parameter controlling for the level of traffic at which congestion effects emerge and become severe.[46]

2. Equation (6.71) predicts a uniform speed for all cars that use simultaneously a road link. However, this uniform car speed is different from the speed of buses. The resulting speed of both modes is proportional to that they would enjoy in absence of traffic, s_{wk}^{F}, with the proportion given by the denominator of (6.71). The free flow speed does not change over years t or time periods p, but differs between highway and urban road links. Finally, the model assumes away congestion effects in the subway network, using a fixed, uniform metro speed, s_M.

3. The stochastic user equilibrium requires that:

$$\begin{aligned} s_{k,C}^{R,p,t}(\boldsymbol{\xi}) - \hat{s}_{k,C}^{R,p,t} &= 0, \\ s_{k,B}^{R,p,t}(\boldsymbol{\xi}) - \hat{s}_{k,B}^{R,p,t} &= 0, \end{aligned} \tag{6.72}$$

where $\hat{s}$ are the expected speeds and s their resulting counterparts given by (6.71).

Solution algorithm

To solve the entire model, MOLES uses *macro-expectations*, i.e. expected values of $\mathrm{t}_{Lt\mathbf{a}}^{\mathrm{e}}$ and $\mathrm{t}_{Ot\mathbf{a}}^{\mathrm{e}}$ for each alternative $\mathbf{a}$, contained within vector $\mathbf{e}$. The initial macro-expectations are denoted by $\mathbf{e}(0) = (\mathbf{t}_{Lt\mathbf{a}}^{\mathrm{e}\,(0)}, \mathbf{t}_{Ot\mathbf{a}}^{\mathrm{e}\,(0)})$. The initial solution of the core model yields the vector $\mathbf{x}^*\big(\mathbf{e}(0)\big)$ containing p_{Hit}, p_{Xit}, S_{it}^{H} and the locational choice probabilities. The corresponding notation for the solution of the core model in an arbitrary iteration j is $\mathbf{x}^*\big(\mathbf{e}(\mathrm{j})\big)$.

Beginning with an initial *micro-expectations* vector $\boldsymbol{\xi}(0)$, which contains all expected speeds ($\hat{s}$) in the network, MOLES computes all blocks of equations from (6.35) to (6.57). Then, it uses the chain rule formulae in (6.58) and (6.59) to obtain the joint probability for each combination of vehicle, mode, commuting route, O-trip destination and O-trip route, conditional on $\boldsymbol{\xi}$. Traffic, measured in passengers in each segment of the network, is then calculated by iterating across household types and their alternatives, and incrementing formulae (6.60) to (6.65). Subsequently, MOLES converts passenger flows to vehicle flows using equations (6.66)-(6.70). It finally calculates resulting speeds using (6.71) and the discrepancy equations in (6.72). If this discrepancy is non-negligible, the micro-expectation vector is updated according to the formula: $\boldsymbol{\xi}(i+1) = \boldsymbol{\xi}(\mathrm{i}) + \beta(s\big(\boldsymbol{\xi}(\mathrm{i})\big) - \boldsymbol{\xi}(\mathrm{i}))$, where β is the update rate and $s\big(\boldsymbol{\xi}(\mathrm{i})\big)$ is the vector of resulting speeds obtained from (6.71). The fixed point iteration continues until the converging iteration for which it holds $s\big(\boldsymbol{\xi}(\mathrm{i}^*)\big) - \boldsymbol{\xi}(\mathrm{i}^*) \approx \mathbf{0}$. The correct expectation vector $\boldsymbol{\xi}(\mathrm{i}^*)$ is then used to update the macro-expectation vector $\mathbf{e}$. To this end, MOLES iterates across each alternative $\mathbf{a}$, collects the candidate routes for commuting and generic trips, as well as their expected travel times. It then computes a weighted average of these travel times using the conditional route choice probabilities as weights. The macro-expectation vector, $\mathbf{e}(\mathrm{j}+1)$, is injected to the core model. MOLES terminates when $\mathbf{e}(\mathrm{j}+1) - \mathbf{e}(\mathrm{j}) \approx \mathbf{0}$.

[45] Setting $a_{S,p} = 0$ eliminates all congestion effects, as the resulting speed equals the free flow speed at all levels of traffic.

[46] Setting $b_S = 0$ implies the same level of delay, independent of traffic level. Setting $b_S = 1$ yields linear congestion effects, delaying the onset of congestion. That is, congestion emerges with moderate traffic and does not explode as traffic volumes increase; Setting b_S to a value much larger than one further delays the onset of congestion effects, but these effects become much more severe at high traffic volumes.

References

(n.a.) (n.d.), *ELECTRICITY INFORMATION 2018 EDITION DATABASE DOCUMENTATION*, http://www.iea.org/t&c/termsandconditions/. [52]

(n.a.) (n.d.), *ELECTRICITY INFORMATION 2019 FINAL EDITION DATABASE DOCUMENTATION*, http://www.iea.org/t&c/termsandconditions/. [51]

ApSIMON, H. et al. (2009), "Synergies in addressing air quality and climate change", *Climate Policy*, Vol. 9/6, https://doi.org/10.3763/cpol.2009.0678. [56]

Barraza, F. et al. (2017), "Temporal evolution of main ambient PM2.5 sources in Santiago, Chile, from 1998 to 2012", *Atmospheric Chemistry and Physics*, Vol. 17/16, pp. 10093-10107, https://doi.org/10.5194/acp-17-10093-2017. [16]

Claeys, G., G. Fredriksson and G. Zachman (2018), *The Distributional Impacts of Climate Policies*, Bruegel, Brussels. [35]

Climate Action Tracker (2019), *Chile*, https://climateactiontracker.org/countries/chile/. [33]

Duncan, B. et al. (2016), "A space-based, high-resolution view of notable changes in urban NO x pollution around the world (2005–2014)", *Journal of Geophysical Research*, Vol. 121/2, pp. 976-996, https://doi.org/10.1002/2015JD024121. [17]

El Ministerio del Medio Ambiente (2013), *Primer Reporte del Estado del Medio Ambiente*, El Ministerio del Medio Ambiente, Santiago. [18]

EU (2003), *Directive 2003/87/EC of the European Parliament and of the Council of 13 October 2003 establishing a scheme for greenhouse gas emission allowance trading within the Community and amending Council Directive 96/61/EC*. [38]

European Environment Agency (2019), "Road Transport Appendix 4 Emission Factors 2019", https://www.eea.europa.eu/publications/emep-eea-guidebook-2019/part-b-sectoral-guidance-chapters/1-energy/1-a-combustion/road-transport-appendix-4-emission/view (accessed on 3 February 2021). [10]

Font, M. (2015), *The State and the Private Sector in Latin America*, Palgrave Macmillan US, New York, https://doi.org/10.1057/9781137015761. [42]

Gallardo, L. et al. (2018), "Evolution of air quality in Santiago: The role of mobility and lessons from the science-policy interface", *Elem Sci Anth*, Vol. 6/1, p. 38, https://doi.org/10.1525/elementa.293. [8]

Garreaud, R. and J. Rutllant (2003), "Coastal Lows along the Subtropical West Coast of South America: Numerical Simulation of a Typical Case", *Monthly Weather Review*, Vol. 131/5, pp. 891-908, https://doi.org/10.1175/1520-0493(2003)131<0891:clatsw>2.0.co;2. [14]

Generadoras de Chile (n.d.), *Generación Eléctrica en Chile*, http://generadoras.cl/generacion-electrica-en-chile (accessed on 18 March 2020). [44]

Hirte, G. and S. Tscharaktschiew (2020), "The role of labor-supply margins in shaping optimal transport taxes", *Economics of Transportation*, Vol. 22, https://doi.org/10.1016/j.ecotra.2020.100156. [62]

IASS Potsdam (2019), *Air Pollution and Climate Change*, Institude for Advanced Sustainability Studies. [30]

IEA (2020), *Electricity Information: Overview*, IEA, Paris. [25]

IEA (2019), *CO2 intensity of power, Chile 2000-2018E*, https://www.iea.org/countries/Chile (accessed on 20 March 2020). [45]

IEA (2019), *Stated Policies Scenario*, https://www.iea.org/reports/world-energy-model/stated-policies-scenario (accessed on 18 March 2020). [47]

IEA (2018), *CO2 Emissions from Fuel Combustion 2018*. [29]

IEA (2018), *Electricity information 2018*, OECD Publishing, Paris, https://doi.org/10.1787. [19]

IEA (2018), *Electricity Information 2018*, IEA, Paris, https://doi.org/10.1787/electricity-2018-en (accessed on 11 February 2019). [53]

IEA (2018), "Emissions per kWh of electricity and heat output (Edition 2018)", *IEA CO2 Emissions from Fuel Combustion Statistics* (database), https://dx.doi.org/10.1787/5f382d97-en (accessed on 20 March 2020). [46]

IEA (2018), *Energy Policies Beyond IEA Countries - Chile Review 2018*. [23]

IEA (2018), *World Energy Balances 2018*, OECD Publishing, Paris, https://dx.doi.org/10.1787/world_energy_bal-2018-en. [50]

IEA (2016), *WEO-2016 Special Report: Energy and Air Pollution*, IEA, Paris. [7]

IPCC (2019), *Global warming of 1.5°C An IPCC Special Report on the impacts of global warming of 1.5°C above pre-industrial levels and related global greenhouse gas emission pathways, in the context of strengthening the global response to the threat of climate change, sustainable development, and efforts to eradicate poverty Edited by Science Officer Science Assistant Graphics Officer Working Group I Technical Support Unit*, http://www.environmentalgraphiti.org. [1]

Jorquera, H. et al. (2005), "Trends in air quality and population exposure in Santiago, Chile, 1989-2001", *International Journal of Environment and Pollution*, Vol. 22/4, p. 507, https://doi.org/10.1504/ijep.2004.005684. [13]

Lanzi, E. and R. Dellink (2019), *Economic interactions between climate change and outdoor air pollution*, OECD, Paris. [6]

Ministerio del Medio Ambiente (2017), *Desafíos de la calefacción para la descontaminación atmosférica*. [20]

Moore, F. (2009), "Climate Change and Air Pollution: Exploring the Synergies and Potential for Mitigation in Industrializing Countries", *Sustainability*, Vol. 1/1, https://doi.org/10.3390/su1010043. [55]

Nash, C. (2015), *Handbook of Research Methods and Applications in Transport Economics and Policy*, Edward Elgar Publishing, https://doi.org/10.4337/9780857937933. [43]

Observatorio Social (UAH) (2014), *Actualización y Recolección de Información del Sistema de Transporte Urbano, IX Etapa: Encuesta Origen Destino Santiago 2012. Encuesta Origen Destino de Viajes*, SECTRA, Santiago, http://www.sectra.gob.cl/biblioteca/detalle1.asp?mfn=3253. [22]

OECD (2020), *Decarbonising Urban Mobility with Land Use and Transport Policies: The Case of Auckland, New Zealand*, OECD Publishing, Paris, https://dx.doi.org/10.1787/095848a3-en. [57]

OECD (2019), *Taxing Energy Use 2019: Using Taxes for Climate Action*, OECD Publishing, Paris, https://dx.doi.org/10.1787/058ca239-en. [48]

OECD (2018), *OECD Economic Surveys: Chile 2018*, OECD Publishing, Paris, https://dx.doi.org/10.1787/eco_surveys-chl-2018-en. [12]

OECD (2018), *Rethinking Urban Sprawl*, OECD Publishing. [27]

OECD (2016), *OECD Environmental Performance Reviews: Chile 2016*, OECD Publishing, Paris. [9]

OECD (2016), *The Economic Consequences of Outdoor Air Pollution*, OECD Publishing, Paris, https://dx.doi.org/10.1787/9789264257474-en. [4]

OECD (2015), *Climate Change Mitigation: Policies and Progress*, OECD Publishing, Paris, https://dx.doi.org/10.1787/9789264238787-en. [24]

OECD (2015), *The Economic Consequences of Climate Change*, OECD Publishing, Paris, https://dx.doi.org/10.1787/9789264235410-en. [2]

OECD (2006), *The Political Economy of Environmentally Related Taxes*, OECD Publishing, Paris, https://dx.doi.org/10.1787/9789264025530-en. [28]

Parry, I. and A. Bento (2001), "Revenue Recycling and the Welfare Effects of Road Pricing", *Scandinavian Journal of Economics*, Vol. 103/4, https://doi.org/10.1111/1467-9442.00264. [61]

Pino, P. et al. (2015), "Chile confronts its environmental health future after 25 years of accelerated growth", *Annals of Global Health*, Vol. 81/3, pp. 354-367, https://doi.org/10.1016/j.aogh.2015.06.008. [15]

Rao, S. et al. (2013), "Better air for better health: Forging synergies in policies for energy access, climate change and air pollution", *Global Environmental Change*, Vol. 23/5, https://doi.org/10.1016/j.gloenvcha.2013.05.003. [54]

Schindler, M. and G. Caruso (2014), "Urban compactness and the trade-off between air pollution emission and exposure: Lessons from a spatially explicit theoretical model", *Computers, Environment and Urban Systems*, Vol. 45, https://doi.org/10.1016/j.compenvurbsys.2014.01.004. [26]

Secretaría Regional Ministerial del Medio Ambiente Región Metropolitana (2018), *Informe Final para la Gestión de Episodios Críticos de Contaminación Atmosférica por Material Particulado Respirable (MP10) Periodo 2017*. [34]

Sims, R. et al. (2014), "Transport", in Cambridge University Press (ed.), *Climate Change 2014: Mitigation of Climate Change. Contribution of Working Group III to the Fifth Assessment Report of the Intergovernmental Panel on Climate Change*, Mitigation of Climate Change, Cambridge. [31]

Sterman, J., L. Siegel and J. Rooney-Varga (2018), "Does replacing coal with wood lower CO2 emissions? Dynamic lifecycle analysis of wood bioenergy", *Environmental Research Letters*, Vol. 13/1, p. 015007, https://doi.org/10.1088/1748-9326/aaa512. [36]

Tikoudis, I. (2020), "Second-Best Road Taxes in Polycentric Networks with Distorted Labor Markets", *The Scandinavian Journal of Economics*, Vol. 122/1, pp. 391-428, https://doi.org/10.1111/sjoe.12322. [60]

Tikoudis, I. (2019), "Second-Best Road Taxes in Polycentric Networks with Distorted Labor Markets", *Scandinavian Journal of Economics*, https://doi.org/10.1111/sjoe.12322. [59]

Tikoudis, I. and W. Oueslati (2021), "MOLES: A New Approach to Modeling the Environmental and Economic Impacts of Urban Policies", *Computational Economics*, https://doi.org/10.1007/s10614-019-09962-3. [63]

Tikoudis, I. and W. Oueslati (2017), "Multi-objective local environmental simulator (MOLES 1.0): Model specification, algorithm design and policy applications", *OECD Environment Working Papers*, No. 122, OECD Publishing, Paris, https://dx.doi.org/10.1787/151cf08a-en. [11]

Tikoudis, I., E. Verhoef and J. van Ommeren (2015), "On revenue recycling and the welfare effects of second-best congestion pricing in a monocentric city", *Journal of Urban Economics*, Vol. 89, https://doi.org/10.1016/j.jue.2015.06.004. [58]

UN Habitat (2014), *Developing local climate change plans : a guide for cities in developing countries*. [5]

UNFCCC (2015), *Paris Agreement*. [49]

US EPA (2016), *Technical Support Document: Technical Update of the Social Cost of Carbon for Regulatory Impact Analysis Under Executive Order 12866 Interagency Working Group on Social Cost of Greenhouse Gases, United States Government With participation by Council of Economic Advisers Council on Environmental Quality See Appendix B for Details on Revisions since*. [21]

von Schneidemesser, E. and P. Monks (2013), "Air quality and climate – synergies and trade-offs", *Environmental Science: Processes & Impacts*, Vol. 15/7, p. 1315, https://doi.org/10.1039/c3em00178d. [39]

WHO (2020), *Climate risks from CO2 and short-lived climate pollutants*, Health and sustainable development. [41]

WHO (2019), *Air pollution*, World Health Organisation. [32]

WHO (2018), *Household air pollution and health*, Fact heets. [37]

WHO (2016), *Ambient air pollution: A global assessment of exposure and burden of disease*, World Health ORganisation, Geneva. [3]

Williams, M. (2012), "Tackling climate change: what is the impact on air pollution?", *Carbon Management*, Vol. 3/5, pp. 511-519, https://doi.org/10.4155/cmt.12.49. [40]

Endnotes

[1] Using a proposed social cost of carbon in year t, V_t (CLP/tonne of CO_2), and pre-multiplying that with a time-invariant carbon content of $c_G = 0.0023$ tonnes CO_2 per litre of gasoline, yields the gasoline carbon tax depicted in Figure 3.1 is $c_G V_t$. The corresponding tax on diesel is $c_D V_t$, where $c_D = 0.00268$. The conversion factor for electricity is year specific as the tonnes of CO_2 per kWh are projected to fall.

[2] For illustrative purposes, consider an arbitrary actual bus route in the left panel of Figure 3.8 consisting of points:

$$r = \left\{\underbrace{\mathbf{x}_1, \mathbf{x}_2, \mathbf{x}_3}_{\mathbf{z}_1}, \underbrace{\mathbf{x}_4}_{\mathbf{z}_2}, \underbrace{\mathbf{x}_5, \mathbf{x}_6}_{\mathbf{z}_3}, \underbrace{\mathbf{x}_7}_{\mathbf{z}_4}\right\}$$

where points $\mathbf{x}_1, \mathbf{x}_2, \mathbf{x}_3$ lie sufficiently with each other close to be projected on the same node of the stylised network, $\mathbf{z}_1$. Similarly points $\mathbf{x}_5, \mathbf{x}_6$ lie sufficiently with each other close to be projected on the same node of the stylised network, $\mathbf{z}_3$. The resulting simplified bus route on the stylised network is $s = \{\mathbf{z}_1, \mathbf{z}_2, \mathbf{z}_3, \mathbf{z}_4\}$ and all elements in it are credited service to $\boldsymbol{r}'$. Repeating for all routes allows the complete point-to-route mapping $\mathbf{z}_{\mathrm{x}} \longmapsto (s_1, s_2, .., s_{\mathrm{K}})$ which returns all K projected bus lines passing from node $\mathbf{z}_{\mathrm{x}}$.

[3] This note builds upon endnote 2.Using the complete point-to-route mappings for a sequence of Q points in the stylised network $\mathbf{z}_1$, $\mathbf{z}_2$,.., $\mathbf{z}_{\mathrm{Q}}$, it is possible to approximate the minimum number of transits involved in traversing it. For instance, if there is a simplified bus route s in the point-to-route mapping of each point $\mathbf{z}$ in the sequence, then that sequence can be traversed without transits.

[4] The negative exponential model is for the fuel consumption (litres/km) is:

$$Q_{Cv} = A_{C,F} + a_{C,F}\left(1 + \gamma_{C,H}\, I_{C,H} + \gamma_{C,U}\left(1 - I_{C,H}\right)\right) \exp\left(\beta_{C,F}(t_v - 2006)\right),$$

where Q_{Cv} denotes fuel consumption, expressed in litres per kilometre; subscript $F = \{\text{gasoline}, \text{diesel}\}$ denotes fuel type; $I_{C,H}$ is and indicator that equals one if the vehicle is driven on a highway and zero if driven in an urban road; $\gamma_{C,H}$ and $\gamma_{C,U}$ are shift parameters that allow the consumption function to adjust when driving on a highway versus urban roads; and t_v is the year at which vehicle v is introduced in the market. The model is parametrised by $a_{C,F}$ and $\beta_{C,F}$.

For electric cars, the energy consumption (kWh/km) is logarithmically related to the year at which each vehicle entered the market:

$$\boldsymbol{F_{Cv} = \left(1 + \gamma_{C,H}\, I_{C,H} + \gamma_{C,U}\left(1 - I_{C,H}\right)\right) \log\left(a_{C,\mathrm{e}} - \beta_{C,\mathrm{e}}\,(t_v - 2015)\right).}$$

[5] Assume the emission factors for a pollutant in a sample of years prior to 2020, $\{t_0, t_1, t_2, .., t_K\}$, is $\{e_0, e_1, e_2, .., e_K\}$. A negative exponential model can be fit to any pair of sequential observations $\{t_i, t_{i+1}\}$ and $\{e_i, e_{i+1}\}$ by solving the system:

$$e_i = a_{i,i+1} \exp\left(-b_{i,i+1}\, t_i\right)$$

$$e_{i+1} = a_{i,i+1} \exp\left(-b_{i,i+1}\, t_{i+1}\right)$$

for the pair-specific parameters $a_{i,i+1}, b_{i,i+1}$. Repeating for all pairs of sequential observations yields the yields the sequence of estimates $\{b_{0,1}, b_{1,2}, .., b_{K-1,K}\}$. The sequence of b-estimates can be used as a proxy for the acceleration or deceleration of technological progress. This study projects the sequence forward, i.e. it computes $\{b_{2020,2030}, b_{2030,2040}, b_{2040,2050}\}$ from b-estimates $\{b_{1982,1990}, b_{1990,2000}, b_{2000,2010}, b_{2010,2020}\}$. The estimates are then used to project $\{e_{2030}, e_{2040}, e_{2050}\}$.

[6] The following emission factors are used:

Emission factors g/km	Euro III	Euro V	Euro VI
CO	2.6700	0.2230	0.2230
VOC	0.4090	0.0220	0.0220
NOx	9.38	3.09	0.60
N2O	0.0010	0.0320	0.0400
NH3	0.0029	0.0110	0.0090
PM 2.5	0.2070	0.0462	0.0023

The following formula calculates the emission factor of the average internal combustion engine bus:

$$e_t = s_{3,t}e_3 + s_{5,t}e_5 + s_{6,t}e_6,$$

where $e_{3,t}$, $e_{5,t}$ and $e_{6,t}$ are the factors for pollutant e and $s_{3,t}, s_{3,t}, s_{3,t}$ are the evolving shares of Euro 3, 5 and 6 buses in the fleet.

[7] Both conditions need to hold for such a reinforcement effect to emerge. The study examined the impact of a 30% horizontal *public transport subsidy*. Its effect was found to be ambiguous. The policy has the potential to induce an overall shift from car to public transport modes. However, in the context of this study, this policy is found to steeply increase the demand for non-commuting trips. It is also likely to strengthen the length of local trips currently taken with soft mobility modes and draw passengers from them. The model predicts that the latter set of effects could offset the former.

[8] To see why the reinforcement effect occurs consider the following crude approximation of the transport related carbon:

$$C = Q\left(aP_cC_c + b(1-P_c)\big((1-P_e)C_B + P_eC_e\big)\right)$$

where Q are passenger kilometres; P_c is the fraction of passenger kilometres taken with car; P_e is the fraction of buses being electric; a, b is the inverse occupancy rates of cars and buses, *i.e.* vehicle km per passenger km; C_c, C_D, C_e is the carbon footprint of a car, diesel and electric bus kilometre. Differentiating C with respect to P_e to get $\dot{C}$, and dividing that by C yields:

$$\frac{\frac{dC}{dP_e}}{C} = \frac{\dot{C}}{C} = -\frac{\big(b(1-P_c)(C_B - C_e)\big)}{\left(aP_cC_c + b(1-P_c)\big((1-P_e)C_B + P_eC_e\big)\right)}.$$

The last expression has both a larger numerator and a smaller denominator when any of the two tax schemes in present. Therefore, the decarbonising effect of bus electrification accelerates in the presence of one of the tax schemes examined in the paper.